THE DISTRIBUTION OF BUOYANT DENSITY OF HUMAN ERYTHROCYTES IN BOVINE ALBUMIN SOLUTIONS

Thesis by

Robert C. Leif

In Partial Fulfillment of the Requirements

for the Degree of

Doctor of Philosophy

California Institute of Technology

Pasadena, California

1964

(Submitted May 25, 1964)

To my wife and my parents

ACKNOWLEDGEMENTS

I wish to thank the California Institute of Technology for a Graduate Research Assistantship and the National Science Foundation for supporting the first year of my research.

I wish to thank Dr. C. M. Pomerat for permission to use the Model B Coulter-Counter at the Pasadena Foundation for Medical Research; Mrs. L. Capers and Dr. D. Hammond for performing the cytological studies presented in this thesis; Dr. G. Keighley for the preparation of $Fe^{59}CL_3$ solutions; and Mr. R. L. Millette, Mr. D. Kabat, and Dr. G. Attardi for permission to cite their unpublished results.

I wish to thank the personnel of both the Machine Shop and the Glass Blowing Shop of the Chemistry Department for transforming half-formed intentions into working instruments.

I am most grateful for discussions with and suggestions made by Drs. M. L. Birnstiel, J. H. Fessler, A. Saha, W. Winocour, and R. Weil, and to Messrs. H. H. Ohlenbusch, R. L. Millette, and A. Lebor .

I wish to thank Drs. F. Weil and A. Saha and Messrs. W. R. Holmquist and W. C. Galley for donating blood to this investigation.

For wise counsel I wish to thank Professor L. Pauling.

For friendship, moral support, assistance in time of need, and sagacity, I wish to thank Dr. E. Zuckerkandl.

For his kindness, understanding, tolerance, and wisdom, I wish to thank and acknowledge my gratitude to my mentor, Dr. J. R. Vinograd.

I wish also to thank Dr. Saha for his friendship, loyalty, and for his integrity in a time of need.

I wish to thank Mrs. L. Lozoya for typing this thesis with dispatch and accuracy.

I wish to thank my parents for supporting me through 21 years of schooling, and for all their generosity and love.

And finally, I wish to thank my wife, Suzanne, whose sweetness has tempered me and who, with industry and craftsmanship, produced most of the figures in this thesis and did the typing of the innumerable drafts.

ABSTRACT

A procedure for preparing and fractionating linear density gradients of bovine serum albumin is described. Reproducible buoyant density distributions of human erythrocytes in these gradients were obtained and individual fractions could be rebanded. The average buoyant density of erythrocytes from four individuals was 1.0808 ± 0.0004 g. cm.$^{-3}$; the average density from a fifth individual was 0.0028 g. cm.$^{-3}$ greater. The entire buoyant density distribution shifts with salt content; the erythrocytes behave as "perfect" osmometers. Salt gradients predictably spread or narrow the distribution, and may be used to increase the resolving power of the density gradient.

Rabbit erythrocytes pulse-labeled with Fe^{59} first appear at the light edge of the distribution, and the mean progresses linearly with time through the distribution. The width of the distribution of labeled cells also increases with time.

A study with the Coulter-Counter Model B of cell volumes in the buoyant density fractions showed that the mean cell volumes on the lighter side remained constant, while on the dense side the mean cell volume decreases. This decrease, if regarded as a water loss, does not quantitatively account for the increase in density.

Microscopic examination of the individual fractions of the buoyant density distribution show that the cells do not appear to be damaged by the manipulations, and that cells in the denser fractions are significantly less biconcave than the average cell. The reticulocytes concentrate in the lighter fractions, but do not clearly separate from the erythrocytes. It is proposed that the buoyant density be regarded as an index of the physiological condition of the erythrocyte. A summary discussion of the aging of the erythrocyte is given.

ABSTRACT OF PROPOSITIONS

1. The carboxyl groups present in filter paper which are responsible for the incomplete elution of peptides and the tailing of proteins during electrophoresis can be reduced by $LiAlH_4$.

2. A two-dimensional method for fractionating cells is proposed. The first dimension is a separation by buoyant density; the second is by electrophoretic mobility.

3. A pulse labeling experiment with both radioactive glycine and iron to determine the relationship between human erythrocyte age and buoyant density is proposed.

4. The use of the Cahn Electrobalance as a Westphal balance is proposed as a way to accurately measure the densities of small volumes of liquids, 0.1-0.3 ml.

5. A modification of the peptide mapping technique is proposed which will render it suitable for taxonomic surveys, allow the discovery of small common peptides, and enhance the possibility of the identification of neutral amino acid substitutions.

TABLE OF CONTENTS

PART PAGE

I. INTRODUCTION

A. The Necessity for Cell Fractionation Techniques

At the present time, a subject of major interest in cell biology is the study of the processes and pathways of differentiation. Such studies would be greatly facilitated if homogeneous populations of cells at each stage of development could be obtained. The chemical differences between these populations could then be ascertained. The primary chemical changes which are responsible for these differences, i.e. the chemical reactions of differentiation, might either be suggested by the chemical differences themselves or studied in experiments involving the differentiation of the homogeneous cell populations. These studies could make use of tissue culture techniques or in vitro labeling of homogeneous cell populations and subsequent implantation back into the body. It is thus desirable to purify cells into homogeneous populations in order to determine their composition and to study their reactions in evolving from one to another.

The dispersal of individual cells either on a microscope or in a culture medium has been a major method in cytochemistry. Unfortunately, dispersion on a microscope slide suffers from the difficulty that the amount of any chemical constituent present in a single cell is minute. In the case of the human erythrocyte, this is only 30 μμg of hemoglobin. No other human cell is known to contain as much of a

single protein in solution. This concentration is sufficient for spectrophotometric studies (1), such as of the amount of alkali resistant hemoglobin in a single erythrocyte (2). However, instead of direct measurements labeling methods have usually been employed. Autoradiography has been used to study the incorporation in individual cells of radioactive isotopes into proteins and nucleic acids. Specific antibodies labeled with a fluorescent dye have shown the presence of an antigen (3,4). Experiments with single cells besides suffering from the defect of the small amount of any substance present also have the following deficiencies: the need of prior specific knowledge of what is to be investigated, the limitation to one or two substances to be investigated in any one cell, and the inability to separate research material into aliquots.

The dispersal and subsequent tissue culture of cells, cloning, is a very powerful technique. One recent dramatic example of the efficacy of this method was the demonstration of the inactivity of part of one of the two X chromosomes present in each cell of the human female (5), the "Lyon Hypothesis" (6). Either one or the other but not both of the alleles, each respectively located on one of the X chromosomes for an enzyme, glucose-6-phosphate dehydrogenase, is expressed. Skin cells of women heterozygous for two electrophoretically distinguishable varieties of this enzyme were cloned.

Either one or the other but never both of the varieties of enzyme was present in these clones. This method is not generally applicable to the study of differentiation. The differences between the two resultant cells of a mitotic division would be obscured during the further differentiation which occurred with the multiplication of the cells into a clone. The relationship of mother and daughter cells could not be established because the mitotic division results in the loss of the mother cell.

Therefore, since dispersal techniques cannot produce sufficient quantities of homogeneous cell populations to allow for the assay of the differences between these populations by chemical techniques, fractionation methods must be devised.

Upon consideration of the vast number and diversity of the types of molecules which comprise an individual cell, it is doubtful that if all of these molecular species were tabulated in each of the cells of an animal the tabulation from any two cells would be identical. Therefore, a simple chemical tabulation will not suffice for a definition of homogeneity. Perhaps the quickest way to approach the subject is to ask what causes cells to be different. The primary answer will of course be genes, or DNA. This must be somewhat further defined for metazoans. For instance, erythrocytes and neurons from a single individual at first glance appear to have very little in common,

though they are expressions of the same DNA. But these observed differences are due to different segments of the DNA being expressed.

Homogeneous cell populations may be defined as possessing identical genetic information, which is identically expressed in an identical environment. The regions of the DNA which are not expressed are presumably, at least in some instances, blocked by the presence of histone (7). Therefore, provisionally, homogeneous cell populations can be defined in biochemical terms as comprising cells which possess the same complement of DNA, histone to DNA attachment, and extracellular biochemical environmental history. The foregoing discussion has neglected cytoplasmic inheritance.

This thesis concerns itself with the application of a physical chemical technique to cellular materials; namely, with a method of purification by centrifugation and the application of this method to human and rabbit erythrocytes.

B. Physical Chemical Methods for Fractionating Cell Populations

Several physical chemical properties have been used for purification or fractionation of cell populations: electrophoretic mobility (8, 9), sedimentation rate (10), partition coefficient between aqueous phases (11), and buoyant density (12).

Fractionation by electrical charge (8, 9) has recently been demonstrated and will be of great use. This method, as evidenced from the observed differences in electrophoretic mobility (13), should separate red cells from white cells, leucocytes from granulocytes, and certain types of malignant cells from the other cells present in the blood. However, it does not fractionate by degree of differentiation. Erythrocytes are not resolved by electrophoresis (8).

Fractionation by sedimentation rate has recently been reported by H. Mel (10). He obtained a separation of erythrocytes from white cells and a separation of bone marrow into nucleated and enucleated cells in a continuous flow apparatus. The dispersed cells were separated by the action of gravity in a density gradient formed by the continuous feeding of twelve uniformly flowing horizontal streams of isotonic solutions which contain 0 to 3.1 wt./vol. per cent dextran.

Partition of cells between two aqueous phases made immiscible by the presence of different polymers has been used to separate bacteria (11). The entropy of mixing associated with the two aqueous polymer solutions is small (14), as it depends on the molarity of the polymers, which in turn is very low. The interaction energy between the polymers depends on the weight fraction of the solution that the polymers constitute (14). Therefore, essentially the type of interaction of the polymers will determine the miscibility of the polymer

solutions. This system shows some promise for cells of higher organisms. This separation of cells appears to be by surface charge. Twenty-four hours are required for the two phases to separate. The method is now highly developed, but the twenty-four hours required for the phases to separate is dangerously long for this sort of manipulation of cells. The settling of mammalian cells in this time in the lighter phase may cause problems.

C. Density Separations of Cells

The last physical chemical method, density fractionations of cells, will be the topic of this thesis. Several reports have appeared in the literature of the variation of "density" among different types of dispersed cells and of physical separations based upon this property (12, 15). Two general separation procedures have been used, packed cell methods (15, 16, 17, 18, 19) and neutral density separations (12, 20, 21, 22, 23).

In the latest version of the packed cell method, Garby and Hjelm (19) subjected a packed cell mass to a strong centrifugal field. The field supposedly stratifies the packed cell mass into a density gradient. This density gradient is fractionated layer-wise by slicing the tube at various levels.

Ferrebee and Geiman (12) achieved the first neutral density

separation of erythrocytes . They separated cells which had been invaded with the malarial parasite, Plasmodium Vivax, from cells which had not been invaded. The cells were layered upon a bovine serum albumin solution which was denser than the infected cells and less dense than the uninfected cells. After centrifugation, the infected cells were separated at the top from the uninfected cells at the bottom of the column of bovine serum albumin. Neutral density separations also have been carried out in silicon oil (21) and aqueous solutions of gum acacia (22).

Fractionations performed with the packed cell method (17) and the neutral density separation (20) have shown that white blood cells and young erythrocytes are less dense than mature erythrocytes (12, 16, 18, 19). Garby and Hjelm (19) have shown with the packed cell method that the youngest and oldest erythrocytes are located respectively at the top and bottom of the packed cell column and that the distribution of radioactivity does move down through the cell column with time. However, at intermediate times during the life span of the cells the radioactivity is widely distributed in the packed cell column.

The above procedures are not suitable for the quantitative investigation of the density distribution in cell populations. It is not clear that the segregation of the cells achieved by the packed cell

technique is truly by density. The neutral density procedure yields only two fractions in each experiment. These restrictions may be overcome by centrifuging the cells in a buoyant density gradient. Narrow buoyant density fractions obtained from such a gradient might provide material for the study of the physical and chemical changes in cells with age.

A single experiment suggesting the possibility of such a procedure for human blood cells has been published by Ferrebee and Geiman (12), who observed a diffuse band of red blood cells after centrifuging a sample of blood in a bovine serum albumin density gradient prepared by layering out albumin solutions of graduated density upon each other.

Mateyko and Kopac (23), in an article published after the major portion of this thesis research had been completed, reported criteria for the suitability of many materials to be used in cell separation based on buoyant density. Their criteria were that the material be:

> "... (1) dispersible or soluble in aqueous solutions; (2) stable at cellular ranges of pH; (3) stable and remain dispersed at extremes of temperature; (4) nonviscous; (5) a substance with a high initial specific gravity adjustable to lower values; (6) a high molecular or particle weight material; (7) a non-penetrating substance; (8) isotonic in the isopycnotic range; and (9) completely innocuous to cells."

An abbreviated list of substances studied by these authors includes: small organic molecules, sucrose, glycerol, and amino acids; natural organic polymers, gum acacia, starch, and dextran; synthetic organic polymers, polyvinyl alcohol and polyvinyl pyrrolidone; proteins, bovine serum albumin, hemoglobin, globin, egg albumin, and gelatin; inorganic colloids, basic solutions of sodium silicate and neutral solutions of colloidal silica (Ludox). Of these substances, the only one found to meet the authors' criteria was colloidal silica.

The commercial solutions of colloidal silica (Ludox) used by Mateyko and Kopac in their investigations ranged in SiO_2 content from fifteen to thirty-one per cent, in density from 1.15 to 1.26 g. $cm.^{-3}$, pH 8.54 to 9.8, and particle diameter from 7μ to 15 μ. The authors also state that these solutions have "an extremely low viscosity" and are stable at neutral pH. However, they recommend that the 0.15 molar salt needed for physiological osmolarity should be added just prior to using the solution.

Mateyko and Kopac report buoyant density separations in colloid silica of cells from the following tissues: amphibian (frog) and mammalian (rat) hepatic, amphibian (frog) renal, and human gynecological tissues. In the case of rat hepatic cells, they found two discrete bands of cells separated by a cell free area. The cells from the two bands were morphologically different. The lighter cells

were typical hepatic cells, while the denser cells were considerably elongated. No attempt at rebanding the isolated density fractions is reported. The gradients used in these experiments were made by layering a low density suspension of cells in a physiological solution upon a dense solution. The gradients were formed by careful stirring at the interface between the light and dense solution or by a gentle tapping of the centrifuge tube. These procedures do not form linear density gradients. These authors were interested in qualitative separations of cells, not quantitative buoyant density distributions.

D. Linear Gradients and Equal Volume Fractions

Qualitative results and separations of cells can be achieved with almost any sort of density gradient. Figure 1 shows the density distribution of erythrocytes in a gradient which contained density plateaus. The erythrocytes appear to be distributed in three distinct narrow bands. This distribution is an artifact. The bands were separated by density plateaus, regions without a density gradient (see figure 2). The density gradient was limited to the region of the bands. Thus, the density range of the fractions in which the cells had banded was greater than it would have been had the gradient been linear throughout the liquid column. These misleading results were quite reproducible. It was later discovered that the density plateaus

were due to improper machining of the cams which determined the fraction of dilute and concentrated solutions in the gradient. These cams were not machined by personnel of the C.I.T. chemistry shop.

If a density distribution of the cells is to be plotted, it is necessary to know both the densities and density ranges of the fractions. The value of the ordinate is directly related to the number of cells or the quantity of a material, and the density of the buoyant solution is the abscissa. The density range in the fraction determines the relative amount of material to be found in the individual fraction. This quantity, the density range of each fraction, corresponds to the volume of each fraction in column chromatography.

The density of each fraction, conceivably, could be measured. But such measurements, if performed with a pycnometer, besides being both time-consuming and difficult, are insufficiently accurate, as the density range of each fraction must be calculated from density differences, 0.0020-0.0030 g. cm.$^{-3}$, which are but five times the experimental error, 0.0004, for the best pycnometric determinations performed in this thesis. Only with reliable linearity of the gradient and fractions of equal volume can the density gradient, and thus the density and density range, of each fraction be calculated from the densities of just two or three fractions.

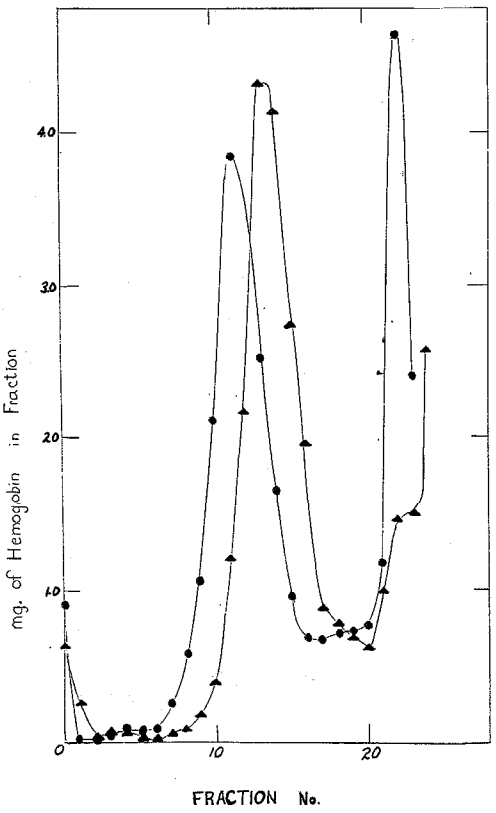

Figure 1. -- Buoyant density distribution of human erythrocytes. Two separate experiments, ● and ▲ . The gradient machine is described in the text. The density gradient produced by the apparatus is shown in figure 2.

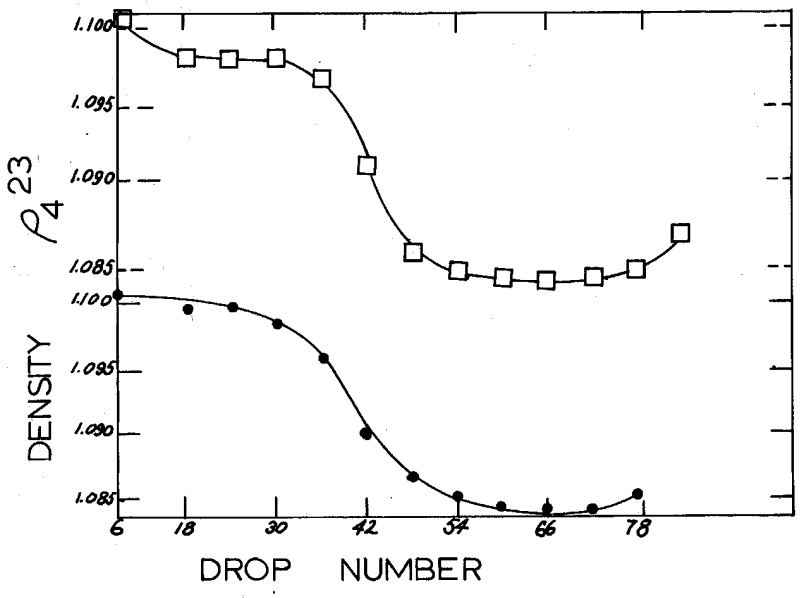

Figure 2.-- The density gradient obtained with the apparatus used for the experiment described in figure 1. Upper, density determined from the refractive index; lower, density determined with a pycnometer. Density plateaus due to improper machining of the cams.

E. Discussion of the Various Procedures for Preparing Linear Density Gradients

For the purposes of this discussion, the kinds of apparatus for the preparation of linear density gradients will be divided into two classes: those which employ syringes or other types of piston drives to control the flow of the solutions and those which do not.

The simplest apparatus of the first class is that described by Kuff, Hogeboom, and Dalton (24). Two syringes, one filled with a dense and the other a light solution, are driven at different rates by programmed cams. The solutions are expelled in varying proportions from the syringes into a mixing chamber and then into a centrifuge tube. Such an apparatus was constructed in this research, but was found to be unsuitable for the formation of linear gradients from the BSA solutions required for banding erythrocytes.

In an apparatus designed by Bock and described by de Duve et al. (25) and Choules (26), the two pistons are connected and advanced simultaneously in their cylinders. The solution from one of the cylinders is forced into the other cylinder, where it is rapidly mixed by a 1700 rpm stirrer with the contents of the other cylinder. This arrangement allows the contents of the cylinder which contains the mixer to be simultaneously linearly enriched with the contents of the other cylinder and to be pumped out during this enrichment. The

output of the cylinder with the stirrer is twice its input. Both the contents of the stirred cylinder and of the other cylinder must flow out through the stirred cylinder.

Bock and Ling (27) and Lakshmanan and Lieberman (28) have shown analytically that the ratio of the output to that of the input of the mixing chamber must equal 2 for the formation of a linear gradient.

The apparatus designed by Bock did not appear promising for the formation of BSA gradients because it involved the use of pistons that could easily be frozen by the BSA solutions, which act as an adhesive, and a 1700 rpm stirrer that could conceivably denature the BSA.

The apparatus described by Bock and Ling (27) is of the second type and does not employ pistons. It consists of two parallel cylinders which are connected at their bases by a capillary and stopcock. The outflow cylinder has a second stopcock and capillary at its base, which is extended by a piece of narrow diameter tubing. A stirrer made from a metal helix of thin wire is attached to a suitable motor, and hangs down into the outflow cylinder. Equal volumes of the two solutions of different densities are pipetted into their respective cylinders, the stirrer is started, and the stopcocks are opened.

The ratio of the output of the outflow cylinder to that of the input is also 2 . However, instead of coupled pistons, the pressure

heads of the liquids in the two cylinders maintain this flow ratio. As the liquid level of the outflow cylinder decreases, liquid from the other cylinder flows into it. This flow maintains the hydrostatic equilibrium between the two sides of the connected cylinders.

The apparatus described by Bock and Ling does make linear sucrose gradients and has been used in semiquantitative work with BSA gradients (29). However, as the BSA solutions used in the cell fractionations are viscous ca. 20 to 40 centipoises, very slow preparation of the gradients would be necessary to insure that the differences in viscosity do not interfere with the maintenance of hydrostatic equilibrium between the two liquid columns.

All of the above apparatuses were designed to form linear gradients. This is, however, only the first half of the apparatus problem. The second half is to collect equal volume fractions. At present, piercing the bottom of a plastic centrifuge tube with a pin and collecting a constant number of drops for each fraction is the procedure used in sampling CsCl (30) and sucrose gradients (31). This is a tedious task and lacks reproducibility for density gradients which are also steep viscosity gradients. The drop size tends to increase as the viscosity decreases. The apparatus developed in this research and described in the next section has been used by others to fractionate sucrose (29) and D_2O-H_2O gradients (32, 33).

II. APPARATUS, MATERIALS, AND METHODS

A. An Apparatus to Prepare and Fractionate Linear Density Gradients

It was decided to construct a dual purpose apparatus, one which would both prepare and fractionate linear density gradients. The problems associated with metering the flow of viscous solutions have been solved by the use of a peristaltic pump. This pump is used instead of equal pressure heads or joined pistons for maintaining the necessary ratio of two for the output to the input of the mixing chamber. This ratio is obtained by connecting two of the pumping tubes of the peristaltic pump by a tee. The outflow of the two tubes was twice that of a single tube. Because the pump meters a constant flow, equal volume fractions were obtained. Since the rates of flow are now externally controlled, the volume of the dense, more viscous solution need not be measured. The end of the gradient will occur when the mixing chamber is empty. Linear density gradients (ca. 0.006 g. $cm.^{-4}$ over a distance of 5 cm.) were prepared from bovine serum albumin solutions with a density gradient machine based on a Technicon peristaltic pump.

B. Construction and Operation of the Gradient Apparatus

The machine, figure 3, consists of five principal parts: a peristaltic pump, a gradient forming assembly, a tube holder, a fraction collector, and a tubing assembly.

A Technicon peristaltic pump, P, model number 1, was slowed to 9/16th of the original speed by interchanging sprockets numbers 37V and 38V. The roller drive gear housing was raised with a 1/8" gasket in order to provide clearance for sprocket 38V. The flow rate of the pump was altered by the exchange of the sprockets in order to allow sufficient time for the mixing of the solutions in the gradient forming assembly. The flow rates of the pump were altered by the exchange of the sprockets rather than narrowing the pumping tubes because of the inconsistency of the flow rates of viscous BSA solutions through tubing of less than 0.030" internal diameter.

The gradient forming assembly consists of a stirrer, S, a mixing chamber, M , a mixing chamber holder, H , and a mixing chamber holder spacer block, B . The mixing chamber and the stirrer are shown in figure 3, and the holder and spacer block in figure 4.

The stirrer blade was fashioned from a Teflon sheet 1.5 x .15 x 6.5 cm. The Teflon sheet was held in a wood vise, twisted with a pair of pliers, and raised in ca. 1 cm. increments

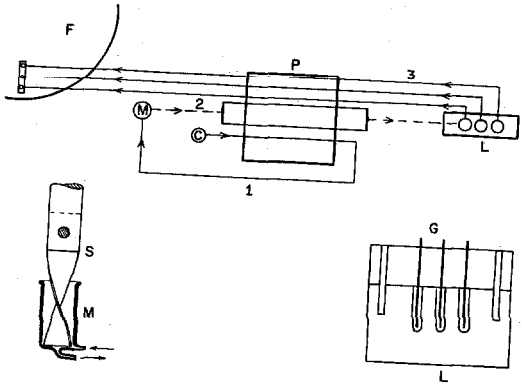

Figure 3.--Equipment for formation and fractionation of BSA gradients. The plastic tubing is 0.030" ID except for the dashed lines, which are 0.040". The pumping tubes were obtained from the Technicon Company. The stirrer blade S was fashioned from Teflon sheet 1.5 x 0.15 x 6.5 cm by twisting 180° over 5 cm. The stirrer is mounted with a Teflon pin on a grooved lucite rod, and rotated 150 rpm. The dimensions of the glass mixing chamber are 1.7 cm ID x 3.0 cm. The glass capillary tubes, G, 1.14 mm OD, 1.0 mm ID x 12 cm, were obtained from the Kensington Scientific Corporation, Berkeley, California (100λ Microcaps). The speed of the Technicon pump, model no. 1, was changed by a factor of 9/16 by exchanging sprockets 37V and 38V. This figure is a diagrammatic description of the apparatus and is not drawn to scale.

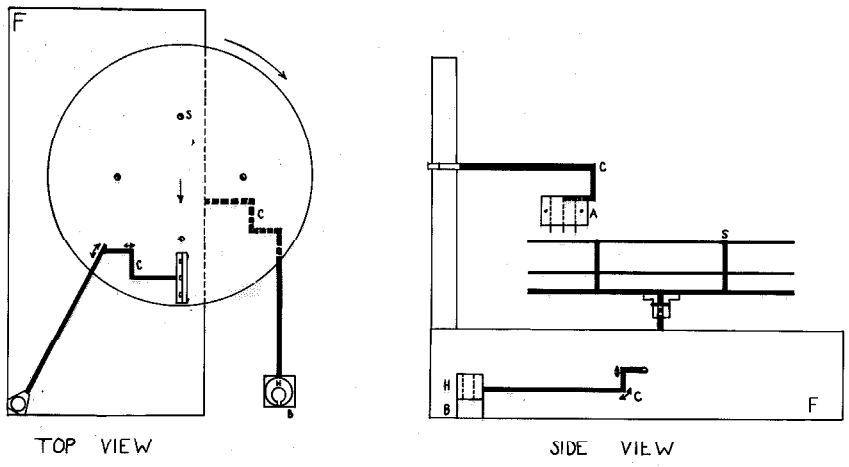

$\frac{1}{12}$" equals one inch

Figure 4.--Modified Gilson fraction collector, F, aluminum spacers with bolt S, mixing chamber holder, H, mixing chamber holder spacer block, B, and the lucite assembly, A. Both the mixing chamber holder and the lucite assembly are attached via contort clamps, C, to the fraction collector. Arrows indicate freedom and direction.

until it had been twisted 180 degrees over a distance of 5 cm. The first cm. of the sheet marred by the pliers was cut off. A hole was punched, as shown in figure 3, in the untwisted last cm. of the sheet. All edges were smoothed and slightly rounded with sandpaper. The stirrer blade was pegged to a lucite shaft. This shaft was in turn attached with a stainless steel collar to the shaft of a 150 rpm synchronous Bodine motor.

The mixing chamber is a small glass beaker with an inlet and an outlet at the base. The mixing chamber holder is a split cylinder of nylon into which the mixing chamber snugly fits. The nylon cylinder is mounted (figure 4) via a stainless steel connecting rod, a contort clamp, C, and an aluminum rod, to the base of the fraction collector. The spacer block is a cube of lucite fitted so as to level the assembly when slid underneath the holder.

The SW 39 tube holder, figure 5, consists of two lucite blocks, top and bottom, which are mounted on an aluminum assembly. The bottom block contains three holes for the SW 39 tubes. The SW 39 tubes contain 5 ml. and are 1/2" in cross-section and 2" in length. The bottom block is sandblasted everywhere except in front and back of the tube holes in order to eliminate stray reflections in the photography of the centrifuge tubes. Two stainless steel rods in the bottom block serve as guides for the top block to slide upon. The top block contains three guide holes for the glass capillaries, G (figures 3 & 5).

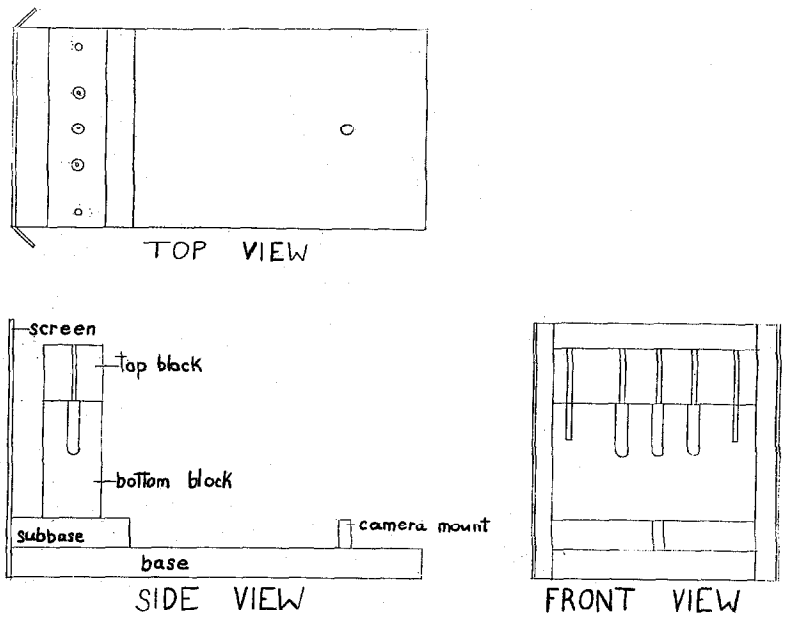

$\frac{1}{7}$" equals one inch

Figure 5.--Tube holder with screen and camera mount.

The bottom block is mounted on an aluminum sub-base, which in turn is mounted on a large aluminum base. A camera mount and a white aluminum screen are attached to the base.

The spiral test tube rack of the Gilson fraction collector was replaced by an equivalent rack constructed for small test tubes, figure 4. It is suggested that this tube rack be further modified to prevent the cracking of small test tubes by covering the base plate with 1/8" neoprene sheet.

The arrangement of tubing shown in figure 3 is most conveniently described in terms of the operation of the apparatus. Tygon tube 1, figure 3, filled and flushed with concentrated BSA, is connected to the inlet of the dry 5 ml. mixing chamber, M, provided with a motor driven Teflon stirrer, S. A 2.35 ml. volume of dilute BSA was pipetted into the mixer. Concentrated BSA from a container, C, usually a polyethylene vial, is pumped into the mixer and the mixed solution into the centrifuge tube mounted in the lucite blocks, L, of the SW 39 tube holder. The arrangement of Tygon tubes 1 and 2 is such that the output from the mixer is twice the input, the condition for the formation of a linear density gradient. Tygon tube 1 is a single 0.030" Technicon pumping tube with 0.030" extensions at both ends. The pumping tubes were pre-selected by the manufacturer. Tygon tube 2 starts as a 0.040" tube which at the pump is split into

two tubes by a glass Y. These two connecting tubes are 0.030" pumping tubes. On the other side of the pump, the two tubes are attached to another glass Y, which in turn is connected to a 0.040" tube. The BSA solutions were delivered to the bottom of the centrifuge tubes through a glass capillary tube. Filling requires 11 minutes and is stopped before efflux of the first bubble.

After centrifuging, the tubes were again mounted in the lucite block. Fourteen equal fractions and the remainder were pumped out layerwise through similar glass capillary tubes, connected to Tygon tubes, into 10 x 75 mm. test tubes in the fraction collector. The fraction collector was actuated at 1.4 minute intervals. Brushing of the Tygon delivery tubing against the test tube rim fractionates the last drop. The Tygon tubes rest in grooves milled into a lucite sheet, and are held in place by a lucite face plate which is screwed by wing nuts to the lucite sheet. This lucite assembly is attached via a contort clamp, C, assembly to a stanchion mounted in the base of the Gilson fraction collector. The volume of each fraction was $0.314 \pm .005$ ml. The volume of the fractions was determined by collection in a weighing bottle of the output during two minutes of operation of the Technicon peristaltic pump. This is 0.234 ml. of water per minute. The time for collection of each fraction was 1.35 minutes. The standard deviation of the fraction size was determined from absorbance measurements of collected fractions which

had been pumped by the Technicon pump. The colored mixture that was fractionated was composed of 15 ml. of a 20% albumin solution and 2 ml. of a 15% hemoglobin solution. The fractions were diluted with CO saturated water and read at 518 mμ (34), the CO- ferrihemoglobin isosbestic wavelength.

The manufacture and fractionation of the gradients along with the preparation of the BSA solution, the preparation of the cell samples, and the centrifugation of the gradients, were performed at 4°C.

C. Test Procedure for Linearity of the Gradient

The linearity of the gradients was tested at three stages: the ratio of the volumes of the influent and effluent Tygon pumping tubes, the linearity of the gradient entering the SW 39 tube, and the linearity of the gradient removed from the SW 39 tube before and after centrifugation.

The ratio of delivery of the influent to effluent Tygon tubes was measured by attaching glass capillaries to both tubes, filling the tubes with the appropriate solutions, and pumping the contents into weighing bottles for ca. two minutes. The volume of liquids in the weighing bottles was then determined from the weights and known densities of the solutions. The pumping ratios were first tested at

room temperature with water, then in the cold room with concentrated BSA and water, and finally, again in the cold room, with concentrated and dilute BSA. Steps one and two establish that the pumping ratio was independent of viscosity and that an adequate safety factor against back flow existed in the system. The ratios of the output to the input with water, concentrated BSA and water, and concentrated and dilute BSA were, respectively, 1.97, 2.06, and 2.01.

In figure 6, the results of the above tests of the linearity of the gradients are shown. The densities of each fraction were determined from the readings of a Zeiss Abbe refractometer with the relation $\rho_4^4 = 1.0540 + 1.543\ (N_{25}^D - 1.3670)$. The relationship was derived from the values obtained for refractive index and density of several solutions made during the testing of the machine (see figure 7).

D. The Advantages and Disadvantages of Bovine Serum as a Gradient Material

Bovine Serum Albumin (BSA) has the following advantages as a gradient material: Serum albumin is a normal constituent of blood. BSA has been used in culture media for human cells (35) and is therefore non-toxic and even thought to exert a protective effect on cells (36). Both rabbit (29) and duck erythrocytes (38) which have been

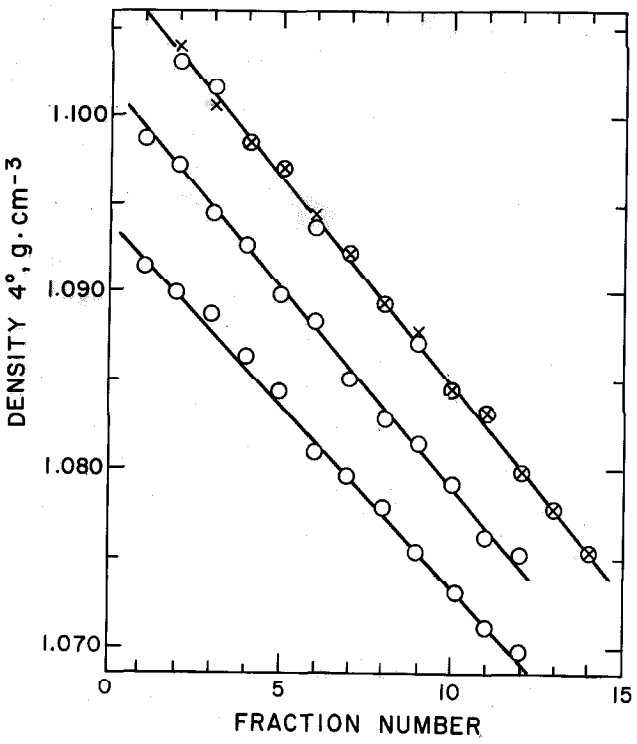

Figure 6.--BSA density gradients. Densities were evaluated from refractometer readings with the relation, $\rho_4^4 = 1.0540 + 1.543\ (N_{25}D - 1.3670)$. Upper line: solutions pumped directly from mixing chamber into fraction collector actuated at 0.70-min. intervals. Two separate experiments, O, X. The ordinate values are displaced upward by 0.0040 gm. cm.$^{-3}$. Middle line: collected from centrifuge tube; not centrifuged. Lower line: centrifuged. Different BSA solutions were used in these experiments.

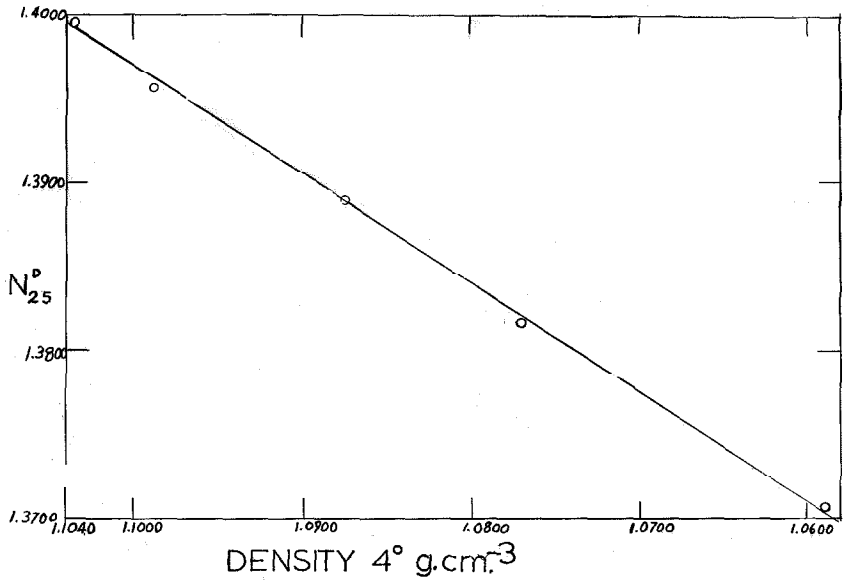

Figure 7. -- The relationship between density and refractive index of concentrated BSA solutions. The ordinate and abscissa are, respectively, the refractive index at 25°C and the density at 4°C of several BSA solutions.

fractionated in BSA gradients retain most of their capacity to incorporate amino acids into TCA insoluble material. The duck cells have also been shown to incorporate radioactive uridine into RNA (37). BSA solutions have previously been used in the neutral density separations of human erythrocytes (12, 20). Serum albumin is a good buffer at physiological pH, and has a low absorbance in the visible spectrum. BSA has the following two disadvantages: concentrated solutions are viscous and the density of the protein is only ca. 1.3 g. $cm.^{-3}$. The maximum density of the most concentrated solution which can be conveniently used for the formation of linear gradients is $\rho_4^4 = 1.10$.

Preparation of the BSA Solutions

Bovine albumin powder, fraction V, purchased from Armour and Company, Chicago, was used throughout this work. The dry powder, Armour Lot X20008, according to the analysis supplied by the manufacturer, contained: 99% albumin (by electrophoresis), 2.65% water, 1.60% ash, not more than 500 ppm heavy metals, and gave a pH of 4.98 upon solution in water. The concentrated BSA solution was prepared as follows: 108 g. of the powder was layered on 200 g. of water containing 50 g. of Amberlite MB-3 resin in a one-half gallon polyethylene refrigerator container provided with a magnetic stirring bar and a tight lid. The mixture was stirred in the

cold. The container was tapped lightly every few hours as needed to bring the BSA powder into contact with liquid, and finally was tilted to wet the remaining powder on the walls. The solution decanted from the resin was centrifuged at 1000 rpm in 250 ml. centrifuge bottles, and decanted into another centrifuge bottle which contained 25 g. of resin. The suspension was intermittently agitated over a two-hour period and then centrifuged in stainless steel tubes for two hours at 20,000 rpm in the Spinco 30 rotor. The top layer of the solution from each tube was removed with a Pasteur pipet and discarded. The solutions were pooled in a tarred vessel.

The following salts were added per 100 g. of deionized BSA solution: 0.2391 g. Na_2CO_3, 0.3030 g. NaCl, 0.1124 g. $MgCl_2 \cdot 6H_2O$, 0.0286 g. KCl. The above mixture neutralizes the BSA, and provides the cation composition and the osmolarity of NKM (29) as calculated for the ca. 67% by weight water present in the BSA solution. The densities of the final solutions were $1.104 \pm .001$ g/ml. From dry weight determinations on one of these BSA solutions, the density of a buffered 33.3% BSA solution was calculated to be 1.1007. The 1.104 g/ml. solutions are actually 63.5% by weight water. The pH determined with pH paper was at 6.8 to 7.2. The dilute solutions were made up by weight assuming additive volumes. All solutions were stored at -60°C in small polyethylene containers. The solutions

were thawed and rethawed as needed in water at room temperature. It was found that the storage of the BSA solutions at 2°C for one week or more caused a substantial shift in the red cell density distribution towards higher density.

The BSA solutions for the study of the effect of salt concentration on buoyant density were prepared from deionized concentrated BSA with $\rho = 1.103$ by addition of 0.106 ml. of a salt solution (12.5 g. KCl and 49.13 g. $MgCl_2 \cdot 6H_2O$ per 100 ml.) to 100 g. of BSA solution containing 0.2391 g. of Na_2CO_3. This stock solution now contains the same cation proportions as NKM and has 40.4% of the osmolarity, assuming here that the BSA is inert. A 25 times concentrated NKM solution was added to aliquots of the stock solution to obtain solutions ranging from 80% to 120% of the osmolarity of NKM. The concentrated solutions were diluted with NKM solutions of the corresponding osmolarity to form the dilute BSA solutions.

In the aging experiments and cytological studies, a mixture of solutes approximately the same as Eagle's saline was introduced into the deionized BSA. Eagle's saline was derived, apparently, by Brecher et al. (38) from Eagle's (39) tissue culture minimal media. This change in buffer was made to facilitate future work with less hardy cell types. The BSA-solute mixture was prepared by addition of 100 g. BSA solution to 0.5 ml. of a concentrate obtained by

evaporation under dry nitrogen of 13.33 ml. of Eagle's saline carbonate (see table 1). The mixture was stirred overnight and remixed with the residual BSA in the weighed container. Finally, 0.261 ml. each of 54 g/100 ml. $CaCl_2$ and 45 g/100 ml. $MgCl_2$ were added. The pH of the concentrated BSA was 6.8. The dilute BSA was prepared by adding a modified Eagle's saline solution. This solution was prepared by titrating Eagle's saline (see table 1) into Eagle's saline chloride, a solution of the same composition as Eagle's saline except for the substitution of additional NaCl for $NaHCO_3$ and the addition of antibiotics to a pH of 6.8.

All chemicals were reagent grade. The water was redistilled in glass. Sterile Alsever's (40) solution was supplied by Delco Chemical Company, Glendale, California.

E. Application of the Cells

Three drops of blood obtained by finger punch were dripped directly into 0.4 ml. of Alsever's solution. Within 20 minutes, 0.30 ml. of this suspension was layered onto the density gradient column in a thickness of 0.25 cm. with a 1 ml. serological pipet. The applied sample contained ca. 5×10^8 cells and ca. 15 mg. of hemoglobin. In the aging experiments, four drops of rabbit blood obtained by slitting a marginal ear vein were dripped into ca. 2 ml.

TABLE I. The Composition of Eagle's Saline and Related Solutions

	Eagle's Saline	Eagle's Saline Carbonate	Eagle's Saline Chloride
	g./liter	g./liter	g./liter
NaCl	6.20	16.56	7.59
Na_2CO_3	----	25.10	----
$NaHCO_3$	2.00	-----	----
$NaH_2PO_4 \cdot H_2O$	0.13	0.74	0.13
KCl	0.36	2.08	0.36
$CaCl_2$	0.18	----	0.18
$MgCl_2 \cdot 6H_2O$	0.15	----	0.15
dextrose	0.90	5.23	0.90
streptomycin sulfate	----	2.92	0.50
	units	units	units
penicillin SK	----	500,000	100,000

of Alsever's solution. The cells were packed in a clinical centrifuge, freed of most of the supernatant fluid by decantation, spun again, and the remaining fluid absorbed into a wad of tissue. The pellet was first dispersed and then blended with a Vortex mixer into 3 ml. of the dense BSA solution. This BSA solution containing the cells was used to prepare the density gradient. As discussed in section III-C, this initial distribution of cells in the gradient column reduces the contamination of the light layers by cells which are driven to the cylindrical walls by the radial field as compared with the introduction of the cells as a layer on top of the gradient column.

F. Centrifugation

The SW 39 tubes were spun in a precooled SW 25 rotor fitted with special nylon adapters in a model L Spinco ultracentrifuge at 20,000 rpm for 60 minutes at ca. 4°C. In preliminary runs in the SW 39 rotor, the results of swirling were observed in a "corkscrew" pattern of red cells near the bottom of the tube. The swirling was substantially reduced by using the heavier rotor and reducing both the acceleration and deceleration as recommended by de Duve et al. (25). The current in the drive circuit and the speed control circuit of the model L ultracentrifuge were adjusted so that the acceleration could be controlled manually from rest. Deceleration was reduced

by the use of the heavier rotor, which also reduces surges in acceleration. A routine program for centrifugation was followed. The speed selector was increased in increments of 500 rpm every 2,000 divisions on the odometer up to 3,000 rpm, in increments of 250 rpm each minute up to 5,000 rpm, and directly to 20,000 rpm.

After one hour of centrifugation, the speed selector was turned to zero. The time selector had been set so that the brake would not be turned on and the rotor was allowed to coast to a stop without braking .

The above procedure substantially decreased the amount of swirling but did not entirely eliminate it. However, the above procedure required manual control of the acceleration of the centrifuge and, as evidenced by the residual swirling, did not sufficiently slow the deceleration of the rotor. Hogeboom and Kuff (41) have recommended the use of a small bucking potential to slow the deceleration of the rotor. The swirling was almost entirely eliminated by the use of an electrical device which semiautomatically programmed the acceleration and deceleration of the centrifuge and provided a suitable bucking potential to slow the deceleration below 3500 rpm. This device regulated the current which, after amplification by a Thyratron tube, is the drive current. The device and an ammeter to monitor the drive current were installed by the Spinco Field Service Engineer.

This electrical device consisted of a bank of resistors which are sequentially added in parallel by a Minarix timer, model number 6CBR-B-120M. The Minarix timer consisted of a clock motor which made a revolution every two hours. Six adjustable cams mounted on the drive shaft of the motor activated six micro-switches. The wiring diagram of the circuits of the device is presented in figure 8. All of the circuits except 6 and 7 are added in parallel by the microswitches. Microswitch 6 is normally closed and wired in series. When it is activated, the circuit to the Thyratron tube is broken. Rheostat 7a and resistor 7b are wired together in series and in parallel to circuits 1 through 5 and resistor 7.

Table 2 summarizes the program of the timer. After the rotor is inserted into the centrifuge, the door is left open. The speed selector is set at 4500 rpm, the maximum allowable for open door operation of the machine. The resistance of rheostat 7a is then adjusted so that the rotor is just short of starting rotation. The Minarix timer is started and closes microswitch 1. The current flowing through resistor 1 very slowly accelerates the rotor. One minute after resistor 2 is added, at 140 rpm, the onset of the natural precession of the drive used for these experiments begins. Because the precession absorbs power, resistor 2a is manually switched on for about one minute until the precession has stopped, 250 rpm. The

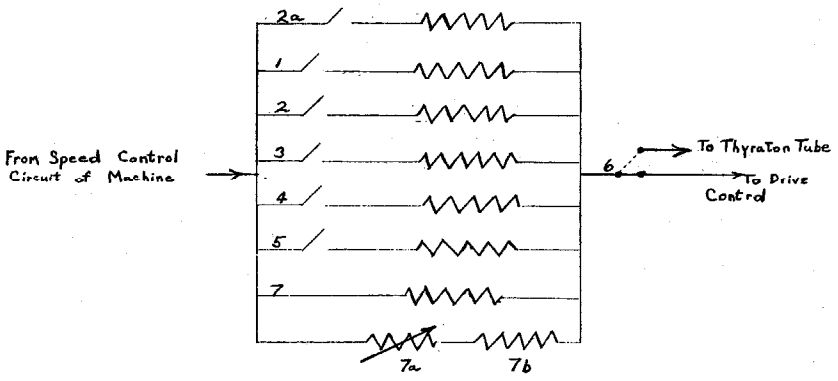

Figure 8. -- Wiring diagram of the circuits of the acceleration and deceleration programmer. Numbered circuits 1, 2, 3, 4, 5, and 6 are actuated by the six micro-switches of the timer. The switch in circuit 2a is manually actuated as indicated in the text and table 2. The values of the resistors and rheostat 7a are given in table 2.

TABLE II

Electrical Acceleration Control

Resistor number	Ohms	Percentage of timer cycle completed when micro-switch is activated	inactivated	Drive current in amperes	RPM at end of period	Normal mode of micro-switch	Comments
1	75,000	0	35	2.3	100	open	
2	50,000	2	"	2.9	700	"	
2a	150,000	3	4	3.1	250		manually opened by auxiliary switch
3	40,000	8	35	3.4	2,800	"	
4	50,000	18	"	3.7	5,000	"	
5	0	28	78	--	20,000	"	
6	circuit broken	78	98	1.0	3,500	closed	wired in series
7	60,000	---	---	1.9	0	---	wired in parallel to the other resistor circuits
7a	0-500,000	---	---	1.9	0	---	
7b	50,000	---	---	1.9	0	---	rheostat 7a and resistor 7b are wired in series

door of the Model L Ultracentrifuge is then closed and the speed selector advanced to 20,000 rpm. The Model L Ultracentrifuge could then be left until just before the end of the period of the timer, which occurs when the SW 25 has accelerated to 3,500 rpm. The Minarix timer was then switched off and turned so that all the micro-switches were open. With all the switches open, the timer has been returned to its starting position. The only current to the Thyratron tube is through resistors 7 and 7b and rheostat 7a. As previously stated, rheostat 7a had been adjusted so that the current was just short of being capable of starting rotation. Prior to the cessation of the rotation of the rotor, a low frequency oscillation of the ammeter occurs. The rotor is stopped when the oscillation disappears. In order to avoid any possibility of causing a sudden stoppage in rotation, rheostat 7a is slowly adjusted to its maximum, 500,000 ohms. The door of the centrifuge can now be opened and the rotor removed. This centrifuge program, or one based on the appropriate feedback from the rate generator of the ultracentrifuge, should be of use in sucrose gradient centrifugation.

In the aging experiment and for the cytological studies, the SW 39 tubes were spun in a precooled Serval HS, Field Aligning rotor fitted with special nylon adapters in an unmodified Serval model RC-2 centrifuge. The buoyant density distributions obtained

with the Serval combination (table III in section III-C and figure 35 in section VI-E) were substantially the same as those obtained with the electrically controlled Spinco rotor and centrifuge combination. No corkscrew pattern of red was ever observed with the Serval combination. The Serval rotor is accelerated to 5000 rpm in ten minutes by gradually increasing the setting of the speed control. The acceleration to 500 rpm took about 3 minutes. The natural precession of the Serval HS rotor occurred between 500 and 1000 rpm, and thus at a greater field strength than that of the SW 25, which occurred at 140-200 rpm. The precession of the Serval rotor is accompanied by a vibration of the whole centrifuge. The Serval HS rotor was allowed to decelerate without braking. No bucking current was used to slow the deceleration of this rotor.

The buckets of the Serval HS rotor are mounted on a universal joint, and thus can align with the sum of the outward centrifugal force and the sideward forces due to acceleration or deceleration. This sum of forces is the force effective on the gradient. The bucket mounts of the HS rotor were lightly greased with molybdenum disulfide lubricant.

G. Density Measurements

Densities were measured in a 0.224 ml. pycnometer made by removing the overflow bulb and drawing out both ends of a 0.3 ml. micropipet. The pycnometer was completely filled by suction, with a side tube and pinch clamp in the suction line. A tygon tube mounted in a Sigmamotor Peristaltic Pump served as the suction line. The pump was provided with a reversing switch. The volume of the pycnometer was determined with water with a precision of $\pm 5 \times 10^{-5}$ ml. The standard error in the determination of the density of the BSA solutions was $\pm$ 0.00045 g. cm.$^{-3}$. Gas bubbles formed in the BSA solutions upon filling the pycnometer. These rose to the top of the pycnometer and were drawn into the suction line after 5 to 20 minutes. All densities were determined between 22° and 26°C and were corrected to 4°C, the temperature at which the density distribution experiments were actually performed.

The thermal expansion of a dilute $\rho_4^4 = 1.0725$ g. cm.$^{-3}$ and concentrated $\rho_4^4 = 1.1056$ BSA solution was determined by dilatometry with a slightly modified twin capillary pycnometer which has been described by Lipkin et al. (42). This pycnometer or dilatometer, which consists of two parallel graduated capillaries joined by a 5 ml. bulb, was modified by bending the end of one of the capillaries ca. 150° and tapering it to a point. The uniformity of the bores of the

dilatometer was tested and found to be satisfactory by comparing the observed increases in volume of water contained in the dilatometer, the sum of the graduations of both capillaries at their menisci, with the actual volume of water as determined from the increases in weight (figure 9). The thermal expansion of water was measured (figure 10) and found to be in good agreement with the data in the literature(43).

The BSA solutions were equilibrated at 37°C for 30 minutes prior to filling the dilatometer. Filling was accomplished by pumping the BSA solutions into the dilatometer with a Sigmamotor peristaltic pump. The solutions were successively equilibrated in constant temperature baths, each equipped with a calibrated precision thermometer. The baths and thermometers were kindly made available by Dr. John F. Catchpool. The 4°C and 0°C determinations were performed in the cold room. Beakers filled with distilled water and with crushed ice and distilled water served as constant temperature baths. The thermal expansion of the two BSA solutions is shown in figure 11.

Densities obtained at room temperature were first corrected to 24°C with a thermal coefficient of expansion, 0.0003 g. cm.$^{-3}$. The 24°C densities were further corrected to 4°C with an expansion coefficient obtained by linear interpolation between the values 0.00024 g. cm.$^{-3}$ °C^{-1} for $\rho_4^{24} = 1.0667$ and 0.00029 g. cm.$^{-3}$ °C^{-1} for $\rho_4^{24} = 1.0999$.

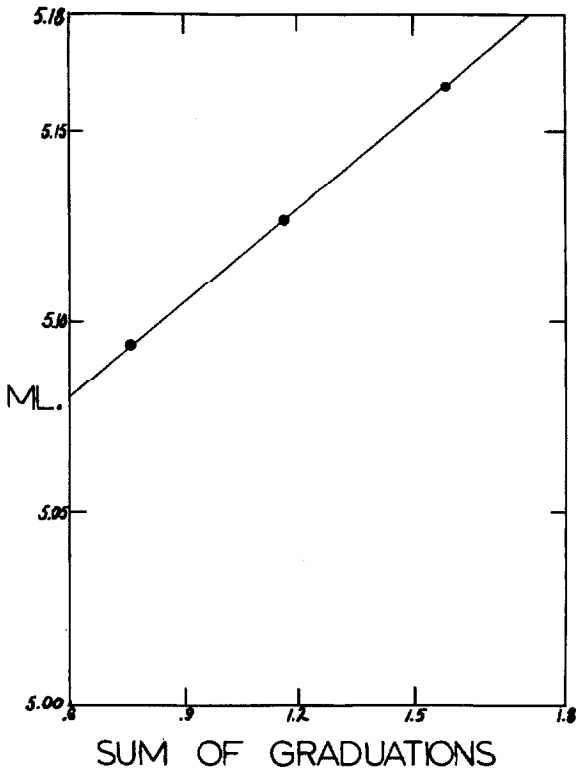

Figure 9. --Test of the uniformity of the bores of the dilatomter. The ordinate and abscissa are, respectively, the volume of water determined from the weight of the filled dilatometer and the sum of the graduations of both capillaries at their menisci.

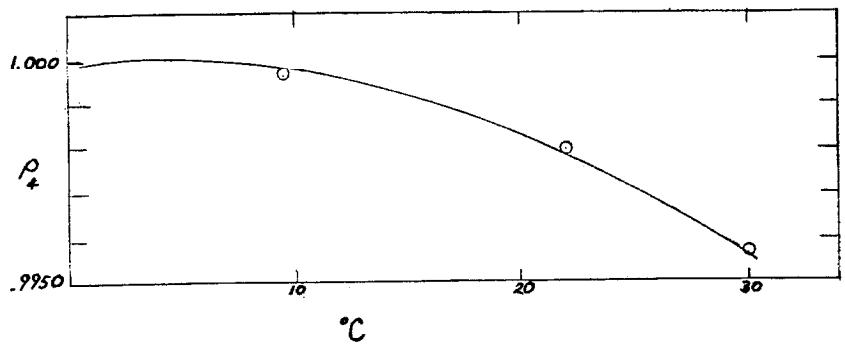

Figure 10.--The measurement of the thermal expansion of water with the dilatometer calibrated in figure 8. The line was drawn with values obtained from the literature.

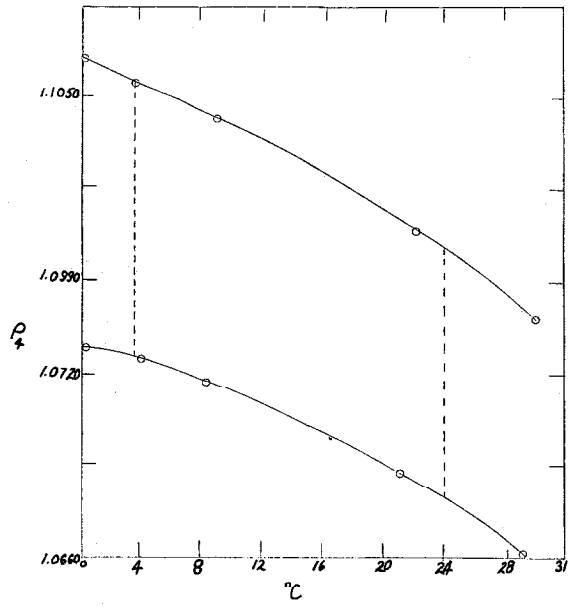

Figure 11.-- The thermal expansion of two BSA solutions. The solid lines connect the experimental points. The dashed lines connect the densities of the two solutions at 4°C and 24°C.

H. The Determination of the Absorbance Profile

The cells were lysed by adding 2.5 ml. of CO-saturated distilled water, inverting the tubes a few times, and stirring with a Vortex mixer for 30 seconds. The lysates were centrifuged at low speeds to remove debris and read at 518 mμ (34) in a Zeiss PMQ spectrophotometer. The results were corrected for the absorbance of the BSA in the fraction. The cells that remained at the bottom of the SW 39 tube were dispersed with the Vortex mixer in a known amount of water, transferred to a test tube, stoppered, and again stirred with the mixer. This method of lysis did not completely free the pelleted cellular debris of hemoglobin. As much as ten per cent of the absorbance is pelleted with the debris. This is probably due to the binding of hemoglobin by the cell walls, ghosts, rather than incomplete lysis of the cells. However, this binding of hemoglobin does not affect the position of the density distribution as a control wash or further lysis of the pellets revealed no density selective binding of absorbance.

In the aging experiment, the fractions were first diluted with CO-saturated NKM solution and spun in a clinical centrifuge. The supernatant solution was decanted and the cells lysed with 2.5 ml. of 0.05 μg/ml. saponin solution. This lysin evidently solubilizes the

cell walls. No pelleted material was observed after centrifugation.

I. The Determination of the Distribution of Cell Volumes

Volume distributions of human erythrocytes were determined by electronic sizing with a Model B Coulter-Counter according to Brecher et al. (38). The flow of small nonconducting objects such as cells through an orifice channel across which a voltage has been applied causes fluctuations in this voltage. The Counter-Counter counts and measures these voltage fluctuations. Approximately 500 volts are applied across the orifice channel by platinum electrodes. The orifice, according to the manufacturer's specifications, is a cylindrical hole 100 μ in diameter and length. The change in resistance ΔR due to the presence of a cell in the orifice channel is given in the manufacturer's literature (44) as:

$$\Delta R = \frac{\rho_o v}{A^2} \cdot \left(\frac{1}{\frac{1}{1 - \rho_o/\rho} - \frac{a}{xA}} \right) \qquad (1)$$

ρ_o = electrolyte resistivity

A = aperture area normal to axis $\pi \frac{D^2}{4}$

v = particle volume

ρ = particle effective resistivity

a = particle area normal to aperture axis

x = $\frac{\text{length parallel to aperture axis}}{\text{diameter of equivalent sphere}}$

The term in parentheses, which is the correction due to factors other than cell volume, is small and can be ignored. Substitution of the known or estimated numerical values of the quantities in this term shows it to differ by less than 2% from unity. The values of the following quantities were obtained from Ponder's monograph ($\rho_o/\rho = 0.02$ (45), $x = 1.10$, and $a = 50\ \mu^2$. The area of the orifice channel calculated from the diameter is $7850\ \mu^2$.

Two types of measurements were made with the Coulter-Counter. In the first, the total number of cells per unit volume was obtained by passing a calibrated volume of a cell suspension through the orifice and noting the number of voltage fluctuations generated. In the second of measurement, the cell suspension is passed through the orifice at a constant rate of flow and the number of cells in twenty-five successive size ranges counted. These size ranges or "windows" correspond to increments of 6.9μ. The number of cells in each of the size ranges is presented in analogue form on a recorder. To obtain volume distributions, these analogue values were reconverted to numerical form.

The Coulter-Counter B used for these experiments was kindly made available by Dr. C. M. Pomerat of the Pasadena Foundation for Medical Research.

The use of this instrument is further described in section VI-A of this thesis.

III. BUOYANT DENSITY DISTRIBUTIONS OF HUMAN ERYTHROCYTES

A. Buoyant Density

The term buoyant density has been used previously (46) to specify the density of a macromolecule as the density of the fluid in which the macromolecule is neutrally buoyant at the temperature, pressure, and activity of water in the buoyant medium. The buoyant density of erythrocytes similarly depends on these factors and probably also on the factors regulating transport across the cell wall.

The pressure at which the cells come to rest is not known because the cells may move in the gradient column due to the pressure decrease that accompanies deceleration. However, this movement of the cells should be minimal. The pressure dependence of the buoyant density of a species depends (46) on differences in compressibility and preferential solvation between the buoyant species and medium. These differences should be small for the suspending BSA solution and the buoyant cells as they both have approximately the same content of salts, water, and protein.

The osmolarity of the two solutions used in the preparation of the density gradient columns was the same. The activity of water is thus expected to be constant throughout the column except for the small effect of the gradient in BSA concentration, which in turn will affect the activity coefficients of the small molecules present. The presence of BSA in these columns does not appreciably contribute to

the osmolarity of the solutions. The extent of this contribution by the BSA will be discussed in section III-L.

B. The Buoyant Density Distribution

Reproducible, approximately bell-shaped profiles of absorbance have been obtained from the blood of five human donors and three rabbits. In the case of one of the humans, R. C. L., a significant fraction of the cells was denser than the maximum density in the column and appeared at the bottom of the tube.

In the course of this work, the density gradients and the total number of cells applied varied from experiment to experiment. The data were appropriately normalized to eliminate the effect of these two variables in the distribution function, $F(\rho)$. The distribution function $F(\rho)$ includes the term $1/g_o$, the reciprocal of the total quantity of material under study, and thus is independent of the total concentration of red cells. This distribution function, $F(\rho) = 1/g_o \; dg/d\rho$, is also independent of the magnitude of the linear density gradients and consequently the density range per fraction. The plot of the distribution function against buoyant density provides a graphical presentation of the normalized data. The total area under the curve is unity, and the area between any two abscissas represents the fraction of material possessing buoyant densities in the indicated range.

Because volume fractions were collected in these experiments, the distribution function is reformulated in terms of volume, V, $F(\rho) = (1/g_o)(dg/dV)(dV/d\rho)$. The derivatives are approximated by the integral values obtained from each volume fraction, $F(\rho) = (1/g_o)(\Delta g/\Delta V)(\Delta V/\Delta \rho)$, where Δg and ΔV are, respectively, the amount of material and the volume of each fraction. The quantity $\Delta g/\Delta V$ is obtained by measuring the amount of material in each fraction; the materials considered were absorbance, radioactivity, and the number of cells. The value of $\Delta \rho/\Delta V$, the density range per fraction, was a constant as the volumes of the fractions were equal and the gradients linear. The value of this quantity was obtained by averaging the densities of a light, a medium, and a dense fraction, as explained below.

C. Artifacts Due to Centrifugation in Tubes with Parallel Walls

Before the calculation of the gradient can be accomplished, the artifacts due to centrifugation in parallel-walled, cylindrical tubes must be discussed. The walls of the cylindrical tube are not radii of the centrifugal field. The cells, like all other species, move in the direction of the radii of the centrifuge rotor. The cells which do not encounter the walls of the centrifuge tube during centrifugation reach equilibrium positions in the lamellae of the solutions which are

buoyant. The travel of cells which are driven to the tube walls by the radial field still stops at their equilibrium position in the direction of the centrifugal field, i.e. at the position of the buoyant solution. These cells are, however, not uniformly distributed in the corresponding cylindrical surfaces or lamellae. The cells which have struck the walls are concentrated near the walls, thus resulting in a nonuniform concentration distribution of cells in the cylindrical lamellae. Two forces act to restore a uniform distribution in the cylindrical lamellae: one is diffusion and the other is the swirling of the tube contents which occurs during acceleration and deceleration.

The human erythrocyte is 30% by weight hemoglobin and contains 30 $\mu\mu$g of this protein; therefore, it weighs 100 $\mu\mu$g, or 6.02×10^{13} Daltons. If the erythrocytes are assumed to be spheres in a BSA solution, $\rho = 1.08$ g. cm.$^{-3}$, or 20 centipoises viscosity, at a temperature of 4°C, the diffusion coefficient is calculated (47) to be 1.4×10^{-12} cm.^{2}/sec. The Brownian movement of the cells in concentrated BSA solution was observed microscopically in this investigation, and in agreement with the very small diffusion coefficient was not clearly detectable. The Brownian movement is, therefore, too weak to have any significant effect on the distribution of the cells.

The redistribution in the tangential direction due to swirling is a very complicated process. However, the data obtained in the early experiments (Table III-a, exp. 3-123a, b, c) with cells from the blood of R.C.L., where swirling of the erythrocyte distribution was visually observable, suggest that swirling loosens the cells which are packed against the walls of the centrifuge tube. Limited swirling probably is still more of a liability than an advantage, as it decreases the resolution of the system.

It can be shown (33, 48) that approximately 25 per cent of the contents of a parallel wall SW 39 centrifuge tube in an SW 25 rotor will be driven to the walls of the tube during sedimentation. This is the fraction of the tube volume which would be eliminated if the walls of the tube were made radial.

A summary of some of the results of the erythrocyte distributions is given in Table III. Two quantities related to the problem of centrifugation in parallel walled centrifuge tubes are presented in Table III. The first of these quantities is the percentage of the total absorbance which appears at lighter densities and is higher in absorbance than the minimum at the less dense side of the bell-shaped distribution. This quantity will be referred to as the tail of the distribution. This material is a result of the cells being driven to the walls during sedimentation. The second quantity is the ratio of the density range between fractions 7

and 12 to that between fractions 2 and 7. The gradients were always linear when measured in the absence of cells; however, the presence of cells, and consequently of the light tail, caused a slight nonlinearity of the gradients. The above two quantities will subsequently be referred to as the tail and the ratio, respectively.

A third new quantity which is not related to the two above, but, however, is necessary to the discussion, is the midpoint of the distribution. The midpoint of the distribution is an average density which reproducibly describes the position of the distribution. The method for determining the midpoint will be discussed in the next section of this thesis.

Most of the experiments presented in Table III are with cells obtained from the blood of R. C. L. The experiments marked with an asterisk were performed with gradients made from the same two BSA solutions. In all of these experiments, the relationship between density and the distance from the center of rotation, R, is the same. The average values for the tail and the ratio in the experiments in Table III-a with the same BSA solutions are, respectively, (9.3 ± 3.6) and $(0.86 \pm .09)$. These values indicate larger artifacts than those in Table III-b (7.5 ± 1.5) and $(0.91 \pm .08)$ obtained from the distributions of bloods from the other donors. The cells from R. C. L., as shown by the average of the midpoints 1.0836 g. $cm.^{-3}$, Table III-a, band at a greater distance from the center of rotation

TABLE III. Tails, Ratios[a], and Midpoints of Buoyant Density Distributions

IIIa: Exp.#	% Tail	Ratio	Midpoint	Donor
117	4.0	0.84	1.0840	R.C.L.
*123a	4.4	0.79	1.0838	"
*123b	3.5	0.84	1.0835	"
*123c	8.0	1.00	1.0829	"
**129a	10.3	0.88	1.0830	"
**129b	11.4	0.74	1.0844	"
**129c	5.4	0.77	1.0828	"
*135a	14.5	0.77	1.0839	"
*135b	11.0	0.72	1.0835	"
*135c	9.6	0.87	1.0836	"
*139a	14.4	0.85	1.0840	"
*139b	9.1	1.00	1.0839	"
*139c	9.3	0.86	1.0837	"
av.	9.3±3.6	0.86±.09	1.0836±3x10^{-4}	

*These experiments were averaged.
**Discarded: Siliclad treated.

IIIb:				
*143	7.2	0.83	1.0807	W.R.H.
*143	7.3	0.79	1.0814	"
*145	8.9	0.85	1.0814	A.S.
*145	7.3	0.91	1.0806	F.W.
*145	10.6	1.01	1.0801	"
*149	5.9	0.93	1.0812	W.G.
*149	5.7	0.90	1.0811	"
*149	6.9	1.06	1.0802	A.S.
av.	7.5±1.5	0.91±.08	1.0808±4 x 10^{-4}	

IIIc:				
101	9.9	0.94	1.0850	†R.C.L.
117	1.8	1.12	1.0841	†‡ "
115	6.3	1.12	1.0790	†‡rabbit 63
115	3.2	0.80	1.0767	†‡ " 64
	5.3±.9	1.00±.14		

†Cells blended into dense BSA solution. Experiments performed with the Serval rotor and centrifuge combination.
‡BSA solutions derived from Eagle's saline.

a $\dfrac{\rho_4^4 7 - \rho_4^4 12}{\rho_4^4 2 - \rho_4^4 7}$

than the cells obtained from other donors, with midpoints close to 1.081 g. cm.$^{-3}$. Therefore, as expected, the magnitude of the artifacts, the tail and the ratio, associated with centrifugation in parallel walled tubes, increases as the average distance sedimented through the gradient column increases.

In another series of experiments, Table III-c, distributions were also obtained with cells from R. C. L. and two rabbits; however, the cells were suspended in the dense BSA solution used in formation of the gradients. The values of the tail and the ratio of these distributions where most of the cells sedimented toward the center of rotation indicate smaller artifacts. They are, respectively, $(5.3 \pm .9)$ and $(1.00 \pm .14)$. This procedure does not eliminate the tail or the nonunity value of the ratio in all experiments because some of the cells are still initially distributed at densities lower than buoyancy and undergo radial spreading during centrifugation.

Both the tail and the nonunity value for the ratio are not due to simple adhesion of the cells to the walls of the "Lusteroid" SW 39 centrifuge tubes. Three experiments were performed in "Lusteroid" tubes which had been heavily coated with "Siliclad," a silicone preparation that reduces the adhesion of cells to surfaces coated with it. The "Siliclad" treatment did not decrease the tail or cause the ratio to approach unity. The results obtained were

non-reproducible and were neglected in taking the averages in Table III-a.

D. Channeling During Fractionation of the BSA Gradient Columns

The cells which have been concentrated at the walls of the centrifuge tube increase the viscosity of the suspending BSA solution. When the contents of the tube are sampled, this concentrated solution tends to remain at the walls, and thus is not included in the appropriate density fractions. This concentrated solution is finally either washed from the tube walls by the meniscus of the gradient column or the density difference becomes large enough so that the solution at the walls collapses into the rest of the liquid column. Experimentally, it is observed that the top of the gradient column, which is clear of red material before fractionation, becomes streaked with red during the last quarter of the fractionation. The distribution of red cells in the test tubes which contain fractions 12 or 13 through 15, unlike that of the other fractions, is uneven. The dense contaminating red BSA solution is concentrated at the bottom of these test tubes.

Not only does channeling introduce an artifact into the erythrocyte distribution, it also complicates the calculation of the

density gradient. The contaminating BSA solution referred to above is not included at its density in the first seven fractions; therefore, these equal volume fractions span a greater part of the density gradient than they should. Thus, the density of the seventh fraction is lower than it should be. Conversely, the next five fractions include most of this viscous dense material which increases the density of the twelfth fraction. Probably, the nature of the contaminating process is more continuous than described above.

E. Procedures for Minimizing the Effect of the Tail and the Nonunity Value of the Density Gradient Ratio

The artifact due to the tail can be circumvented by ignoring these points and when distributions are to be compared, by truncating the distributions at some minimal concentration of material. The artifact of a larger density range in fractions 2 through 7 as compared with 7 - 12 cannot be as easily treated. However, an averaging procedure, which is successful in that it compensates for this artifact at least to the degree that reproducible average positions of the distributions can be obtained, has been developed. The density range per fraction was obtained as the average of the ranges obtained between the second and seventh, and the second and the twelfth fraction. The density of each fraction was evaluated from

that of the second fraction and the density differences per fraction. Greater weight was given to the second fraction because it is least affected by the above drainage errors.

F. An Optimal Shape for a Preparative Centrifuge Tube

It should, at least from the viewpoint of the author of this thesis, be easier to build sector-shaped tubes than to investigate thoroughly the effects of centrifugation in nonsectorial-shaped tubes.

Just recently, the Spinco Corporation has manufactured sectorial shaped tubes. But because of the small capacity of these tubes, 1.2 ml., they were unsuitable for the BSA fractionation of cells. The small capacity of the tubes could be easily remedied. These tubes are similar in shape to the sector-shaped center pieces used in analytical centrifugation. This shape with four flat walls is not the optimal shape for preparative centrifugation. A centrifuge tube that starts as an ellipse and finishes as a circle at the bottom is what is needed. The radius of the circle and the major axis of the ellipse are equal. The minor axis of the ellipse at any distance from the center of rotation is equal to $\frac{R}{R_b} \cdot r$, where the quantities R, R_b, and r are, respectively, the distance from center of rotation, the distance from the center of rotation at the bottom of the tube, and the radius of the tube at its bottom.

G. The Midpoint of the Distributions

In order to compare the displacements in density among the approximately symmetrical distributions, figure 12, it is desirable to select an average position which in turn corresponds to an average density. This average should contain as many reliable experimental data as possible, and should weight each according to its reliability. Any average incorporates a weighting factor. If this factor is unity for all terms, then each term will have been equally weighted. The average density is represented by the summation $\frac{\Sigma\, Yi \cdot \rho}{\Sigma\, Yi}$, where the Yi's are the weighting factors. In order to maximize the repeatability of the average density, weighting factors proportional to the reliability of the points at a given density should be employed; in the next section, a study of the precision of the individual points will be presented (Table 5). In brief, it was found that only points with values of $F(\rho)$ greater than or equal to twenty were reliable. All points with $F(\rho)$ values greater than twenty had approximately the same precision, $\pm$ 10%. In these experiments, a more continuous distribution of absorbance could not be obtained because of the 0.224 ml. volumes required for the density determinations. The distributions are presented as histograms made up of 15 points that are connected by smooth curves.

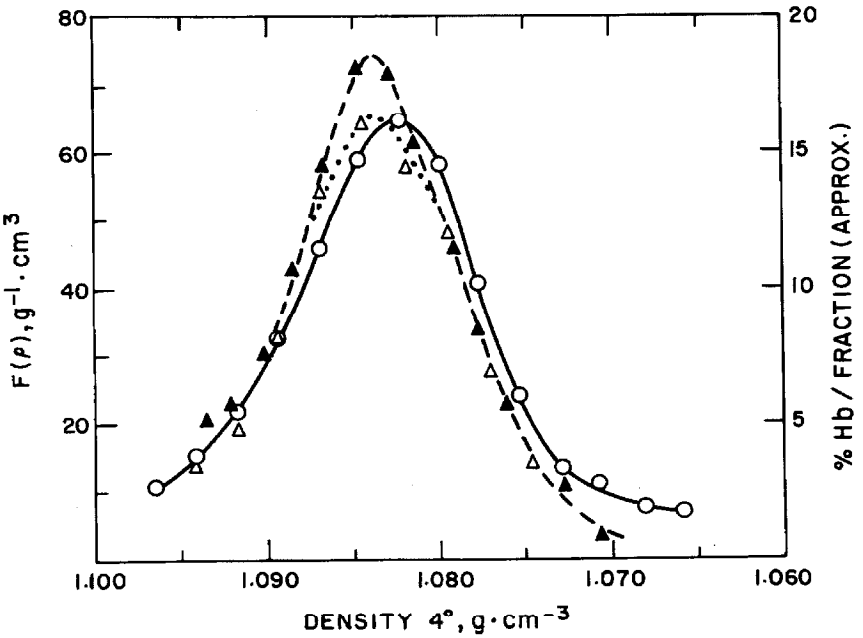

Figure 12. -- Buoyant density distributions of erythrocytes from R.C.L. Three separate experiments.

The three most frequent averages used to represent distributions are the mean, $\frac{\sum_{1}^{15} F(\rho)\cdot\rho}{\sum_{1}^{15} F(\rho)}$, the median, ρ_m, at $\frac{\sum_{1}^{\rho_m} F(\rho)}{\sum_{1}^{15} F(\rho)} = 0.5$; and the mode, ρ, at $F(\rho)_{max}$. The limits for the summations correspond to the number of equal size fractions in the gradients. The upper limit of the numerator in the expression for the median is designated by ρ_m, the density which evenly divides the mass of the distribution. All three averages, as will be shown below, are unsuitable for these distributions.

The mean appears to be the obvious choice, as it can be directly obtained from the experimental data and does not involve values obtained from the smooth curves connecting the points. However, the mean is sensitive to the tails of the distribution. The tail on the dense side, which contains cells denser than the bottom of the gradient column, must be obtained by extrapolation. The light tail is also unreliable because it is contaminated, during drainage (as stated above), by dense cells. If the distributions were bounded by minimum and maximum values of ρ, then a mean which did not include the tails of the distribution could be calculated. An unambiguous but arbitrary method of selecting the values of ρ is to bound the distributions by some minimal value of $F(\rho)$. As stated previously, $F(\rho) = 20$ is the minimal reliable value and, therefore, was chosen as the bound. This procedure introduces

the requirement that fractional values of $\Delta\rho$ be introduced into the calculation of the mean.

The weighting factor, Yi, of the mean is $F(\rho)$. This factor does not weight all points with $F(\rho)$ values greater than 20 equally and, therefore, the mean or the truncated mean density described above will not be the most repeatable average density.

The median is not a suitable measure of the average buoyant density because of the contamination of the lighter part of the distribution by dense cells. The mode is also not suitable because it relies on only one point, and this point lies on an interpolated curve between the points of the histogram.

The following method was, therefore, employed to estimate the midpoint of the density distributions. The method is a slight modification of a graphical procedure used to estimate the mode of a distribution. It consists of locating at constant ordinates the midpoints, halfway between the limbs of the curve. These points are connected by a best straight line. The value of the abscissa at the intersection of this line with the maximum of the distribution is the mode. Because of the histogram nature of the distributions, the value of the maximum cannot be determined with precision. The midpoints of the distribution located at intervals of 10 starting with $F(\rho) = 20$ are therefore numerically averaged. This procedure

gives the proper, approximately equal weight to the points in the distribution.

For sharp distributions with maxima greater than 100, the midpoints located at intervals of 20 starting with $F(\rho) = 30$ were averaged. This average of the midpoints will subsequently be referred to as the midpoint. The values of the midpoint, the bounded mean, and a mean determined by plotting the distribution on Gaussian paper (49) were always in good agreement, and any one of these averages would have yielded the same experimental findings as the average midpoint (Table IV). All shifts of the distributions to be presented are quite apparent to the eye.

It was found, in the comparison of the distributions of erythrocyte volumes obtained by electronic sizing, that the standard deviations of the midpoint similar to that described above was approximately one-third as large as that evaluated from the mean. This improvement was due to the exclusion of the tails of the distribution.

H. Buoyant Density Distributions from A Single Donor

The buoyant density distribution curves for the erythrocytes from a single donor, R. C. L., are shown in figure 12. These curves, which give the results of three separate centrifugations,

TABLE IV. Comparison of the Results of Buoyant Density Distributions of Erythrocytes

IVa: Exp. #	Midpoint	Truncated mean	Donor	Blood Group	Stature	Relative mean cell volume
117	1.0840	1.0838	R.C.L.	B	corpulent	
*123a	1.0838	1.0838	"	"	"	
*123b	1.0835	1.0837	"	"	"	
*123c	1.0829	1.0833	"	"	"	
**129a	1.0830	1.0834	"	"	"	
**129b	1.0844	1.0847				
**129c	1.0828	1.0827				
*135a	1.0839	1.0833	"	"	"	
*135b	1.0835	1.0830				
*135c	1.0836	1.0824				
*139a	1.0840	1.0839	"	"	"	
*139b	1.0839	1.0838				
*139c	1.0837	1.0835				
av.	$1.0836 \pm 3 \times 10^{-4}$	$1.0834 \pm 5 \times 10^{-4}$				1.00
*143	1.0807		W.R.H.	O	thin-normal	
*143	1.0814		"	"	"	1.04
*145	1.0814	1.815	A.S.	B	normal	
*145	1.0806		F.W.		corpulent	
*145	1.0801		"		"	1.06
*149	1.0812		W.G.	A	normal	
*149	1.0811		W.G.	"	"	1.04
*149	1.0802		A.S.	B	normal	1.02
av.	$1.0808 \pm 4 \times 10^{-4}$					

*These experiments with blood from R.C.L. and the other donors were averaged separately.
**Discarded; Siliclad treated.

TABLE IV. (continued)

IVb:	Exp. #	Midpoint	Donor	
	291	1.0831	R.C.L.	
	293	1.0844	R.C.L.	
	291	1.0827	R.C.L.	venipuncture
	293	1.0843	R.C.L.	venipuncture after standing 24 hrs.

demonstrate the reproducibility of the method. Two further determinations were performed with each of those performed above. There were thus nine separate experiments in all. The average of the midpoints from these nine experiments (see Table IV), which were performed over a period of one month, was $1.0836 \pm 3 \times 10^{-4}$ g. cm.$^{-3}$. The bounded means were approximately the same. The average was $1.0834 \pm 5 \times 10^{-4}$ g. cm.$^{-3}$. The standard deviation of the midpoints corresponds to about 1/7 of a fraction.

In various experiments, Tables III and IV (performed over a six-month period), blood from R. C. L. was analyzed whenever a control was necessary. There was no significant variation from this value (1.0836 g. cm.$^{-3}$), in spite of changes in centrifuge rotors, solute composition at constant osmolarity, and lot number of BSA.

Buoyant density distributions were obtained in experiments with veinous blood stored in Alsever's solution at 4°C for periods of 3 and 24 hours. These samples were analyzed together with a sample of blood obtained by finger punch. Again, the distributions were substantially the same. The value of the means, as shown in Table IV, from the vein-puncture blood were 1.0827 at 3 hours and 1.0843 at 24 hours. The values of the finger puncture controls were 1.0831 and 1.0844, respectively.

It is concluded that normal human erythrocytes can be stored for 24 hours without any change in buoyant density.

In section II-D, it was mentioned that aged BSA solutions markedly increased the buoyant density of the erythrocytes. It might be added that if after centrifugation the density distribution of cells in the centrifuge tube is not fractionated but is stored at 2°C and then centrifuged again after two or three days, a large pellet of cells which had previously been buoyant will form at the bottom of the centrifuge tube. Neither of these effects has been studied further. They do, however, indicate that deterioration of the red cells leads to an increase in buoyant density. It will be shown later that the aging of the rabbit erythrocyte in the blood is accompanied by an increase in buoyant density.

I. The Shape of the Buoyant Density Distributions

The shape of the buoyant density distributions in nine experiments was somewhat variable (Table V). The sources of error in the nine experiments include: the swirling of some of the gradient columns, the incomplete lysis or separation of the hemoglobin from the erythrocyte cell walls, ghosts, and the contamination of the lighter part of the distributions by dense cells, as has been discussed previously. This contamination is not reproducible, and

TABLE Va. Analysis of the Data from Nine Experiments with Cells from R. C. L.

	123			135			139					
Density	a	b	c	a	b	c	a	b	c	aver.	σ	σ as % F(ρ)
1.0950	15.5	16.3	13.1	16.6	(13.3)†	14.8	11.7	12.5	13.3	14.2	1.7	12
1.0925	20.7	20.4	19.3	21.7	(20.8)†	20.9	20.1	17.3	20.8	20.2	1.3	6
1.0900	33.5	30.1	29.8	30.1	29.6	28.6	30.6	29.2	33.1	30.5	1.4	5
1.0875	50.3	52.6	43.0	44.8	41.8	41.7	43.7	50.7	42.8	45.7	3.9	9
1.0850	72.0	68.2	57.6	55.2	51.8	52.1	49.7	63.9	50.8	57.9	7.7	13
1.0825	63.8	71.8	64.5	56.8	51.1	53.7	43.7	59.2	51.0	57.3	8.1	14
1.0800	51.9	53.2	68.7	47.2	44.5	45.2	39.8	49.2	44.8	49.4	7.8	16
1.0775	34.0	37.3	38.6	28.4	36.1	40.1	28.8	27.8	33.2	33.8	4.4	13
1.0750	19.2	18.3	21.8	17.2	24.1	24.8	18.1	15.2	22.0	19.5	2.9	15
1.0725	11.3	9.7	12.5	12.2	15.6	11.5	14.4	10.8	15.5	12.6	1.8	15
1.0700	7.2	6.3	9.6	10.8	11.3	9.8	12.3	8.8	10.7	9.6	1.8	19
sum	379.4	384.2	378.5	341.0	340.0	343.2	312.9	335.8	338.0		*4.7	**13.1

TABLE Vb. Data from Table Va Adjusted So that the Sum of F(ρ) from Each Individual Experiment is 350 $g.^{-1}cm.^{3}$

1.0950	14.3	14.9	12.1	17.1	(13.7)†	14.6	13.1	13.1	13.8	12.4	2.2	17
1.0925	19.1	18.6	17.9	22.3	(21.5)†	20.6	22.5	18.1	21.6	20.1	1.8	9
1.0900	31.0	27.5	27.6	31.0	30.5	28.2	34.3	30.5	34.3	30.5	2.4	8
1.0875	46.5	48.0	39.8	46.1	43.1	41.1	49.0	53.0	44.4	45.7	3.9	9
1.0850	66.6	62.3	53.4	56.8	53.4	51.3	55.7	66.7	52.7	57.7	5.7	10
1.0825	59.0	65.5	59.8	58.4	52.7	52.9	49.0	61.8	52.9	56.9	5.2	9
1.0800	48.0	48.6	63.7	48.5	45.9	44.5	44.6	51.4	46.5	49.1	5.6	11
1.0775	31.4	34.0	35.8	29.2	37.2	39.5	32.3	29.0	34.4	33.6	3.3	10
1.0750	17.7	16.7	20.2	17.7	24.9	24.4	20.3	15.9	22.8	20.1	3.2	16
1.0725	10.4	8.9	11.6	12.5	16.1	11.3	16.1	11.3	16.1	12.7	2.6	20
1.0700	6.7	5.8	8.9	11.1	11.7	9.7	13.8	9.2	11.1	9.8	2.4	23
											*3.7	**13.8

TABLE Vb. (continued)

* The numbers presented in columns 2-12 are values of $F(\rho)$.

** The variance obtained from the sum of the σ^2 of all nine experiments.

† Extrapolated from curve. Fraction lost. Not included in average.

caused the area of the usable part of the distribution to vary. Even if the unreliable edges of the experimental curves are excluded and the remainder of the curves adjusted to equal areas, the adjusted curves are not superimposable. The changes in procedure adopted for the "Aging Experiment" would have improved the quality of these experiments.

The most probable shape of the buoyant density distribution of erythrocytes from R. C. L. was obtained by averaging the nine previously mentioned experiments (Table V-a). The values of $F(\rho)$ were read off of the smooth curves which connect the points of the histograms in 0.0025 g. cm.$^{-3}$ increments from 1.0700 to 1.0950 g. cm.$^{-3}$. These values were averaged and the standard deviations were calculated (Table V-a). The sum of the squares of the standard deviations could be reduced by 37 per cent by adjusting the sum of the values of $F(\rho)$ (Table V-a) of each of the nine initial distributions to equal 350 g.$^{-1}$ cm^{3} (Table V-b). However, if instead of this sum of the squares of the standard deviations which is expressed in $F(\rho)$, the sum is expressed as a percentage error for each fraction taken, no improvement is found. The average of the nine adjusted distributions is presented in figure 13. This distribution, when plotted on Gaussian paper (49), does not accurately fit a straight line (figure 14). Neither does the average of the

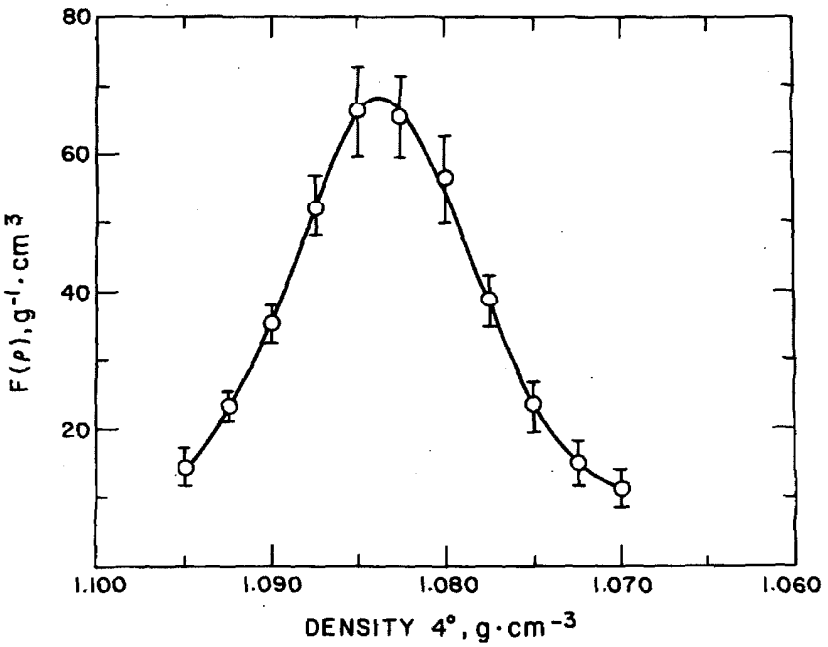

Figure 13.--Most probable distribution of erythrocytes from R.C.L. Ordinates averaged at the indicated densities in nine experiments (table IVb). Area under curve normalized to unity. The error bars indicate the standard deviations.

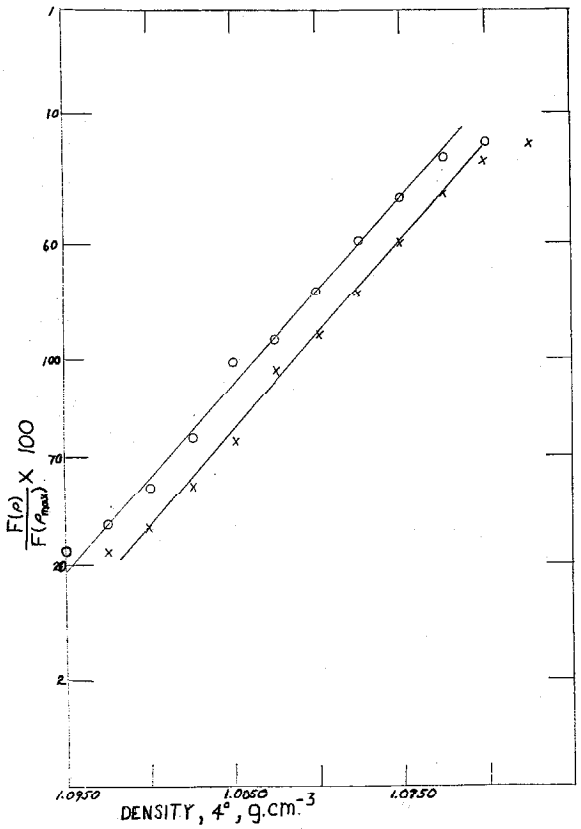

Figure 14.--Plot of the values of $F(\rho)$ given in table IV on Gaussian paper. The ordinate is the ratio of the value of $F(\rho)$ to that of the maximum of the distribution, $F(\rho_{max})$, multiplied by 100. O, the average values of $F(\rho)$ from the nine distributions (table IVa). X, the values from the distributions adjusted to constant area (table IVb); the abscissa values are displaced 0.0020 g. cm.$^{-3}$ to lower densities. A mean buoyant density can be obtained from these plots. This mean buoyant density is the intercept at the maximum value of $F(\rho)$. The values of the means of the distributions of O and X are, respectively, 1.0837 and 1.0838 g.cm.$^{-3}$.

nine distributions which had not been adjusted to equal areas (figure 14).

Two distributions from blood of another individual, W. G., whose erythrocytes band at lighter densities and thus are less affected by the nonsectorial shape of the centrifuge tube, are also plotted on Gaussian paper (figure 15). One of these does fit a straight line. It should be stated that this was the best run that had ever been made with the system. Obviously, it is impossible to decide whether or not these distributions are in general Gaussians.

The dispersion or 2σ width of a Gaussian can be obtained from these plots on Gaussian paper (49). It is the density range between the two ordinant values at 60% of the peak height. Though the erythrocyte distributions have not been established to be Gaussians, the dispersions obtained from these plots should be a good approximation of the true dispersions, and therefore useful for the comparison of different distributions. The values of the dispersions for the blood of R. C. L. were obtained from the plots of the values presented in Tables IVa and IVb. They are, respectively, 0.0122 and 0.0121 g. cm.$^{-3}$. The values obtained from the two distributions of W. G. cells are, respectively, 0.0090 and 0.0091 g. cm.$^{-3}$.

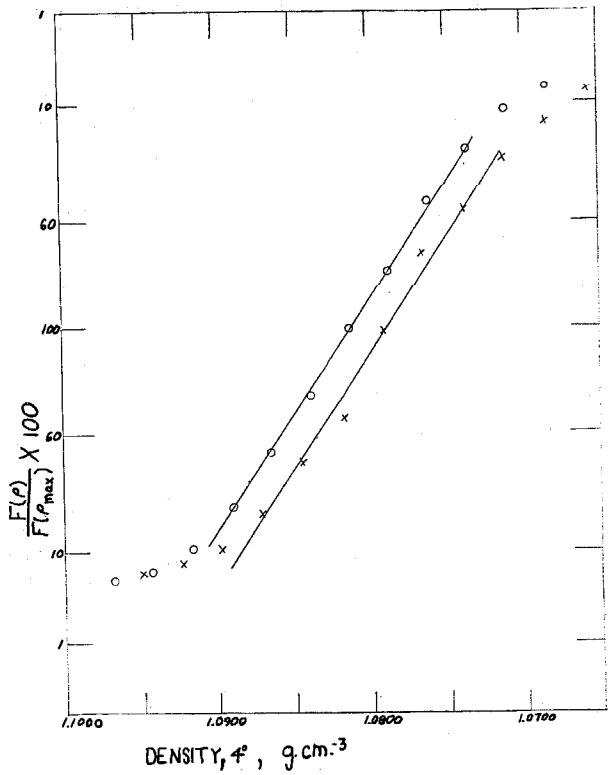

Figure 15.-- Two separate distributions, O and X, of cells from W.G. plotted on Gaussian paper. The abscissa values of X are displaced 0.0020 g. cm.$^{-3}$ to lower densities. The values of the means of the distributions of O and X are, respectively, 1.0813 and 1.0812 g. cm.$^{-3}$.

J. The Rebanding Experiments

Evidence that the observed buoyant density distributions are free of artifacts was sought in "rebanding" experiments. A three-fold normal concentration of cells was applied in a 0.3 ml. layer onto a BSA density gradient. After subsequent centrifugation, two of the fractions were collected in the same test tube. These were thoroughly mixed by gentle horizontal rolling of the test tube. The two fractions used were number four and either eight, nine, or ten. In the experiment presented here, fractions four and ten were mixed. The other two experiments gave substantially the same results. The mixture was drawn into one of the dry pump lines and discharged at first slowly into a new BSA gradient so as to locate the isodensity position. With the glass capillary properly adjusted, one fraction of the mixture was injected. The new gradient, which contained an extra fraction, was then centrifuged, photographed, and fractionated.

The photographs (figure 16) show the density fractions to have rebanded at their expected densities in the new gradient and to be narrow density fractions, which each occupy only the expected one fraction of the gradient. The position of the various fractions shown in the photographs was calculated from the position of the meniscus, the dimensions of the SW 39 tube given in the manual for

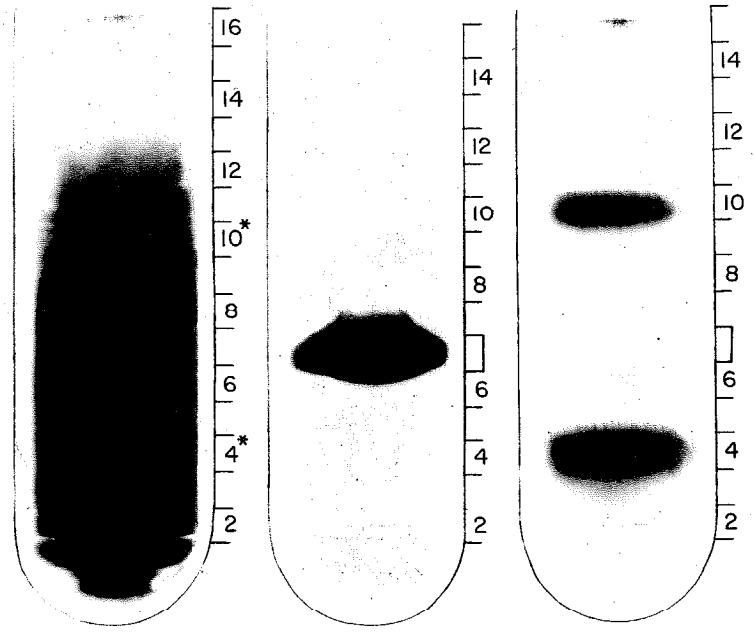

Figure 16. -- Rebanding experiment. Photographs of erythrocyte distributions: (A) original distribution. (B) mixture of 4* and 10* from (A). (C) after centrifugation of (B). Note that an extra layer of BSA is present in (B) and (C).

the Model L centrifuge, and the assumption that the bottom of the tube is hemi-spherical. The validity of these calculations was corroborated by the observation that the isodensity level for the mixture occurred at the anticipated position for the seventh fraction.

The absorbance distributions of the individual fractions from both gradients are shown in figure 17. The bulk of the absorbance from each of the two zones was distributed in the two expected fractions. The fractionations could not be arranged to be absolutely in phase with the original gradient. This may be due to a lack of reproducibility in forming the gradients. It should be noted that these experiments were performed before the final procedures for obtaining buoyant density distributions had been completely developed. The BSA was not deionized, though this lot had the lowest salt content, 0.4% ash, of any used. A slight salt gradient was superimposed on the density gradient and spread the distribution (see section IV-C). This spreading would, however, not have affected the results of these experiments. The gradient machine was based on a Sigmamotor Pump and equal volumes were determined by a cam connected to the pump drive, which actuated a microswitch that stopped the pump. The density determinations were about half as precise as the other ones in this thesis.

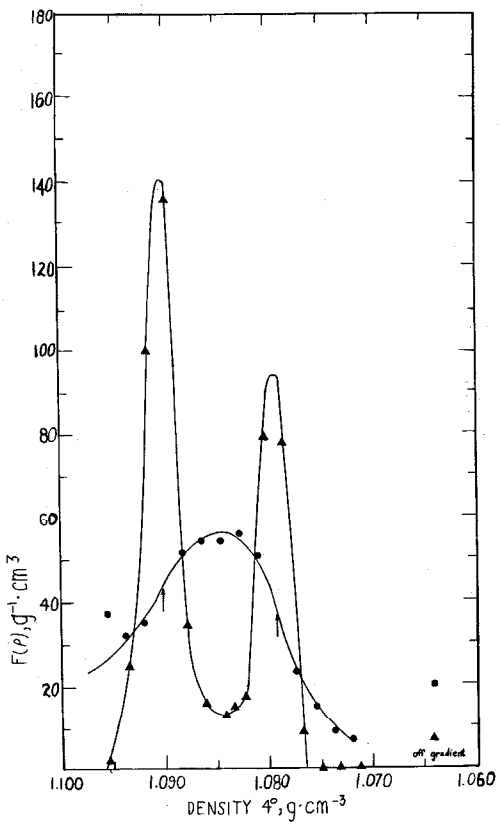

Figure 17.--Graphical presentation of rebanding experiment shown in figure 16. ● , original distribution. ▲, distribution of rebanded fractions, 4* and 10*.

K. Comparison of Erythrocyte Buoyant Density Distributions of Different Individuals

The erythrocytes of four other normal males, in their twenties, were examined (Table IV). The means, 1.0809, 1.0804, 1.0808, and 1.0812 g. cm.$^{-3}$, were significantly smaller than the mean, 1.0836, for the cells from R. C. L. Two distributions of cells from one of these individuals, W. G., are compared with the average distribution of cells from R. C. L. in figure 18. No direct correlation (Table IV-a) between blood group or stature is apparent in this sample, which is too small to be statistically significant. It might be added that R. C. L. lost ten per cent of his body weight during the six-month period over which the mean buoyant density of his erythrocytes remained constant.

The mean cell volumes of the bloods obtained from these individuals and R. C. L. were determined by electronic sizing (sections II-I and VI-A). The mean volumes of all five individuals were within the normal range. However, the mean cell volumes obtained from the bloods of the four other normal males were all larger than that obtained from the blood of R. C. L. The average difference was 3.6 cubic micra. This difference corresponds to the increase in cell volume expected for a shift in buoyant density solely due to water. The derivation of an equation that relates buoyant

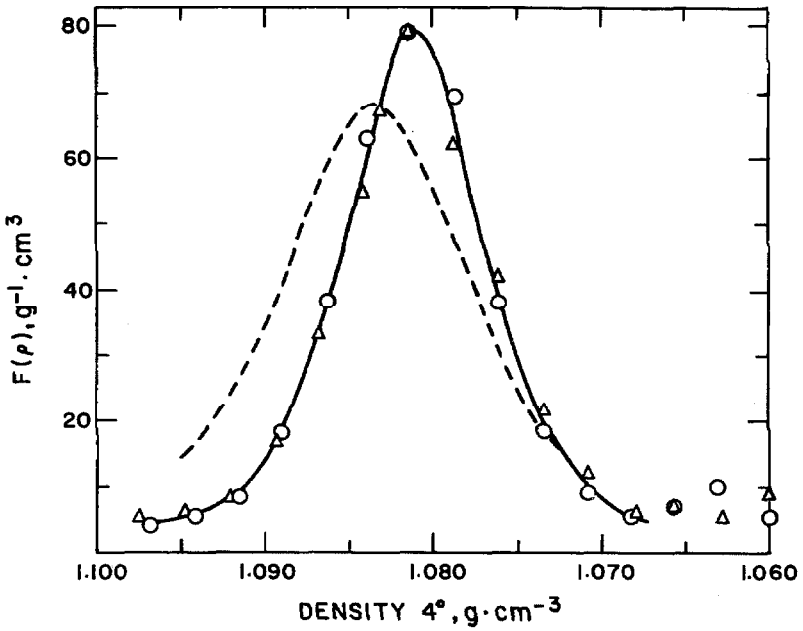

Figure 18.--Comparison of figure 13 with results of two experiments with another donor, W. G. These results have previously been plotted on Gaussian paper, figure 15.

density to changes in cell volume due to water will be discussed later (section IV-A). The interrelation between average buoyant density and average cell volume suggests that it would be of interest to measure these quantities from a large number of individuals. At present, electronic sizing is not nearly as sensitive as buoyant density to these small shifts in density and volume.

L. A Comparison of the Reported Values for the Density of Human Erythrocytes

The average density values found in this study, 1.0836 to 1.0804, with an average value of 1.0814, are significantly less than values previously reported by others (17, 21, 22, 12, 20, 50). The reported values range from 1.0845 (17) to 1.0996 (50) in experiments performed at room temperatures.

The density determinations reported in the literature can be divided into two groups. The first consists of centrifuging the blood and determining the density of the packed cells. The second consists of determining the buoyant density of the cells in either aqueous or nonaqueous systems.

Ponder (50) has used the first method in its simplest form. He sucked packed cells into a pycnometer and directly obtained a density, 1.0996 g. cm.$^{-3}$. Ponder packed the cells for 2 hours at

4,000 rpm "in a large International centrifuge." Powell (17) also obtained a density of packed cells, 1.0845 g. cm.$^{-3}$. He employed density markers, drops of calibrated mixtures of silicone oils. These drops were introduced into the cell suspension and they distributed according to buoyant densities in the density gradient formed under the influence of the centrifugal field by the packed cells. After fixation of the cells by dialysis with formaldehyde, serial sections of the cell mass were microscopically observed. The silicone oil droplets were found in the serial sections. Powell packed the cells for 30 minutes in "a 10 x 1 cm. tube at 3000 r.p.m."

The above experiments are criticized because the total volume of packed cells, hematocrit, decreases as the centrifugal field is increased (figure 19) (45).

Ponder ascribes this shrinkage of the packed cell mass to the forcing out of intracellular water by the closer packing of the cells. If some of the intracellular water were forced out of the packed cells by this procedure, then the values of all these densities would be too high. In these experiments, the cells are not neutrally buoyant. The hydrostatic pressure head caused by the column of suspending liquid and cells compresses each cell. This compression can squeeze out some of the cellular water. The cell wall is

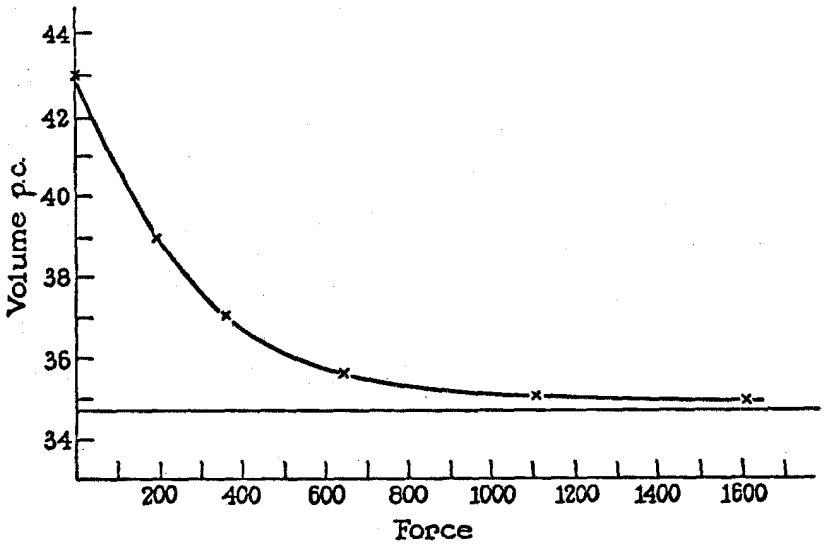

Figure 19.--"Typical relation between volume of red cells and centrifugal force applied, with spinning, to constant volume in each case. Ordinate per cent volume; abscissa, centrifugal force in arbitrary units. The smallest volume shown corresponds to a rate of spinning of about 16,000 rpm and a radius of 10 cm." Taken from E. Ponder, Hemolysis and Related Phenomena, Grune and Stratton, New York, 1948.

permeable to water. The effect of hydrostatic heads to equalize the free energy of two phases containing differing concentrations of solutes and separated by a semipermeable membrane is well known. Furthermore, some of the pores or pumps could be distended by forcing a biconcave disc to distort for closest packing. The relationship between the density of the cells in plasma under physiological conditions and the density observed in pelleted cells is likely to be complex.

Ponder (50) attempted to determine the buoyant density of small clumps of packed cells in a bromobenzene-benzene Linderstrom-Lang column (51). He found that the cells steadily drifted towards increasing density and thought this was due to solubilization of the cellular lipid in the organic solvent.

Neutral density separations have been performed with silicone oil solutions (21). In this work, the mean cell density is reported to correspond to that of a mixture of silicone oils which were varied so that after centrifugation half of the cells remained at the top of the solution and half below. Most criticism of this work stems from the supposed mode of separation. The cells most probably pack on top of the silicone oil phase and then the whole packed cell mass is forced to sink between the silicone oil and the centrifuge wall. Mechanical shear, as well as the osmotic effects

previously discussed concerning pelleted cells would occur. The mean buoyant density of the cells in aqueous solutions was determined in a manner similar to that for the determinations with silicone oil mixtures.

Only three materials have so far been used to form aqueous solutions of sufficient density to band cells. These are gum acacia (22), Ludox (colloidal silicic acid (23)), and BSA. The density of the erythrocyte has not been determined in Ludox. The erythrocyte under physiological conditions is coated with albumin. This albumin layer interacts with the cells and is known to exert a substantial protective effect against hemolysis (45). Therefore, the first criticism of any solution other than an albumin solution is that it does not contain albumin. In the future, especially in work with Ludox, which appears to be particularly promising (cf. Mateyko and Kopac), this criticism could possibly be eliminated by the addition of some albumin to the solutions. In fact, the author of this thesis foresees the necessity for such a procedure in order to band cells of buoyant density greater than 1.0950 g. cm.$^{-3}$.

In the experiments with gum acacia so far reported, no attempt seems to have been made to control solute concentration.

The classical neutral density separations according to the method of Ferrebee by Ferrebee et al. (12, 52) and Vallee et al. (20, 53, 54), were not directed towards quantitative measurements

of cell buoyant density. First, density measurements were performed with a hygrometer, which was adequate for the purposes of obtaining reproducible separations of cells, but unsuitable for accurate work, especially with these viscous solutions. The concentration of solutes in the non-deionized BSA was determined from the freezing point depression. Salts were added so that the osmolarity of the BSA solutions equaled that of the plasma. The solutions were equilibrated with CO_2 from the atmosphere and stored at 4°C. Vallee and co-workers (53) report that the density of the cells changes during the experiments. As has been previously stated, storage of the BSA solutions at 4°C results in substantial increases in buoyant density.

Some ambiguities involved in the absolute values of the buoyant densities reported in this thesis are now discussed. The buoyant densities reported here were not obtained at physiological conditions, in so far as the experiments were performed at 4°C rather than 37°C. The major reason for the choice of temperature was that the loss of K^+ ion in the time period of the experiment (2-3 hours) is negligible at 4°C, but not at 37°C (45). The justification of the present experimental conditions is that they are very similar to those used for the storage of whole blood (40), but, of course, the albumin had to be increased six-fold.

The six-fold increase in albumin concentration significantly alters the osmolarity of the solutions, and thus requires correction of the buoyant densities obtained to the osmolarity of plasma. This alteration of the osmolarity of the solutions by the BSA could be due to anion binding, introduction of significant amounts of uncharged solutes which were a contaminant of the powdered BSA, or large changes in the activity of the other solutes due to the presence of the BSA. These individual effects cannot be readily evaluated; however, they, together with any other effects, have been collectively evaluated by Scatchard et al. (55)

Scatchard et al. have measured the osmotic pressure of concentrated BSA solutions at neutral pH. The concentration of salt was measured on both sides of the membrane. The osmotic pressures of these solutions, when expressed in terms of solute concentration, are insufficient to account for the observed differences in the salt concentration of the two phases. For instance, a 28.5% BSA solution at pH 6.31 develops an osmotic pressure of 0.373 atmospheres. The BSA solution and dialysate were 0.1815 and 0.1603 M in NaCl, respectively.

The salt concentration of the BSA solution, when corrected for the osmotic pressure, is that which would correspond to equal water activities on both sides of the membrane; the stable situation

if the membrane were permeable only to water. The osmotic pressure, when expressed in terms of solute concentration, equals 0.0155 M or, in terms of NaCl concentration, 0.0077 M. When 0.0077 is subtracted from 0.1815, the molarity of the BSA solution, the result is 0.1738, which is significantly greater than 0.1603, the salt concentration of the dialysate. Therefore, the molarities of the concentrated BSA solutions have to be multiplied by 0.1603/0.1738 or 0.924 in order to calculate the molarity of an aqueous solution which possesses the same water activity as the BSA solution.

The average of the midpoints, 1.0814, of all five individuals so far studied must be corrected for the above effect and the miscalculation of the water content in the concentrated BSA solutions that was mentioned in section II-D. The derivation of these corrections is presented in sections IV-B and IV-C. It will be shown that the derivative of the buoyant density with respect to the variable, the ratio of the solute activity in a solution to the solute activity in plasma, is 0.059 g. cm.$^{-3}$. The correction of the molarities of the concentrated BSA solutions by the ratio 0.924 results in a density increase of 0.076 x 0.059 g. cm.$^{-3}$ or 0.0045 g. cm.$^{-3}$. However, this correction is partially offset by the factor 1.05 for the actual 63.5% water present rather than the

66.7% assumed water content of the concentrated BSA solutions. The buoyant density decrease associated with the ratio 1.05 is (-0.05) x 0.059 g. cm.$^{-3}$ or -0.0030 g. cm.$^{-3}$. The average of the midpoints corrected for both of the above effects is 1.0829 g. cm.$^{-3}$. This value is significantly lower, 0.0066 g. cm.$^{-3}$, than the lowest previously published result (17), which, when corrected to 4°C, is estimated to be 1.0895 g. cm.$^{-3}$. Because the coefficient of thermal expansion of the erythrocyte is presently unknown, the coefficient for a BSA solution of similar composition had to be used in this estimate.

IV. TONICITY AND TONICITY GRADIENTS

A. The Effect of Tonicity on Buoyant Density

The effect of tonicity on buoyant density is of interest for two reasons. It offers the possibility of making quantitative studies of erythrocyte osmotic behavior. It provides a means of evaluating any density shifts caused by slight deviations in tonicity of the BSA solutions.

The swelling and shrinking of erythrocytes in solutions of different tonicity (ratio of solute osmolarity to the osmolarity of plasma) is well known, but the quantitative relationship is still a matter of controversy (45). Ponder (45) has derived an equation, 3.10, for the effect of tonicity on cell volume.

$$V = \left(\frac{V_w}{V}\right)_{iso} \left(\frac{1}{T} - 1\right) V_{iso} + V_{iso} \quad \text{(Ponder's eq. 3.10)}$$

Here V is the volume of the cell at tonicity, T, of the suspending solution. V_{iso} and $\left(\frac{V_w}{V}\right)_{iso}$ are, respectively, the volume of the cell and the ratio, 0.70, according to Ponder, of the volume of water in the cell to the total volume of the cell at isotonic conditions. A solution is referred to as isotonic, i.e. T = 1, when the water activity is equal to that of plasma. The cells are assumed to be permeable to water, impermeable to at least one solute, and to obey Van't Hoff's Law. Sodium ion is the main excluded solute in the following experiments.

The osmotic behavior of erythrocytes in general and human erythrocytes in particular in previous studies was not well described by equation 3.10. The volume changes were smaller than expected. This has led Ponder to introduce an arbitrary coefficient, R, into equation 3.10.

$$V = R\left(\frac{V_w}{V}\right)_{iso}\left(\frac{1}{T} - 1\right)V_{iso} + V_{iso} \quad \text{(Ponder's eq. 3.11)}$$

The coefficient was rationalized on the supposition that some of the cellular water was bound and not in equilibrium with the water in the plasma. MacLeod and Ponder (56) established, however, that all of the cellular water was free to equilibrate with ethylene glycol solutions. Hearst and Vinograd (57) have demonstrated that the water bound to DNA is in equilibrium with the solvent water. Ponder (45) in turn suggested that the nonideality of the cellular solutions is due to the high concentration of hemoglobin present. He believes "that simplified osmotic laws are not likely to apply to such a system (the red cell), which, instead of being regarded even as a concentrated solution, might better be regarded as an expanded crystal."

The values of R reported for human erythrocytes cited by Ponder (45) range between 0.5 and 1.0, with most of the values centered about 0.7. These values of R were obtained from

measurements of changes in cell volume with changes in tonicity of the suspending medium. Changes in the volume of cells have been observed by centrifuging aliquots of a cell suspension in a hematocrit tube. Fractional changes in cell volume have been estimated from microscopic measurements of cell areas and calculation of the volumes of cells in dried cell smears. Measurements of changes in cell volume have also been indirectly obtained by measuring the change in the fraction of the cell suspension occupied by the suspending solution. These are called "dead volume" measurements. The fraction of the suspension occupied by the cells is dead to some measurable process; for instance, the conduction of ions or the distribution of a dye.

The above methods for obtaining determinations of changes in cell volume are all discussed at length by Ponder (45). None of these methods directly measures the volume of individual cells in the suspension. At present, there are two other methods available for studying the change in cell volume with tonicity. The first method is to observe the changes in cell volume with a Counter-Counter. The other method is to observe the shifts in the buoyant density distribution of the cells. The latter method, as well as all of the above methods, is based on the assumption that the indicated volume changes are caused by changes in the cellular water content.

Measurements with a Coulter-Counter of the mean cell volumes of erythrocytes at different tonicities have recently been reported (Nevius 1963 (58)). Nevius's data for the mean cell volume against per cent NaCl in the suspending solution have been recalculated for figure 20, so as to obtain a plot of mean cell volume relative to mean cell volume at unit tonicity against tonicity. The results are in striking disagreement with all previously published data and with the results reported in this dissertation. His data fit Ponder's equation (3.11) if a value of R = 2.3 is used. A value of R greater than unity indicates that the cellular fluid is not only entirely available for osmotic absorption of water, but that additional active transport factors which pump water into the cell are operative and are sensitive to tonicity. It is more likely that the high value obtained for R results from comparing volume distributions at different resistivities of the suspending solution. The resistivity is approximately inversely related to the salt concentration or tonicity. Nevius attempted to eliminate this possibility by measuring the volume distributions of mica particles at various salt concentrations. He states that there were no observed differences, but does not include any data.

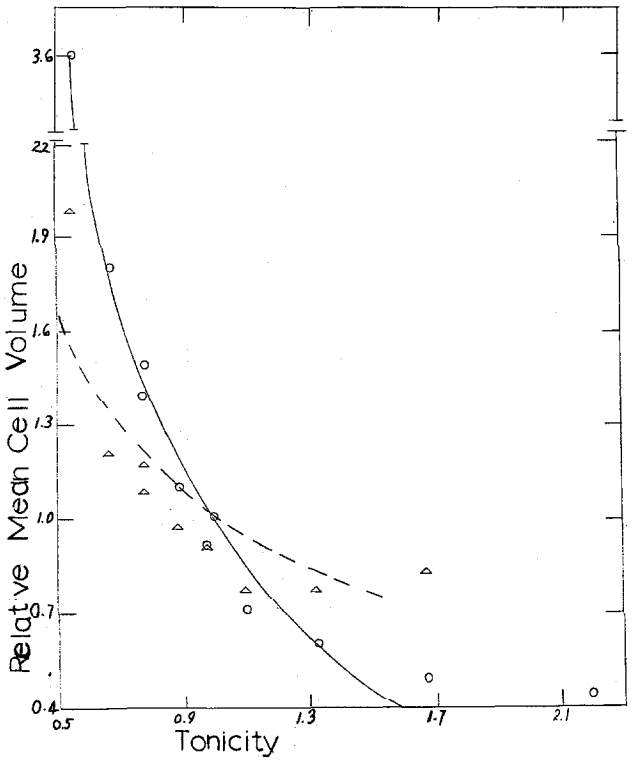

Figure 20. -- O, measurements with a Coulter-Counter by Nevius of the mean cell volume at various tonicities. The solid line is a plot of Ponder's equation (3.11) with R = 2.3. Δ , the above data multiplied by the tonicity of the suspending solutions--see text. The dashed line is a plot of Ponder's equation (3.10) with R = 1.

The apparent volume of the cell is measured as the resistance change due to the presence of a cell in the aperture of the Coulter-Counter, and is, according to equation 1, proportional to the resistivity of the suspending solution. Therefore, in order to render the volume measurements independent of the resistivity or tonicity of the suspending salt solutions, the apparent volumes must be divided by the resistivity or multiplied by the tonicity. The results of multiplying the apparent cell volumes by the tonicity of the salt solutions are also shown in figure 20. The experimental points now lie slightly below but parallel to the theoretical curve for R = 1. Although these data are not good enough to prove that the erythrocytes are perfect osmometers, they will be used to support the interpretation of the buoyant density studies to be presented.

Before the studies on the effect of tonicity on buoyant density are presented, certain mathematical relationships are derived. The relationship between volume and buoyant density for cells in which only the volume of water changes is first derived. The result is then substituted into Ponder's equation 3.10.

Several new quantities are used: M, M_{iso}, and ΔM are, respectively, the mass of the cell at tonicity, T, the mass of the cell at isotonicity, and the difference between the first two quantities, $M - M_{iso}$. The quantity ΔV is $V - V_{iso}$. The quantities ρ and ρ_{iso}

are the buoyant densities of the cell at tonicity, T, and at unit tonicity. The quantity ρ_w is the density of water at 4°C.

The density of a cell at tonicity T defined in terms of the cellular mass and volume at unit tonicity and the mass and the volume increments due to the absorption of water is:

$$\rho = \frac{M}{V} = \frac{M_{iso} + \Delta M}{V_{iso} + \Delta V} \tag{2}$$

and

$$\rho = \frac{V_{iso}\,\rho_{iso} + \rho_w \Delta V}{V_{iso} + \Delta V} \quad . \tag{3}$$

Upon rearranging terms, the following expressions are obtained:

$$\frac{\Delta V}{V_{iso}} = \frac{\rho_{iso} - \rho}{\rho - \rho_w} \tag{4}$$

or

$$V = \left(\frac{\rho_{iso} - \rho}{\rho - \rho_w} \right) V_{iso} + V_{iso} \quad . \tag{5}$$

Ponder's equation 3.10 can be restated:

$$V_{iso} + \Delta V = \left(\frac{V_w}{V} \right)_{iso} \left(\frac{1}{T} - 1 \right) V_{iso} + V_{iso} \tag{6}$$

Subtract V_{iso} from both sides of equation 6 and rearrange terms.

$$\frac{\Delta V}{V_{iso}} = \left(\frac{1}{T} - 1\right)\left(\frac{V_w}{V}\right)_{iso} \tag{7}$$

Combine equation 7 with equation 4:

$$\frac{\rho_{iso} - \rho}{\rho - \rho_w} = \left(\frac{V_w}{V}\right)_{iso}\left(\frac{1}{T} - 1\right) \tag{8}$$

Multiply by $\rho - \rho_w$ and collect terms:

$$\rho + \left(\frac{V_w}{V}\right)_{iso}\left(\frac{1}{T} - 1\right)\rho = \left(\frac{V_w}{V}\right)_{iso}\left(\frac{1}{T} - 1\right)\rho_w + \rho_{iso} \tag{9}$$

Solve for ρ:

$$\rho = \frac{\left(\frac{V_w}{V}\right)_{iso}\rho_w\left(\frac{1}{T} - 1\right) + \rho_{iso}}{1 + \left(\frac{V_w}{V}\right)_{iso}\left(\frac{1}{T} - 1\right)} \tag{10}$$

The buoyant density shift due to a change of 0.1 in the tonicity of the suspending medium for $(V_w/V)_{iso} = 0.70$ is 0.0059 g. cm.$^{-3}$. This density shift is readily measurable, as it is 18 times the standard deviation of the midpoint. The corresponding change in volume is seven per cent.

The shift in buoyant density is, at present, the effect of tonicity that can be the most sensitively measured. This sensitivity in measurement makes studies possible over a much narrower, and thus more physiological, range of tonicities.

B. Experimental Procedures and Results

Two series of buoyant density distributions with erythrocytes from R. C. L. in BSA gradients at various constant tonicities: 0.8, 0.9, 1.0, 1.1, and 1.2 were performed. Each pair of dense and light BSA solutions used in formation of these gradients were at the same tonicity, as described in section II-D.

The buoyant density distributions from one series and the midpoints from both series are shown in figure 21. The entire distribution shifted with salt concentration. The relation between the shift as given by the midpoint of the distribution and the tonicity of the BSA gradient is well represented by equation 10, which is the solid line in the figure. The midpoints of the distributions at a tonicity of 1.2 were estimated with the assumption that the shape of the curve was the same as that obtained at tonicity 1.1.

This agreement between the experimentally determined density shifts due to tonicity changes and those predicted by equation 10 in which R had been set equal to unity establishes, at least for these experimental conditions, that erythrocytes are perfect osmometers. The data obtained by Nevius with the Counter-Counter, as discussed above, are in agreement with this finding.

It is now possible to evaluate the error in buoyant density

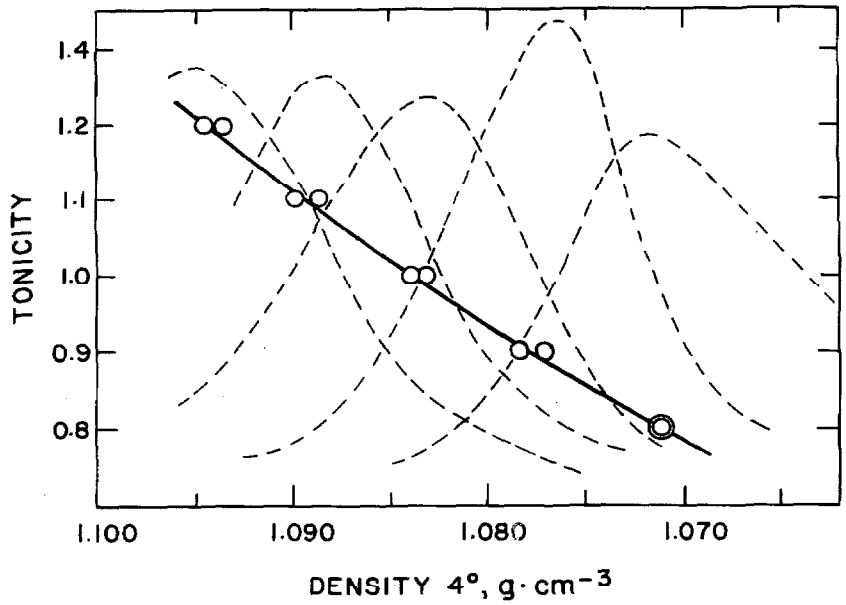

Figure 21.-- Effect of salt concentration on the buoyant density distribution of erythrocytes in BSA. Dashed lines give one set of observed distributions at relative salt concentrations listed from left to right, 1.2, 1.1, 1.0, 0.9, and 0.8. The experimental points represent the means of the distributions. The line was calculated with equation (10) and ρ_{iso} = 1.0836 g. cm.$^{-3}$.

which results from the uncertainty in the tonicity of the BSA solutions used in these studies. A five per cent error in tonicity corresponds to a density shift of 0.0030 g. cm.$^{-3}$. A reasonable estimate, as indicated earlier, of the tonicity of the BSA solutions used in obtaining the distributions is 0.974. The correction to the buoyant densities associated with this tonicity is an increase of 0.0015 g. cm.$^{-3}$. A reasonable estimate of the overall error in the determination of the absolute value of the tonicity of the BSA solutions is plus or minus five per cent or, in density units, $\pm$ 0.0030 g. cm.$^{-3}$. The average density of the human erythrocyte, according to the data in the previous section, should be 1.0829 $\pm$ 0.0030.

C. The Effective Density Gradient in the BSA-Erythrocyte-Salt-Water System

In this system, the density gradient effective in resolving cells of different buoyant density is a composite of the real or physical density gradient set up by the BSA and a gradient in tonicity, dT/dr, associated with the distribution of any nonpermeable solutes. The effect of the gradient of BSA on the gradient of tonicity is negligible (section III-L). The tonicity experiments allow the calculation of the effect of unequal solute concentrations in the

original dilute and concentrated BSA. The effective density gradient, $(d\rho/dr)_{eff}$, has been shown in buoyant density studies of dissolved macromolecules (46) to be the sum of the physical density gradient, $d\rho/dr$, and a further density gradient which describes the response of the buoyant species to changes in solute activity, $(d\rho/dr)_{eff} = d\rho/dr - da/dr \quad d\rho/da$, where a is the activity of the solute. This equation may be expressed in terms of tonicity and the experimental variable V, the liquid volume in the centrifuge tube, which in turn depends on the radial distances, r.

$$\frac{d\rho}{dV}_{eff} = \frac{d\rho}{dV} - \frac{dT}{dV} \quad \frac{d\rho}{dT} \quad . \tag{11}$$

Tonicity is here assumed to be proportional to solute concentration. It might be noted that equation 11 is applicable for experiments performed in centrifuge tubes of arbitrary shapes. The method for evaluating $d\rho/dV$ has been described in section III-E. The value of dT/dV was obtained as the product $\frac{\Delta T}{\Delta \rho} \cdot \frac{d\rho}{dV}$, where ΔT and $\Delta \rho$ are the difference in tonicity and density, respectively, in the two BSA solutions used in preparation of the gradient. The derivative $d\rho/dT$ can be evaluated from figure 21, or, after differentiation, from equation 10:

$$\frac{d\rho}{dT} = \frac{(\rho - \rho_w) + (\frac{V}{V_w})_{iso} (\rho_{iso} - \rho)}{1 - T \left[1 - (\frac{V}{V_w})_{iso}\right]} \tag{12}$$

At T = 1, the differential equation becomes:

$$\left(\frac{d\rho}{dT}\right)_{iso} = (\rho - \rho_w)\left(\frac{V_w}{V}\right)_{iso} \qquad (13)$$

The derivative for the mean density of cells from R. C. L. is 0.059 g. cm.$^{-3}$. This value is correct only when the BSA solution is isotonic at a density corresponding to the midpoint of the cells, 1.0836 g. cm.$^{-3}$. This value, however, can be used as a good approximation in experiments with shallow tonicity gradients, providing the distribution is centered near the isotonic region of the BSA column. In a rigorous analysis, the different values of ρ and V_w/V would have to be introduced into equation 12.

The physical density gradients in this study are approximately $d\rho/dr = 6 \times 10^{-3}$ g. cm.$^{-4}$, or $d\rho/dV = 6 \times 10^{-3}$ g. cm.$^{-6}$ in the SW 39 tube. It is readily possible, as indicated by equation 11, to prepare positive, zero, or negative effective density gradients by appropriate adjustment of the salt level in the initial BSA solutions. A value of $dT/dV = -0.1$ per cm.$^{-3}$ results in a zero effective gradient.

In the case of positive effective density gradients, tonicity gradients may be used to spread or narrow the distributions. This spreading or narrowing can be achieved with the same physical gradient but differing concentrations of nonpermeable solutes in the

dilute and concentrated BSA solutions used in formation of the BSA columns. If the dilute solution is less than isotonic and the concentrated solution greater than isotonic, then a positive tonicity gradient will be superimposed on the physical gradient. This discussion will be simplified with the assumption that the midpoint of the distribution occurs at the isotonic position in the BSA column. If a cell possesses a density greater than the midpoint buoyant density, it will be centrifuged into a hypertonic BSA solution, and its buoyant density will increase due to a loss of water. It will thus come to rest at a denser position in the gradient. Conversely, a light cell will be centrifuged into a hypertonic BSA solution and become lighter because of the absorption of water. These effects broaden the distribution as would a shallower physical gradient. Thus, a positive tonicity gradient decreases the effective density gradient.

In the opposite case, when the dilute solution is hypertonic and the concentrated solution hypotonic, the light cells will be at lower water activity and become denser; the dense cells at higher water activity become lighter. These effects narrow the distribution as would a steeper physical gradient. Thus, a negative tonicity gradient increases the effective density gradient. In the case of either a positive or negative tonicity gradient, the ordering in density of the cells is unaffected. No matter how the distributions are stretched or

compressed by tonicity gradients, a one-to-one correspondence exists between all the points in the density gradients as long as the effective gradients remain positive and linear.

If only the physical gradient is considered, the values of $F(\rho)$ and the sharpness of the distributions will vary when tonicity gradients are added to physical gradients. In order to render the distribution function independent of the effect of tonicity gradients, it may be redefined: $F(\rho)_{eff} = 1/g_o \quad dg/d\rho_{eff}$. Thus, $F(\rho)_{eff}$, when multiplied by $\frac{d\rho_{eff}}{dV} / \frac{d\rho}{dV}$, equals $F(\rho)$. This simple relationship between the expected values of the distribution functions permits the calculation of the effect of tonicity gradients on the physical distribution function, $F(\rho)$.

When the optical density profiles of the cells obtained after centrifugation in tonicity gradients are presented as distribution functions in the physical gradient, the values obtained for $F(\rho)$ at individual points in the distribution will equal the values obtained in experiments without tonicity gradients multiplied by $\frac{d\rho}{dV}^{eff} / \frac{d\rho}{dV}$. Also, since $F(\rho)$ is independent of the physical gradient, the resolution in density at any two points, e.g. the width at half maximum, should be reciprocally related to the above quantity. Any two points on the distribution represent discrete density fractions, which are capable of being rebanded separately from the rest of the buoyant

density distribution. The effective density gradient can be measured from, and is reciprocally related to, the distance or density range between these fractions.

D. Experimental Results

In figure 22, the results of three experiments with approximately the same physical gradient, but widely different positive effective density gradients, are shown. The full line is the control distribution obtained without a tonicity gradient, $\frac{d\rho}{dV}_{eff} / \frac{d\rho}{dV} = 1.00$, the dotted line is the distribution obtained with $\frac{d\rho}{dV}_{eff} / \frac{d\rho}{dV} = 1.68$. The tonicities of the concentrated and dilute BSA solutions were 0.80 and 1.20, respectively. In this experiment, the distribution was sharpened by the negative tonicity gradient. The dashed line is the distribution with $\frac{d\rho}{dV}_{eff} / \frac{d\rho}{dV} = 0.72$. The tonicities of the concentrated and dilute BSA solutions were 1.10 and 0.90. In this experiment, the distribution was broadened by the positive tonicity gradient. The ratios of the maximum height and reciprocal of the widths at half maximum from both of the experiments which had tonicity gradients to the values obtained in the control experiment are in reasonable agreement with the values of $\frac{d\rho}{dV}_{eff} / \frac{d\rho}{dV}$. For the sharp distribution, $\frac{d\rho}{dV}_{eff} / \frac{d\rho}{dV} = 1.68$, the ratio of the maximum height to that of the control was 1.52, and the ratio of the reciprocal

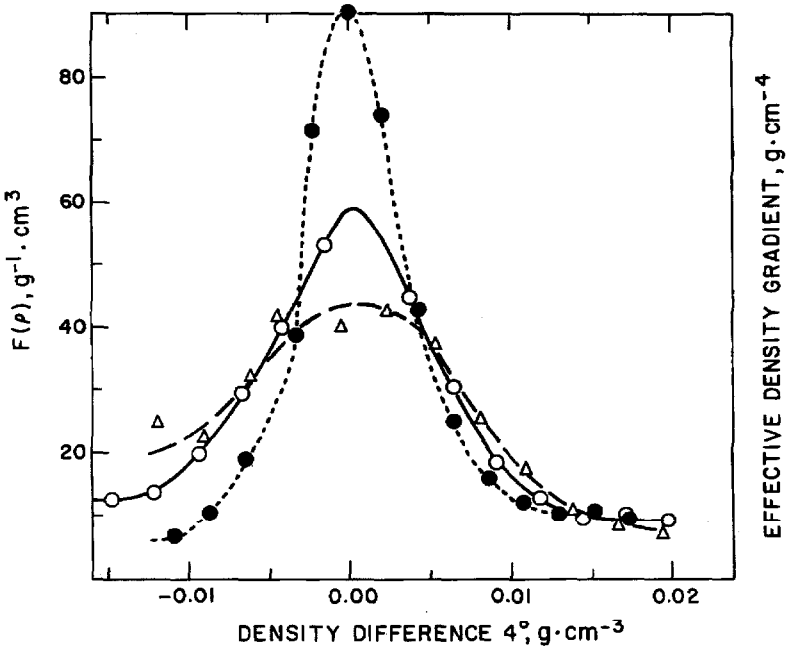

Figure 22.--Effect of salt gradients on the buoyant density distribution of erythrocytes in a BSA density gradient. Solid line: distribution obtained with no salt gradient. Dotted line: distribution obtained with $(d\rho/dV)_{eff}/(d\rho/dV) = 1.68$. Tonicities of the concentrated and dilute BSA solutions were 0.80 and 1.20, respectively. Dashed line: distribution with the above ratio = 0.72. Tonicities of the concentrated and dilute BSA solutions were 1.10 and 0.90, respectively.

of the width at half maximum to that of the control was 1.89. These quantities for the broad distribution, $\frac{d\rho}{dV}_{eff} / \frac{d\rho}{dV} = 0.72$, were, respectively, 0.74 and 0.67.

E. Zero and Negative Effective Gradients

A zero effective density gradient corresponds to a neutral density separation. A negative effective density gradient results in a complex distribution, which is dependent on the initial location of the cells. If the cells are introduced above their buoyant density, they will float because they continuously become less dense than the suspending BSA solution. Conversely, if they are introduced below their buoyant density, they will sink because they continuously become denser than the BSA solution.

F. Advantages and Disadvantages of Tonicity Gradients

The main advantage of the use of tonicity gradients is the increased resolution of the buoyant density distribution obtainable without reducing the physical gradient. It is possible that cell populations of the same buoyant density could be fractionated due to differences in $d\rho/dT$ with the use of tonicity gradients. A possible

disadvantage is that the cells will be exposed to a nonphysiological condition.

V. ERYTHROCYTE AGE AND BUOYANT DENSITY

A. The Relationship between Erythrocyte Age and Buoyant Density

Many reports of the separation of young from old erythrocytes have appeared in the literature (12, 16, 18, 19, 59, 60, 61). Except for the procedure of serial osmotic lysis (62, 63), these separations are usually based on "density." Centrifugally packed cell masses which presumably contain cells stratified by density are fractionated layer-wise (18, 19). This density gradient of cells is far more viscous than the BSA gradients used in the experiments presented in this thesis. The data of Garby and Hjelm (19) are the most recent, and appear to be the best yet obtained with this method. The youngest and oldest cells were found, respectively, at the top and bottom of the packed cell mass, but cells of intermediate ages were apparently not fractionated. Another pulse labeling experiment similar to the one below has been reported by P. Clark (64). In her experiments, the density gradients were formed by layering several BSA solutions of differing concentration. Reproducible distributions of radioactivity were not obtained in this work.

In view of the above reports, a quantitative fractionation of erythrocytes by buoyant density might be expected to provide material for the study of the physical and chemical changes in erythrocytes associated with aging. Quite possibly, density fractions

of populations of other cell types would also provide cell fractions of differing age or degree of maturation.

Any hypothesis which correlates aging with buoyant density must take into account the following facts. The buoyant density distribution remains constant in an individual. The total number of cells at each density remains constant, a result which is given in the next section. The total number of cells in the circulation of an animal is a steady state; the input of new, young cells equals the removal of old cells from circulation. The removal of old cells in man is very selective and appears to involve mainly those cells which have been in circulation for approximately 120 days (65, 66, 67). In the rabbit, the removal of old cells is qualitatively similar. In this animal, the survival time is 45-70 days (68, 69, 70). The removal mechanism, however, appears to be less selective in rabbits because there is some removal of erythrocytes at ages considerably less than 60 days (68, 69, 70). In the formulation of the following first hypothesis, the survival time of all of the cells will be considered constant. Thus, the number of cells at any given age equals the number of cells at any other given age. This is a very good approximation for human cells (65), except for the very old cells 14 or less days before their removal from the circulation.

The simplest hypothesis (figure 23), which takes account of the above, invokes a push-pull mechanism. The newly formed

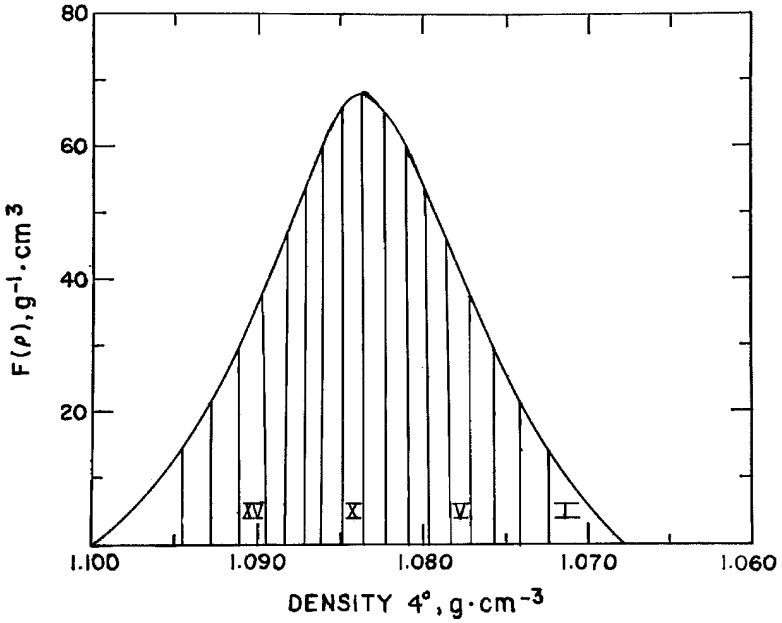

Figure 23.--Hypothetical aging of human erythrocytes. The buoyant density distribution is from figure 13. The tails at both the light and dense edges of the distribution have been added. The Roman numerals refer to time in weeks after entrance of the cells into the circulation. The idealized density range of the cells as they progress through the distribution is shown by the vertical divisions.

erythrocytes would be homogeneous in density and distributed in a narrow band at the lighter edge of the density distribution. These cells would progress linearly with time as lamellae of equal areas through the bell-shaped distribution until they reach a dense position at the end of the distribution and are removed from circulation. In consequence of the simple linear progression of the lamellae, the velocity of the motion through the density gradient must be inversely proportional to the concentration of cells in each lamella. Such a model from a teleological point of view would be quite plausible. During maturation, the young cells, upon leaving the bone marrow, rapidly increase in density. Upon maturation of the cells, the density increasing process slows down so as to pile them up in the center of the density distribution, the optimum physiological state. The mature cells sojourn here for the bulk of their lifetimes, and finally, when their hemoglobin has aged and is no longer physiologically useful, again rapidly increase in density until they are removed from circulation.

In vivo pulse labeling with radioactive iron has previously been used to determine erythrocyte life spans (68, 69) and to follow the physical separation of young from old erythrocytes (18, 19, 59, 61). A study of the time dependence of the relationship between the Fe^{59} labeled cell distributions and the unlabeled cell distribution will be presented in the following experiments. Rabbit erythrocytes were the

test material. The isotope, Fe^{59}, is irreversibly incorporated in the erythrocyte (71). The erythrocyte iron is situated almost entirely as the nondiffusible heme in the hemoglobin molecule (72). Upon the demise of the old erythrocytes, the iron is recycled with ca. 80% efficiency into the new erythrocyte (73). This recycling may be expected to obscure the progress of the label at late ages. Recycling, however, provides evidence that the hematopoetic activity of the bone marrow has not been greatly altered by the presence of the radioactive material.

It was felt that a test of a new method, no matter how interesting, did not warrant the exposure of human volunteers to 100 μ curie doses of Fe^{59}. The packed rabbit erythrocytes stratify by density and age similarly to human cells (60, 62). In a later section of this thesis, data from this experiment with rabbit cells will have to be applied in conjunction with volume distributions and cytological data from the density fractions of human erythrocytes to provide the basis of a discussion of erythrocyte aging. This mingling of data from two orders is frequently necessary in the development of provisional biological theories.

Two adult buck rabbits, #63 and #64, were each injected in a marginal ear vein with 12 microcuries of $Fe^{59}Cl_3$, and a third, #62, with 6 microcuries. The specific activity of the iron was

5.5 millicuries/mg. The $Fe^{59}Cl_3$ was diluted for injection with a buffer which was 0.005 M. in KH_2PO_4 and 0.15 M. in NaCl. The pH of the buffer was adjusted to 3.5 by the addition of 1.0 N. HCl. The buffered $Fe^{59}Cl_3$ solutions were supplied by Dr. G. Keighly.

B. Determination of Radioactivity

The hemoglobin in the saponin lysates was precipitated with 0.5 ml. of 50% TCA solution. These fractions had been previously separated from BSA as described in section II-H. Enough residual BSA was present to act as carrier in the fractions. The precipitates were centrifuged fifteen minutes at 1000 rpm in the International refrigerated centrifuge, separated from the supernatant by decantation, finely divided by the action of a Vortex mixer, washed with 2.5 ml. of 5% TCA, and dissolved with the use of the Vortex mixer in 0.5 ml. of 50 V. % acetic acid and formic acid. The tubes were allowed to stand for at least 90 minutes to insure dissolution of the precipitates. The solutions were then decanted in two steps onto glass planchets, which were dried under an infrared lamp after each decantation. The tubes were washed out with 0.3 ml. of the acid mixture, which was plated onto the same planchet. The dried glass planchets were mounted on sand-blasted aluminum planchets.

This raised the glass planchets closer to the counter window and protected the planchet holders from contamination. Radioactivity was assayed for the time required for one-thousand counts with a Nuclear Chicago low background counter. The background was 2.5 cpm with glass planchets. The radioactivity profile was normalized and presented in exactly the same way as the absorbance profile.

Results

The detailed results of the absorbance, radioactivity, and specific activity, cpm/mg, obtained from all of the experiments performed with the bloods of the three rabbits, #62, #63, #64, are presented at the end of this section. The labeled cells first appear in the lighter fractions. In time, these cells become denser. The width of the distribution generally increases with time.

In figure 24 are presented three distributions of radioactivity and one of absorbance from the same rabbit, #64. The absorbance distribution is from the experiment performed two days after injection of the label. The positions on the density coordinate of the other two distributions of radioactivity, 16 and 35 days after injection, were determined by matching their midpoints of absorbance with that of the two-day distribution. The values of $F(\rho)$ of the 16- and 35-day distribution of radioactivity were corrected by the ratio

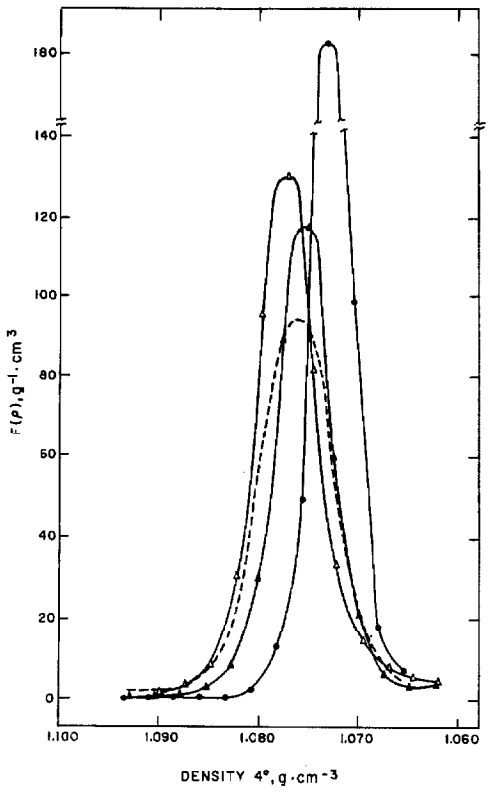

Figure 24. -- Buoyant density distributions of radioactive erythrocytes from rabbit 64. ●, Two days after injection of $Fe^{59}Cl_3$; ▲, 16 days; Δ, 35 days. The dashed line represents the erythrocyte distribution. Other distributions from this rabbit and rabbits 62 and 63 are given in figures 26, 27, and 28.

of the maximum of the two-day distribution of absorbance to that of the maximum of absorbance of the experiment from which the radioactivity distribution was obtained.

In the initial, two-day, distribution shown in this figure, about 72% of the label is found in two adjacent fractions that contain 24% of the cells. After 35 days, the densest distribution of radioactivity shown in figure 24, the band width of the label has increased so that only 43% of the label is found in adjacent fractions, that contain 33% of the cells. The distribution of radioactivity can also be characterized by the absence of the label. At two days after injection, only 1.2% of the label is present in the densest 22% of the cells. After 35 days, the radioactivity is significantly displaced from the light wing of the absorbance distribution. Only 25% of the label is present in the lightest 43% of the absorbance.

The midpoint of the Fe^{59} distribution progresses linearly with time through the first 60% of the cell distribution (figure 25). Further motion of the midpoint is hidden by the recycling of the label. After ca. 40 days, the Fe^{59} that has been released upon the death of old cells and reutilized in new cells begins to be significant in the distribution. That this recycling has occurred can be shown by comparing the distributions of radioactivity from rabbit #62 at 43 and 62 days after injection (figure 26). The distribution of

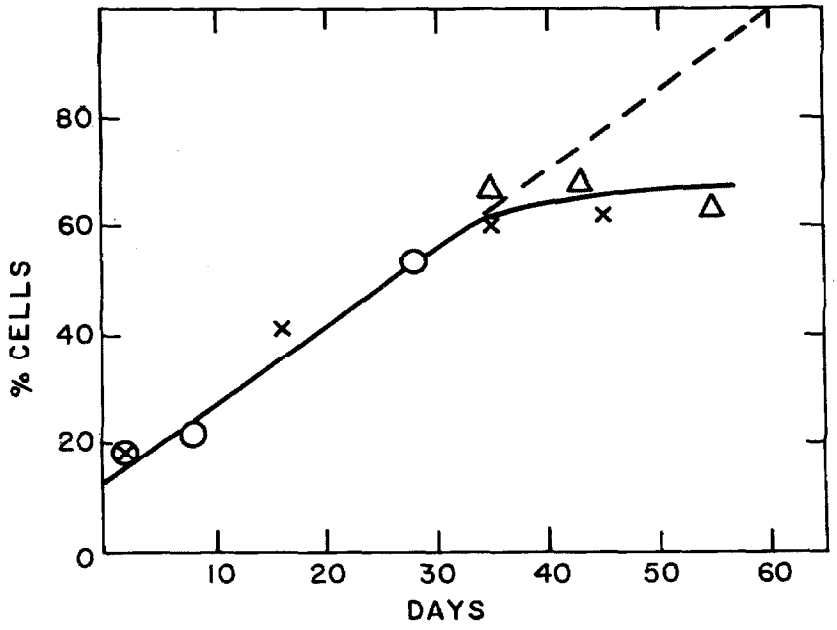

Figure 25.-- Progress of the midpoint of the radioactivity through the erythrocyte distribution. Results from three rabbits: 62, Δ; 63, O; and 64, X.

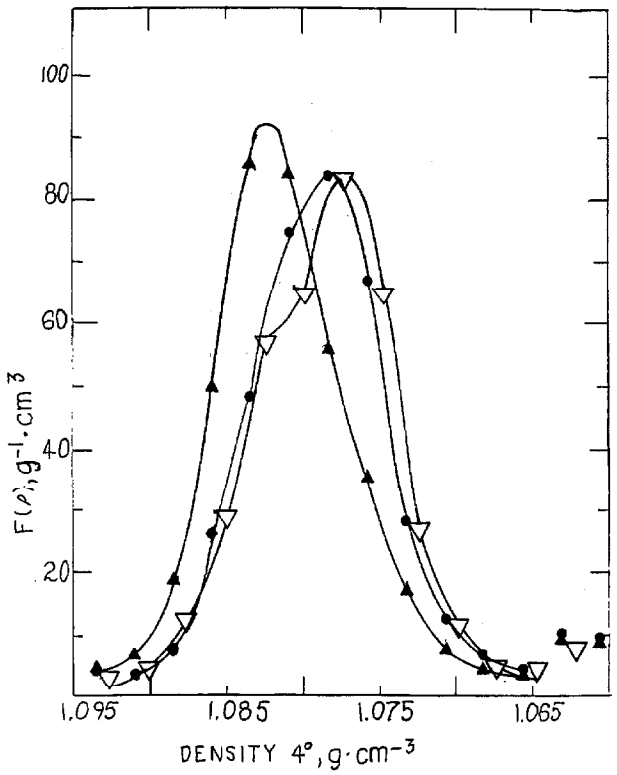

Figure 26.--Buoyant density distribution of erythrocytes showing recycled radioactivity. ● Absorbance distribution and radioactivity distribution ▲ 43 days after injection of $Fe^{59}Cl_3$; radioactivity distribution ▽ 62 days after injection. Note the distribution of radioactivity at 62 days appears at lower densities than the 43 day distribution.

radioactivity at 62 days is at lighter buoyant densities than at 43 days. From ca. 30 days onward after injection, the specific activity profiles begin to look bimodal. This is probably an indication of recycling. However, as the distribution of radioactivity spreads over the distribution of absorbance, the specific activity will begin to look bimodal because of the bell shape of the distribution. If the value of $F(\rho)$ for the radioactivity were to remain constant over the entire distribution of absorbance, the distribution of specific activity would be bimodal. Also, as has been mentioned in section III-D of this thesis, the lighter cells always become contaminated with the denser cells. The recycling does show that the erythropoetic system of the animal is not greatly affected by exposure to the isotope.

The extrapolated intercept of the motion of the midpoints is 61 days with a graphical uncertainty of about $\pm$ 5 days. The result agrees with the reported lifespan of the rabbit erythrocyte, 45-70 days (68, 69, 70). The agreement is consistent with the notion that the progression of the label through the distribution corresponds to the aging of the red cells. The non-zero intercept of the midpoint is attributed to the drainage errors mentioned previously. It might be added that these drainage errors and other previously mentioned artifacts of fractionation always decrease the resolution of the system.

Discussion

The initial width of the distribution of radioactivity is approximately eight times that expected from the hypothesis. The radioactivity as stated above is at two days concentrated in 24% of the cells instead of the 3 per cent of the distribution expected for 2 out of 60 days. This widening cannot be due entirely to artifacts of fractionation, because in the rebanding experiment, only a doubling in width was found, and in part this doubling was caused by the failure to fractionate in phase with the original gradient. Also in contradiction to the hypothesis, the width of the distribution of radioactivity appears to be increasing with time. According to the proposed hypothesis, the radioactivity was to occupy lamellae of equal area in the distribution of absorbance. The width of the distribution of radioactivity was, therefore, supposed to decrease in order to compensate for the increasing concentration of absorbance.

The linear progression of the midpoint, which agrees with the hypothesis, and the widening, which disagrees, suggest that the initial hypothesis is an oversimplification of the relationship of aging and density. The density of the average cell is apparently directly related to age, but the density of an individual cell is not directly related to age. In section VII-A, a provisional theory of erythrocyte development consistent with the above data and the data

in other sections of this thesis will be presented.

The ability of the buoyant density method to separate very young cells from the rest of the cell population is indicated by the ratio of the extremes of specific activity (742 to 10 c.p.m./mg.) in the two-day distribution of cells from rabbit #64. The residual activity found at the bottom of the density distributions at early times may be a contamination by light cells brought down with the glass capillary used for sampling, or may be a resultant of the rapid aging of a very small population of cells (63, 74) or of the release of defective, stillborn, cells from the bone marrow.

PLEASE NOTE: Figure 27 not received with dissertation. Filmed as received.

UNIVERSITY MICROFILMS, INC.

Figure 27.--Results of individual experiments with cells from rabbit #63. Buoyant density distributions of radioactivity, ▲; absorbance, ●; and specific activity, □ . The values of the specific activity in cpm/mg. are the values given in the ordinate for $F(\rho)$. The time in days after injection of $Fe^{59}CL_3$ is indicated at the bottom of the individual figures.

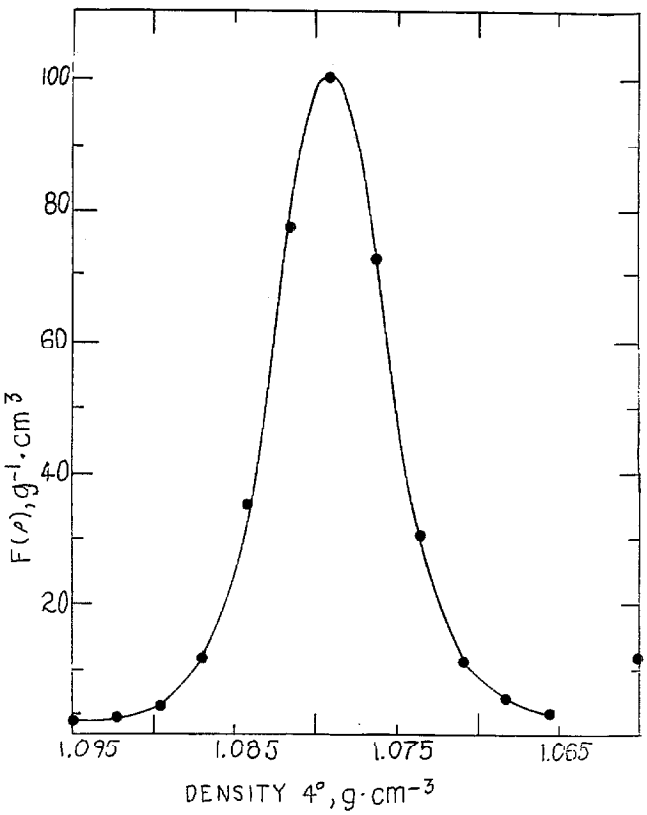

Figure 27a. -- Buoyant density distribution of absorbance obtained prior to injection. The densities were determined with a pycnometer.

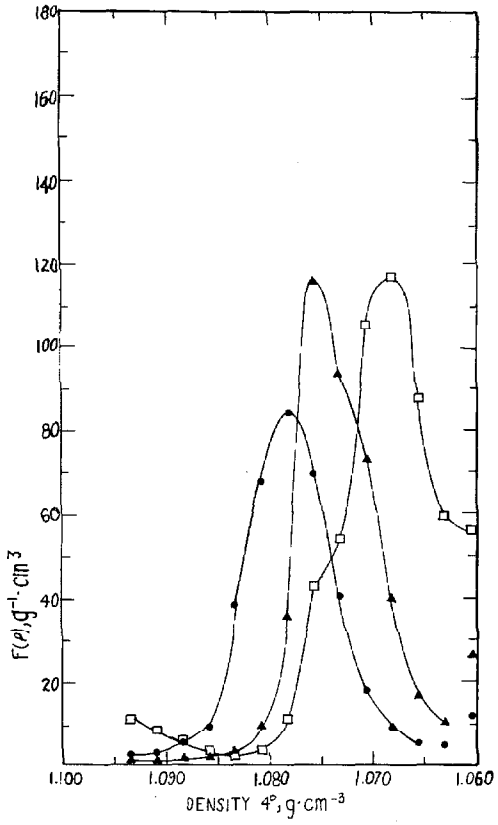

Figure 27b. -- 2 days after injection.

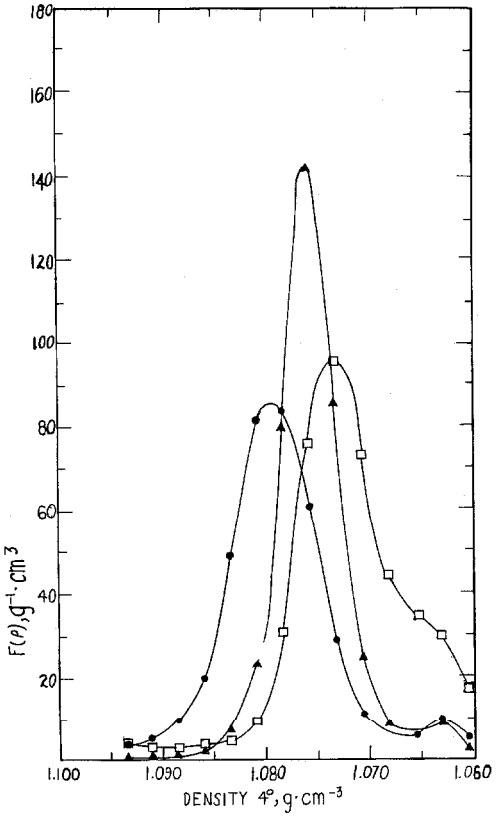

Figure 27c. -- 8 days after injection.

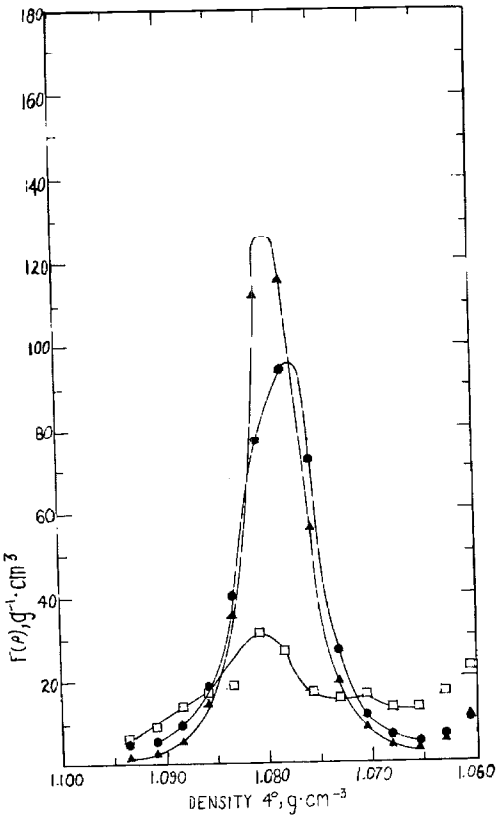

Figure 27d. -- 28 days after injection.

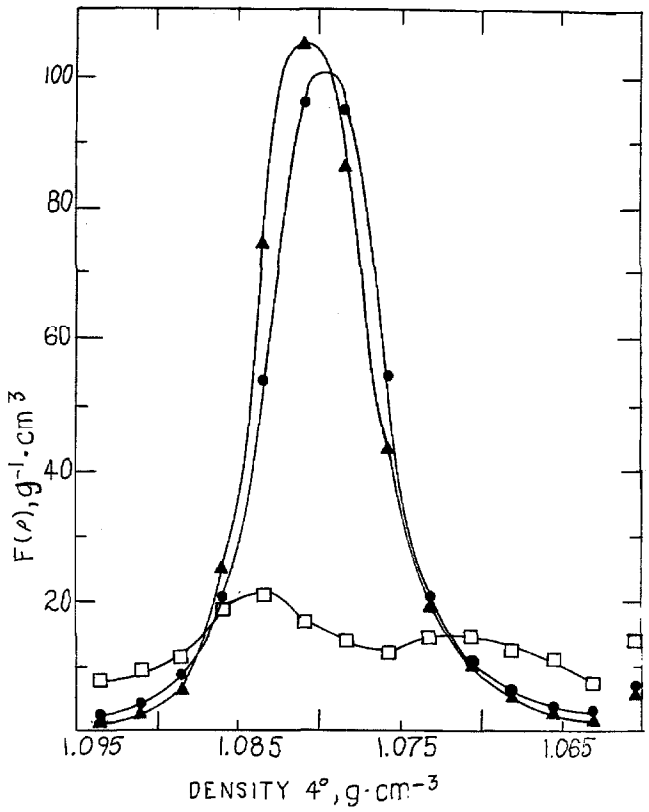

Figure 27e. -- 49 days after injection.

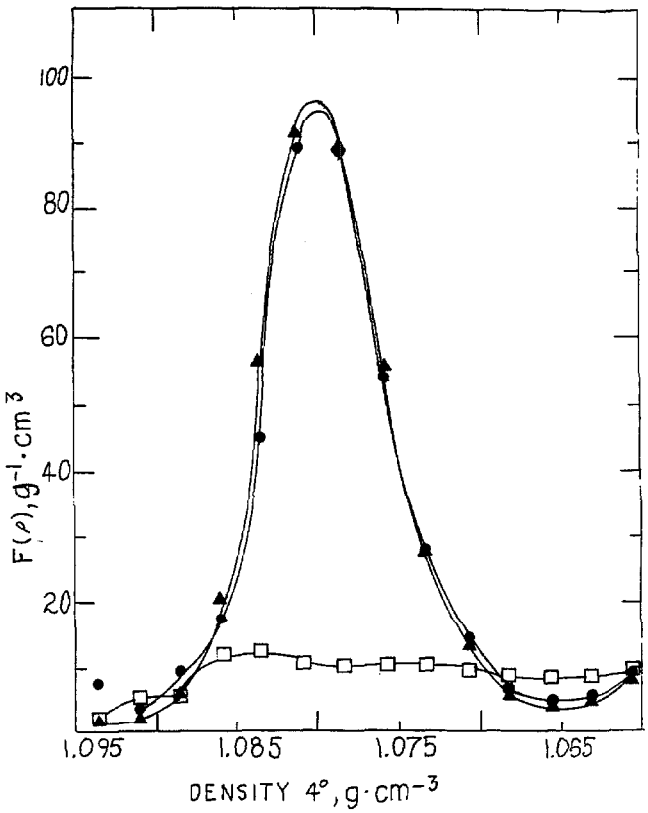

Figure 27f. -- 57 days after injection.

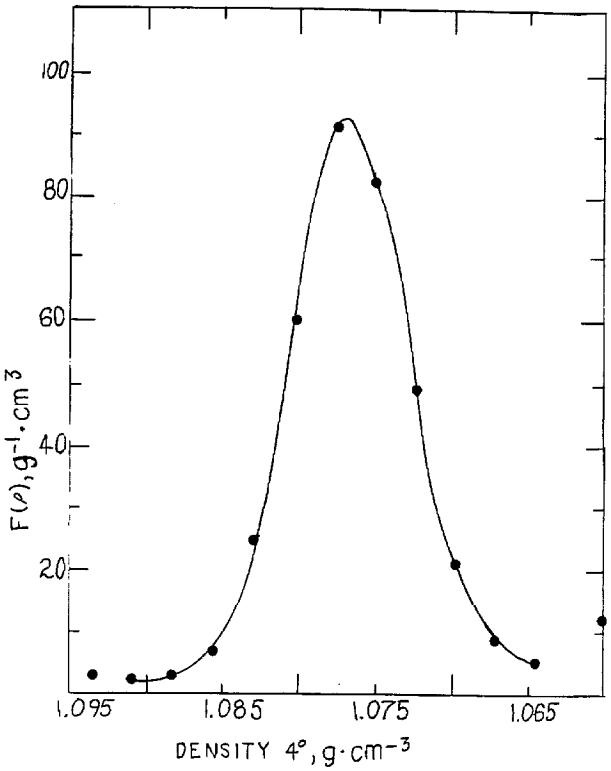

Figure 28. -- Same as figure 27, but distributions obtained with cells from rabbit #64.

Figure 28a. -- Buoyant density distribution of absorbance obtained prior to objection. The densities were determined with a pycnometer.

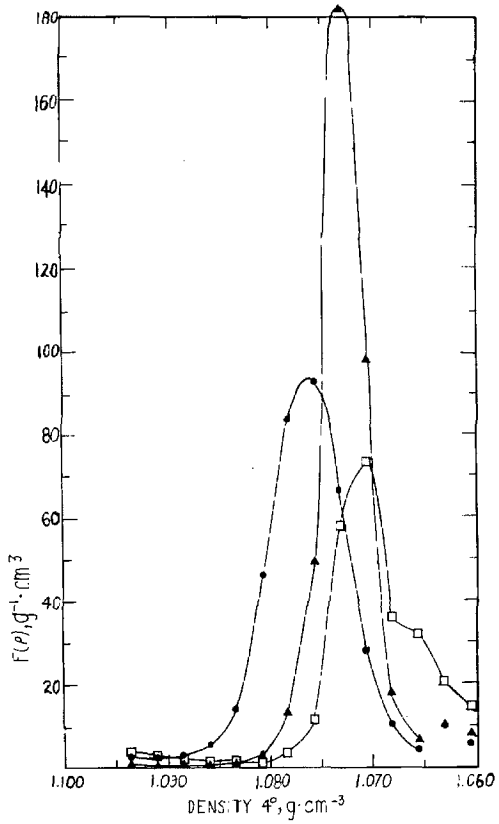

Figure 28b. -- 2 days after injection.

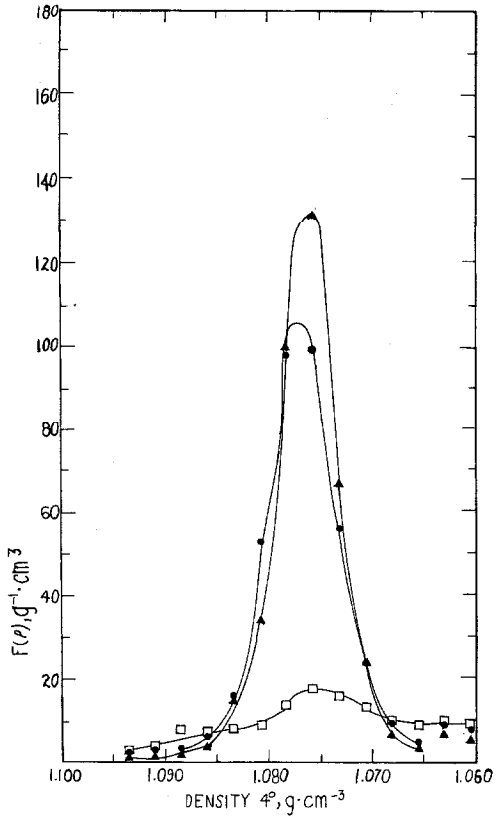

Figure 28c. -- 16 days after injection.

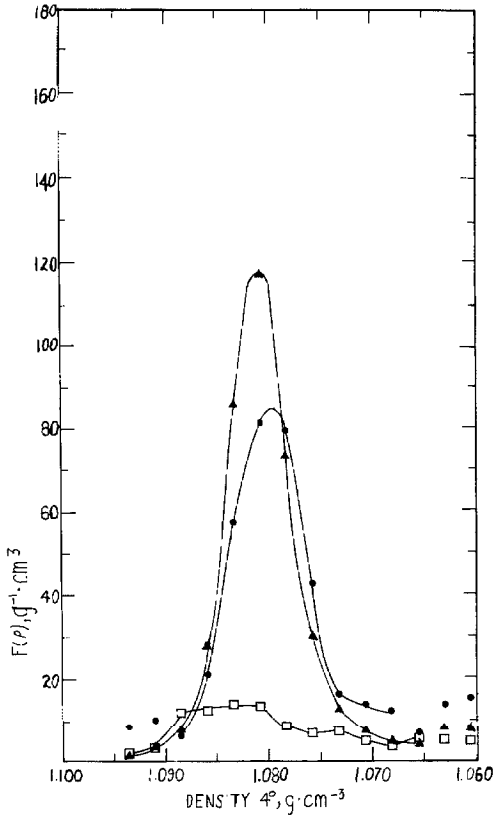

Figure 28d. -- 35 days after injection.

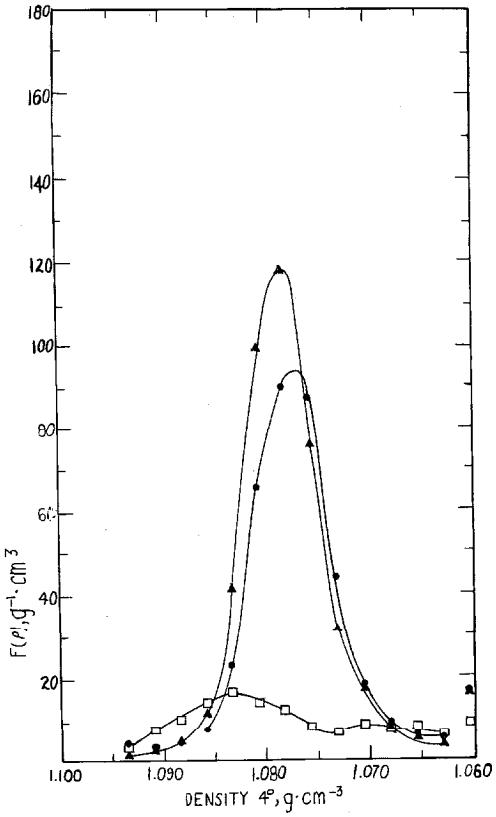

Figure 28e. -- 45 days after injection.

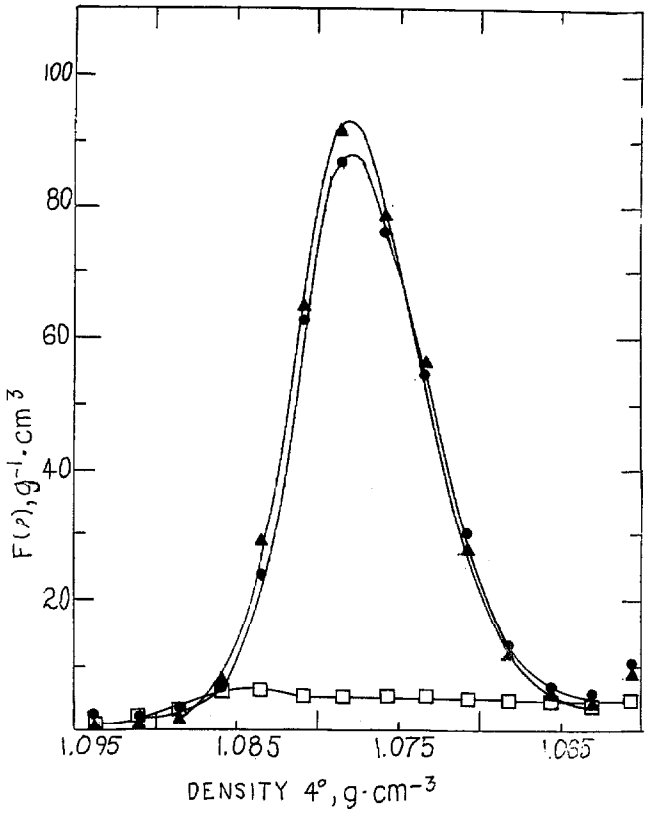

Figure 28f. -- 60 days after injection.

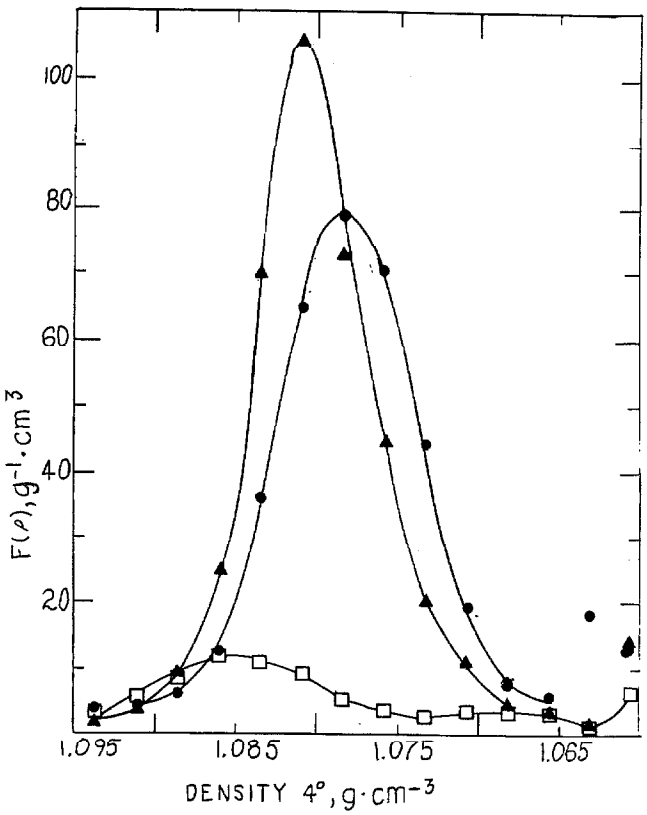

Figure 29. -- Distribution of cells from rabbit 62 at 35 days after injection. Buoyant density distribution of radioactivity, ▲ absorbance, ● , and specific activity, □ . The ordinate values for F(ρ) are also the values of the specific activity in cpm/mg.

VI. CHARACTERIZATION OF THE DENSITY FRACTIONS

A. The Relationship between Buoyant Density and Cell Volume

Price-Jones (76) was the first to show that human erythrocytes constitute a heterogeneous population in size. He measured the dimensions of erythrocyte preparations microscopically. At the present time, this heterogeneity in size is more easily and accurately observed in volume distributions obtained with the Counter-Counter (38). Cell volume distributions of the individual buoyant density fractions of the blood from R. C. L. were determined with this instrument. The detailed results of these determinations are presented at the end of this section.

The measurements were undertaken for two reasons. A change in density can be regarded as a change in mass or a change in volume or both. Assays of the cell volumes and hemoglobin content would indicate the contribution of volume and mass changes to the buoyant density changes. In addition, a correlation between buoyant density and chronological age has been observed in the previous section, and it was desirable to extend this correlation to changes in volume. With data on both the buoyant density and the volume changes which occur upon aging, the preliminary description of cell aging given in the last section will be improved.

In the discussion of the cell volume distribution, the notion of a steady state is again invoked. Just as the input of young cells equals the removal of old cells, the input distribution of cell volumes must be the same as the output distribution of cell volumes. In this case, however, the cells may continually and uniformly change in volume while in circulation.

Three simple hypotheses for the relationship between the cell volume distribution and the buoyant density of the fractions from a sample of blood will be presented. In the first, it is assumed that the newly formed erythrocytes constitute a population with a uniform large volume and a uniform low buoyant density. As the cells age, they shrink and increase in buoyant density. The buoyant density changes in this and the two other hypotheses to be presented are then attributed to some change in composition of the cell. The obvious possibility is a loss of one of the major light components of the cell, most plausibly water.

This first hypothesis can be eliminated by comparing the previously published volume distributions, or those obtained from unfractionated R. C. L. cells, with the volume distribution calculated by means of equation 5 and from the density distributions of the erythrocytes (figure 13). The experimentally determined volume distributions are much wider than those calculated (figure 31, upper).

In the second hypothesis, the relationship between buoyant density and cell volume is less direct. The volume distribution of the newly formed light erythrocytes is the same as the volume distribution for the entire population. The shape of this volume distribution remains constant during the life span of the cells and correspondingly throughout the density distribution. The entire volume distribution could also dehydrate and shrink or undergo any other density increasing process during aging. If this shrinkage occurs, it should be evident in the trend of the corrected means or midpoints of these volume distributions obtained from the density fractions. These values should decrease according to equation 5 if the density increase is solely due to a loss of cellular water.

The third hypothesis is an amended version of the second. The constraint that the input of cells to the circulation and output of cells from the circulation possesses the same relative volume distribution because of the steady state requirement is still in effect. However, in contradistinction to the second hypothesis, the entire volume distribution need not be present in the initial density fraction. The input and output of the different fractions of the volume distribution could be dependent on the density. Therefore, the density range of the input, circulation, and output of the different fractions of the cell volume distribution could differ. An example of such a density dependent fractionation of the cell volume distribution might

serve as an explanation for the density range of the two-day-old rabbit erythrocytes. This density range could be ascribed to the smaller cells entering into the circulation at lower densities than the larger cells. If the density of the output of the cells possessed a volume dependence similar to that of the input, then a gradient in cell volumes would exist which could mask any density-dependent decrease in the entire volume distribution. Any such buoyant density fractionation of cell volumes would also be a fractionation by cellular dry weight, as well as by the major constituent of the dry weight, the cellular hemoglobin.

Experimental

Volume distributions of the density fractions and unfractionated cells were obtained with a Coulter-Counter B. The fractions were first diluted ten-fold by the addition of 2.7 ml. of Eagle's saline. The unfractionated cells were diluted with Eagle's saline to approximately the same cell concentration as that of the fractions. These suspensions were kept cold. One-half ml. from each of these suspensions was diluted immediately prior to counting into 100 ml. of Eagle's saline at ca. 25°C. Three determinations of the volume distributions of the unfractionated cells were performed as control experiments. In two of these, the cells were dispersed in concentrated BSA. These are referred to as the BSA controls. The third

experiment was performed with an aliquot of the sample which had been layered on the gradient column. One of the BSA controls was analyzed at the beginning and the other at the end of the Coulter-Counter analyses. In all experiments, the number of cells were counted before and after the size distribution analyses, which were performed in triplicate. All of the volume distributions were obtained within eight hours of the finger punch collection of the blood. No significant density change occurred in 24 hours (see section III-H). In order to minimize the effect of any instrumental drift, the samples were taken in the following order: BSA control 1, bottom, 5, 10, 15, 1, 6, 11, 14, 9, 4, 2, 13, 7, 3, 8, 12, original finger punch suspension, and BSA control 2.

One ml. of the samples in Eagle's saline was centrifuged, resuspended in 2 ml. of CO-saturated distilled water. The cell lysates were centrifuged and read as before at 518 mμ. The ratio of absorbance to the number of cells counted by the Coulter-Counter is shown in Table VI. This ratio was converted to μμg per cell by equating the ratio, $\frac{\sum_{1}^{15} A}{\sum_{1}^{15} N.}$, with 30 μμg per cell, the value for the cellular hemoglobin determined at Children's Hospital, Los Angeles. The quantity N is the relative number of cells in each fraction, and the quantity A is the absorbance

at 518 mμ.

The densities of the fractions could not be measured as this measurement involves warming the fractions to room temperature. The densities were estimated from the results of previous gradients with the same BSA solutions.

The midpoints of the volume distributions were calculated as before, except that odd integral ordinate values greater than or equal to 7 per cent were averaged.

The value of the mean of the volume distributions obtained with the Coulter-Counter was found to depend on the concentration of the cells. See the results of R. C. L.(1) and(2) Table VI. The concentration of cells in the fractions is not constant; therefore, the means of the distribution had to be corrected for the concentration of cells present in the fraction. This correction factor was determined by comparing the means of two volume distributions, R. C. L. (1) and (2), of unfractionated cells from R. C. L. (figure 30). The cell concentrations were 52,800 and 6,100. The means of the distributions were, respectively, 12,61 and 12.09 windows. The midpoints were 10.47 and 10.35 windows. Windows are the volume units of the Coulter-Counter. The correction factor, therefore, is .52 windows divided by 46,700 cells, or -0.111 windows per 1000 cells. However, the difference between the midpoints of the above two distributions--

TABLE VI. Cell Volume Distributions Obtained with the Coulter-Counter

Material		#1	#2	N #1&2	Mid-point	Mean	Corr. Mean	A.	$\frac{A.}{N}$	Count #3	$\frac{\gamma\gamma}{\text{cell}}$
BSA Control 1		301	293	297	11.31	12.94	12.61			541	
BSA Control 2		228	227	227	10.85	12.65	12.40			215	
Blank		1	1	1	-----	-----	-----			1	
Unfractionated		580	578	579	10.91	12.62	11.97			541	
Fraction # and estimated density											
Bottom		77	77	77	10.09	11.58	11.49	0.030	390	72	49
1	1.0957	126	127	127	10.51	12.17	12.03	0.032	252	116	32
2	1.0937	147	161	154	10.64	12.20	12.03	0.039	253	150	32
3	1.0917	227	224	226	10.65	12.34	12.09	0.051	226	200	28
4	1.0896	369	368	369	10.82	12.67	12.16	0.081	220	342	28
5	1.0876	510	526	520	11.48	13.64	13.08	0.124	239	525	30
6	1.0855	645	638	641	11.06	13.23	12.52	0.148	231	581	29
7	1.0835	751	744	747	11.09	13.40	12.57	0.177	237	673	30
8	1.0815	745	745	745	11.15	13.44	12.61	0.181	243	745	31
9	1.0794	614	610	612	11.15	13.22	12.54	0.146	238	607	30
10	1.0774	439	436	437	11.29	13.18	12.69	0.096	219	424	28
11	1.0753	247	241	244	11.15	13.04	12.77	0.052	213	224	27
12	1.0733	117	118	118	11.17	13.00	12.87	0.028	238	116	30
13	1.0713	78	88	83	11.19	12.74	12.65	0.026	314	83	40
14	1.0692	32	38	35	11.07	12.70	12.66	0.008	230	40	29
15	-----	38	37	37	10.97	12.41	12.37	0.010	267	33	34

TABLE VI. (continued)

	#1	#2	#1&2	Mid-point	Mean	Ratio of mean to that of R.C.L.
R.C.L. (1)	537	520	528	10.47	12.61	1.00
R.C.L. (2)	64	59	61	10.35	12.09	0.95
F.W.	822	777	800		13.32	1.06
W.G.	783	778	776		13.15	1.04
A.S.	598	567	582		12.92	1.02
W.R.H.	1193	1214	1203		14.12	1.04
R.C.L. (3)	1121	1132	1126		13.53	1.00

#Expressed in hundreds.

Notes: The bottom fractions are always contaminated with some extraneous absorbance.

Cell counts 1 and 2 were performed before cell volume distribution analysis; count 3 was performed after volume distribution analysis.

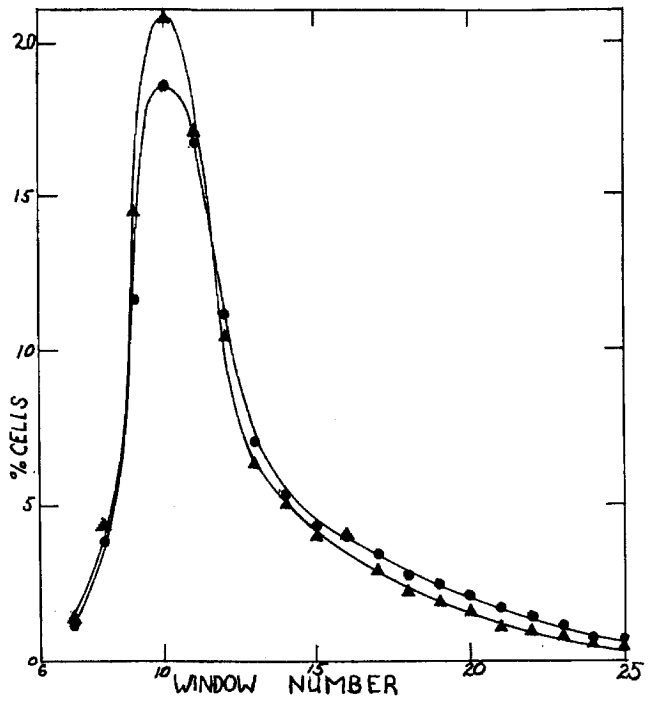

Figure 30.--Volume distribution of erythrocytes by electronic size determination. ●, R.C.L. (1); ▲, R.C.L. (2) (see table VIII). The concentration of cells in R.C.L. (1) was approximately ten times that in R.C.L. (2). Coincidences of two cells simultaneously passing through the Coulter-Counter orifice are probably responsible for shifting distribution R.C.L. (1) to larger volumes.

respectively 10.47 and 10.35 windows--is not significant. The midpoints, therefore, did not need correction. The factor to convert the corrected mean window to cubic micra 3.91 cu. micra/window was determined from the average of the corrected means of the two BSA controls and the mean cell volume of R. C. L. 86.5 cu. micra. The mean cell volume of R. C. L. was determined according to Brecher et al. (38). This determination was performed at Children's Hospital, Los Angeles. The midpoints were similarly converted into cubic micra.

Results and Discussion

Figure 31 (lower) shows the volume distributions of fractions 1, 7, and 12. These density fractions are as heterogeneous in cell volumes as the unfractionated cells (figure 31, upper). This volume heterogeneity of the fractions, together with the previously mentioned lack of agreement between the actual and calculated range of cell volumes, proves that the density fractions are not fractions of the volume or Price-Jones (75) distributions. The first hypothesis is thus eliminated from consideration.

In figures 32 (lower and upper), the solid line is the mean cell volume calculated for the density range under consideration from equation 5. For this calculation, only the water content of the cells was varied. Equation 5 gives relative volumes. The theoretical line was made to intersect the experimentally determined values at 1.0836 g. $cm.^{-3}$, the mean of the buoyant density distribution. The experimental values of the corrected means, figure 32(upper), and the midpoints, figure 32(lower) of the volume distributions of the lighter fractions remain constant, and the observed change in density, 0.0122 g. $cm.^{-3}$, on the dense side of the distribution is only in part, 0.0057 g. $cm.^{-3}$, explainable by dehydration.

The values for the cellular hemoglobin of the cells in density fractions are shown in the insert at the bottom of figure 32. The

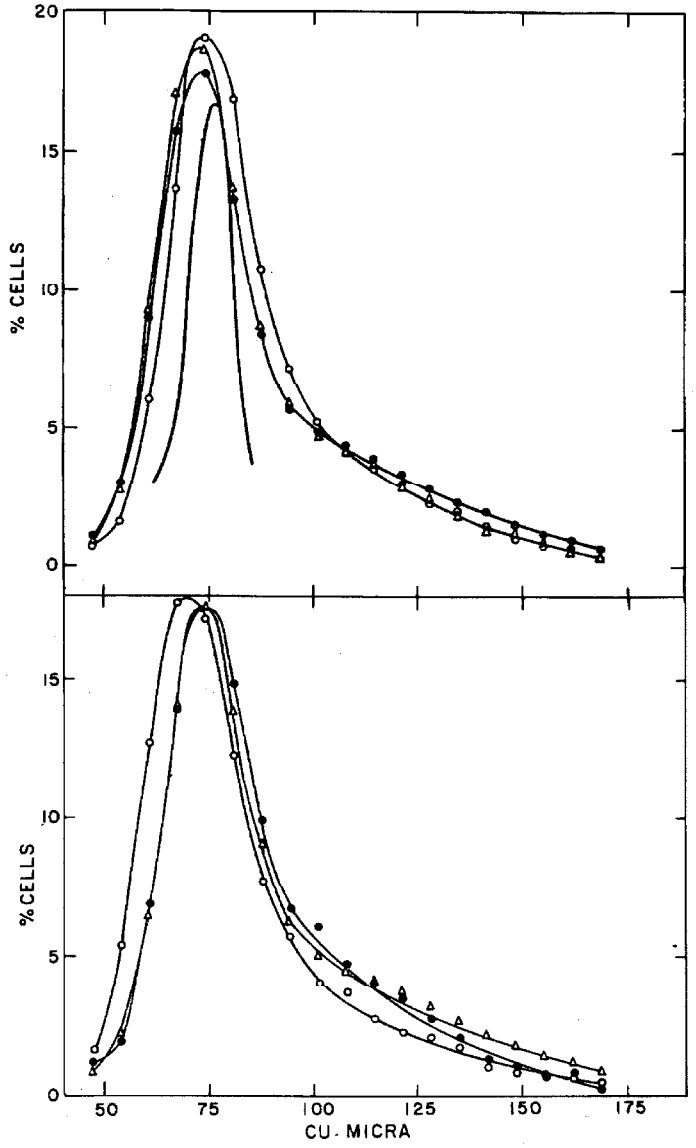

Figure 31.--Volume distribution of erythrocytes by electronic size determinations. Upper: unfractionated cells. ●, untreated cells; O, Δ, cells suspended in concentrated BSA. The narrow band is the volume distribution calculated from density distribution (figure 13) with

$$V = (\rho - \rho_0/\rho_w - \rho)\, V_0 + V_0 \quad \text{(eq. 5)}$$

where ρ_0 and V_0 are the original density and volume, respectively, and ρ_w is the density of water. Lower: fractionated cells. O, fraction 1; Δ, fraction 7; ●, fraction 12.

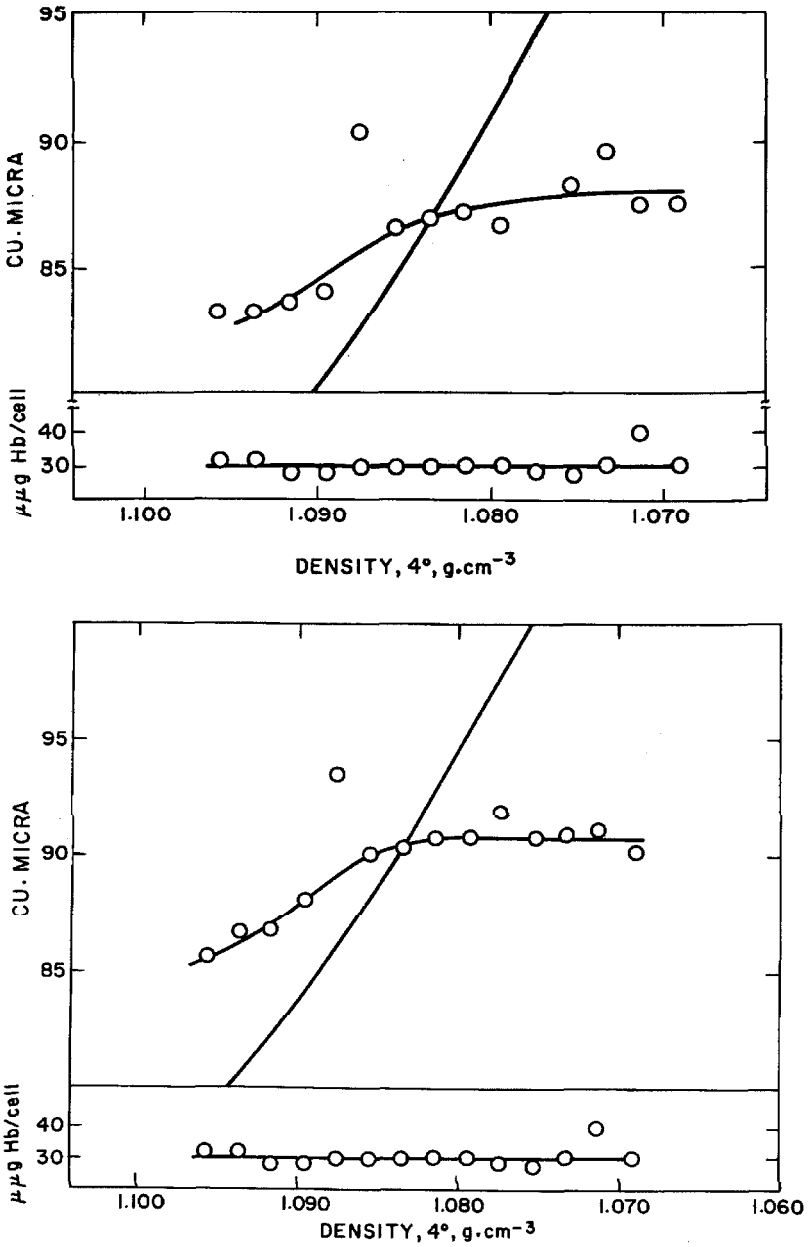

Figure 32.--Upper: mean volumes of cells in the buoyant density fractions. Lower: midpoint of the volumes of cells in the buoyant density fractions. The theoretical line in both the upper and lower graphs was calculated with the equation in the legend for figure 31 (eq. 5). Lower insert: the amount of hemoglobin per cell.

cellular hemoglobin remains constant at 30 μμg throughout the density distribution. The standard deviation is ± 5%. Therefore, no fractionation by cell volume takes place during the aging of the cells, thus eliminating hypothesis three from consideration. Hypotheses one and three having been eliminated, hypothesis two is left. In agreement with hypothesis two, the youngest cells possess a broad distribution in volumes and the rate of buoyant density increase does not depend upon cell volume. Since the volume distribution and hemoglobin content of the cells remained constant over an entire buoyant density distribution, no fluctuation in cell volume or hemoglobin content occurred during the preceding survival time of a cell, 120 days.

The main factor responsible for the range of buoyant densities, 0.0244 g. cm.$^{-3}$, is at present unknown. This range is still 0.0187 g. cm.$^{-3}$, after the change in water content is subtracted.

Both the cellular lipid and K^+ content have been shown to decrease with increasing density in fractionations of packed cell masses (59). As these fractionations by density are not complete, the observed differences between the youngest and oldest cells would tend to be smaller than those which actually exist.

Even if it is assumed, in spite of the necessary presence of lipid for the integrity of the cell wall, that the total cellular lipid is

consumed during the cellular life span, the overall lipid content (76), 5.17 mg./g. cells, is far too small to account for the density increase. A reasonable but arbitrary distribution of lipid content among the cells would be for the youngest to have twice the average lipid content and the oldest none at all. This total range, 10.34 mg./g. cells, for the cellular lipid, would result in a buoyant density shift of 0.0021 g. $cm.^{-3}$, if a value of 0.90 g. $cm.^{-3}$ is assumed for the density of the lipid. This value, 0.90 g. $cm.^{-3}$, is a very low estimate (Table VII). A density shift of 0.0166 is still left to be explained. The density gain due to the loss of cellular lipid could conceivably be greatly magnified if the cellular lipid, perhaps in conjunction with the cellular protein, organized the cellular water into clathrates (77). The loss of cellular lipid would then result in an increase in density of a larger mass of cellular water originally present in the form of the clathrate water.

The decrease in the concentration of K^+ ion that occurs as the cells increase in buoyant density cannot be responsible for this buoyant density increase. The K^+ ion is dense, and its loss certainly cannot increase the density of the cell. The Na^+ ion is less dense than the K^+ ion, and therefore replacement of K^+ ion by Na^+ ion, which occurs at least partially as the cells increase in density (59), cannot increase the density of the cells. Any osmotic effects or

TABLE VII.

VIIa. Lipid Content of Human Erythrocytes[a]

Substance	Mg./100 g. of Erythrocytes	Density
Free Cholesterol	108	ρ_{19}^{19}[b] 1.052
Cholesterol Esters	14	---
Phospholipid	272	---
Unknown	47	---
Unknown, more polar than phospholipid	74	---
Distribution of Phospholipid		
Ethanolamine phosphoglyceride	81	---
Serine phosphoglyceride	28	---
Choline phosphoglyceride	100	---
Sphingomylin	58	---

[a] Taken from Farquhar, W. J. and E. H. Ahrens, Jr., J. Clin. Invest., 42, 675 (1963). The lipid content in this paper was expressed in mg./100 ml. of packed cells; this quantity was divided by 1.08 to obtain the content in mg./100 g.

VIIb. Densities of Some Lipids and Related Substances

Substance	Density
Glycerol	ρ_{15}^{15} 1.26557[b]
Glycerolphosphoric acid	ρ 1.60[b]
Lecithin	ρ_{4}^{24} 1.0305[b]
DL Serine	ρ 1.537[b]
Tripalmitin	ρ_{4}^{70} 0.8730[b]
Palmitic acid	ρ_{4}^{64} 0.853[b]

[b] The Merck Index, Seventh Edition, P. G. Stecher, editor: Chemical Monographs, published by Merck & Co., Inc., New Jersey, 1960.

transport of water of hydration associated with the loss of K^+ ion or its replacement by Na^+ ion need not be discussed, as these volume changes would be included in the volume changes already assayed in the volume distributions of the density fractions.

B. Microscopic Examination of the Density Fractions

During the course of these studies, the morphology of the cells was examined microscopically to determine whether the BSA solutions caused any visible changes. Furthermore, the erythrocyte morphology, reticulocyte content, and distribution of white cells of the density fractions were studied.

The cells in two sets of density fractions of R. C. L. blood were examined in some detail. In one of the experiments, the cells were originally dispersed in the concentrated BSA solution. In the other, the cells were layered on top of the gradient. Both experiments gave essentially the same results. The erythrocyte morphology and white cell distribution data are from the experiment with the cells dispersed in the concentrated BSA solution. In both experiments, the fractions were diluted 10-fold with Alsever's solution. One-half ml. aliquots were removed for later absorbance determinations of the hemoglobin. The cells from each of the fractions were centrifuged, resuspended in 0.2 ml. of homologous

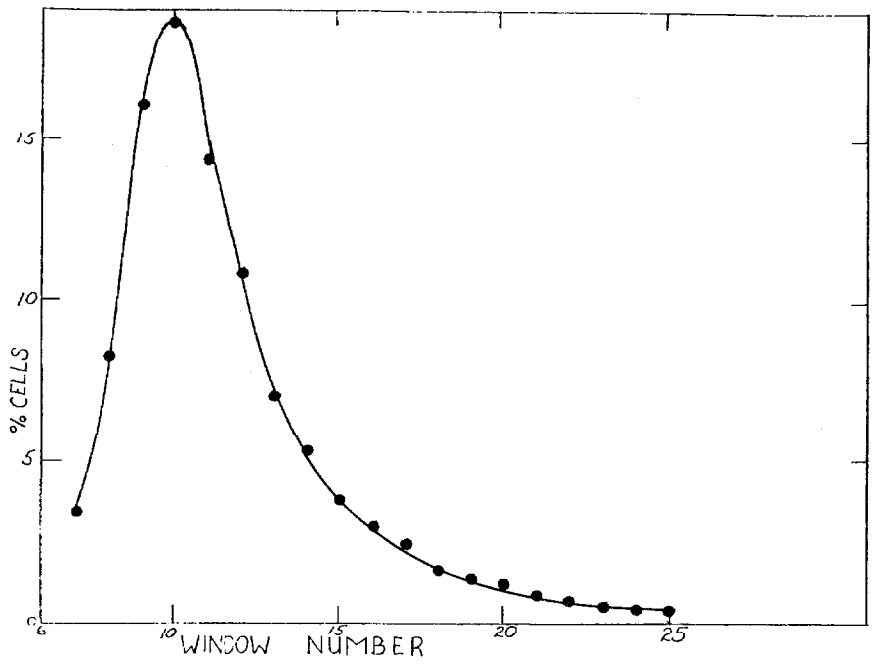

Figure 33.--Volume distributions not shown in figure 31. The number of the fraction from which the cells were obtained is shown at the bottom of each figure.

Figure 33a.-- Bottom fraction.

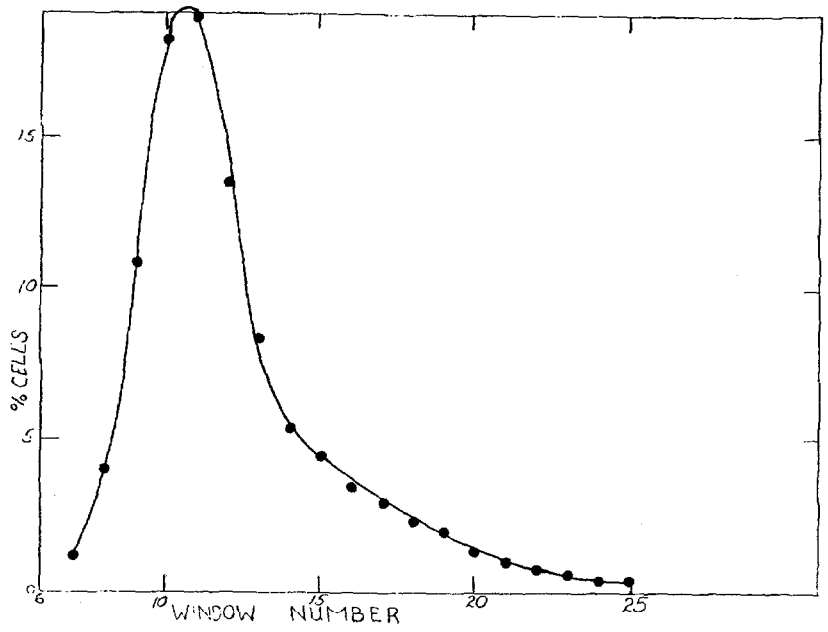

Figure 33b. -- Fraction 2.

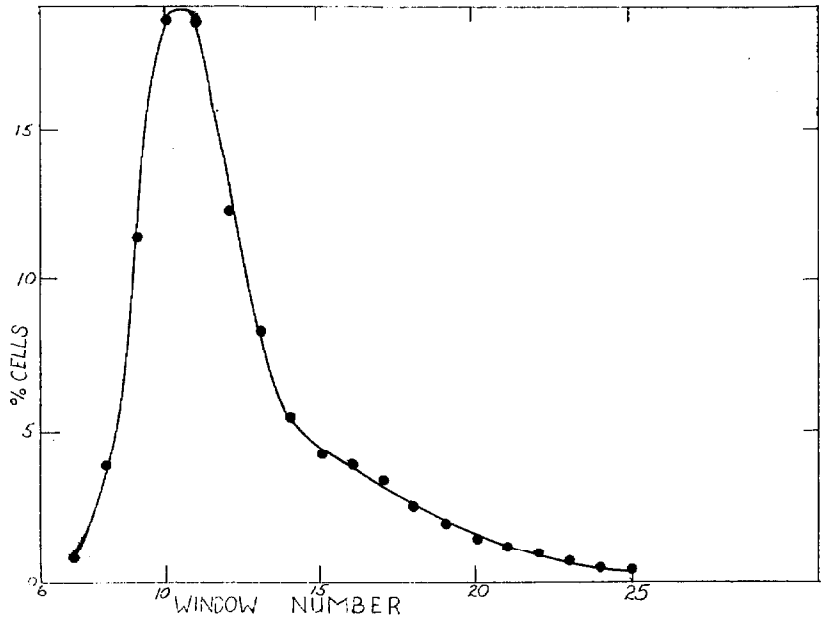

Figure 33c. -- Fraction 3.

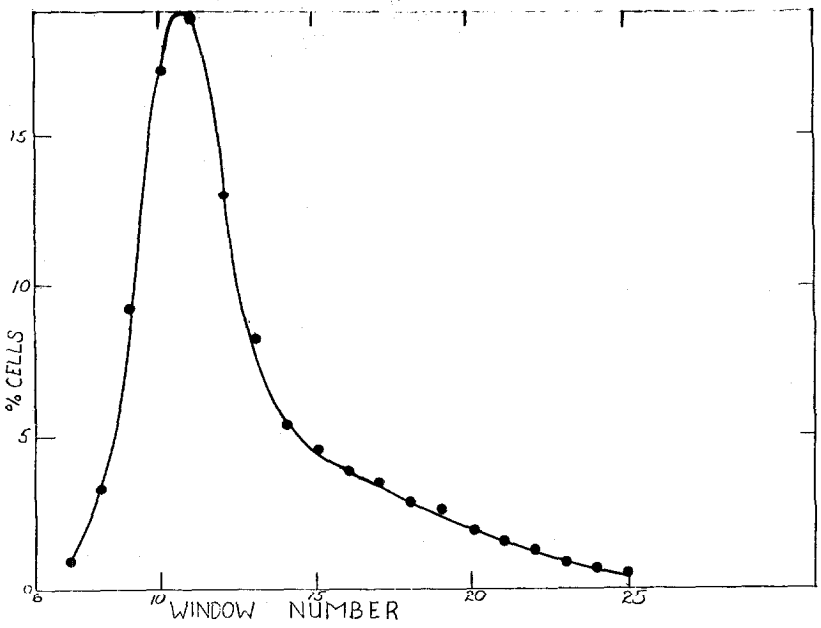

Figure 33d. -- Fraction 4.

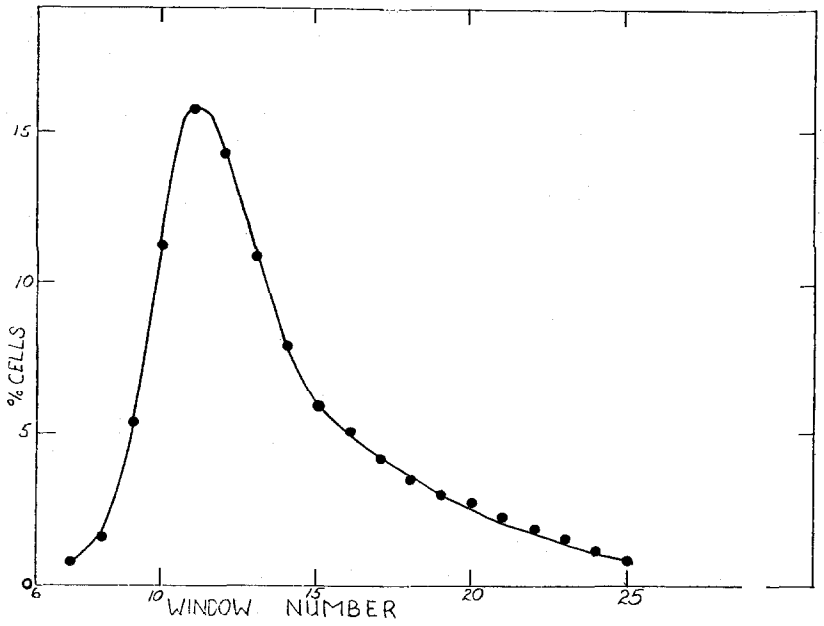

Figure e. -- Fraction 5.

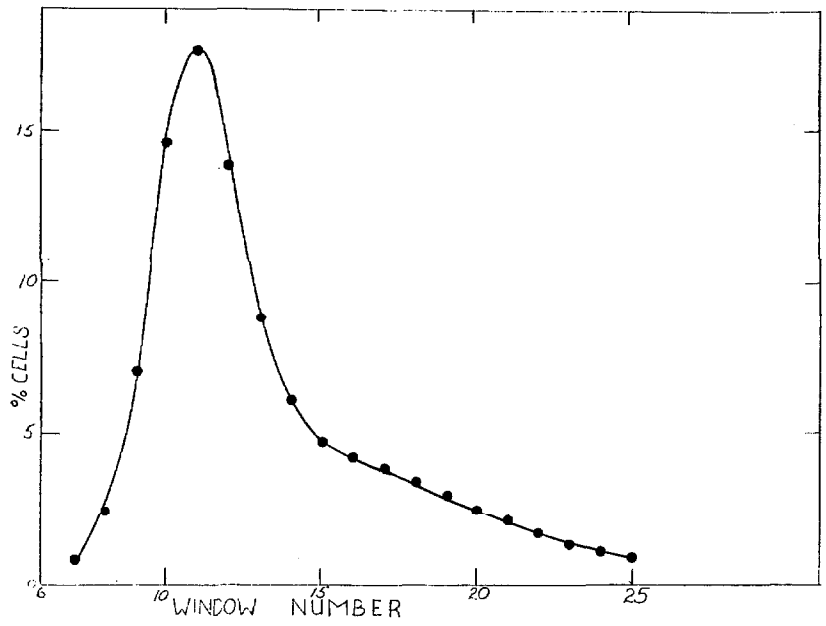

Figure 33f. -- Fraction 6.

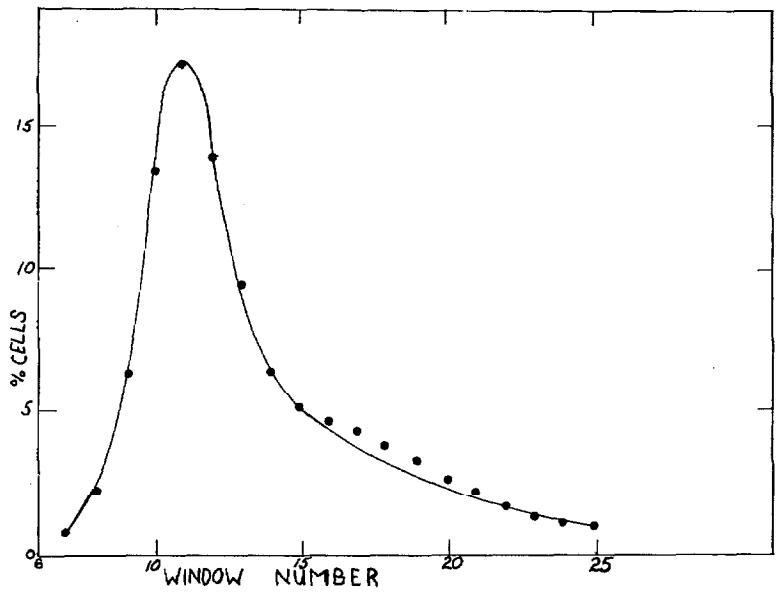

Figure 33g. -- Fraction 8.

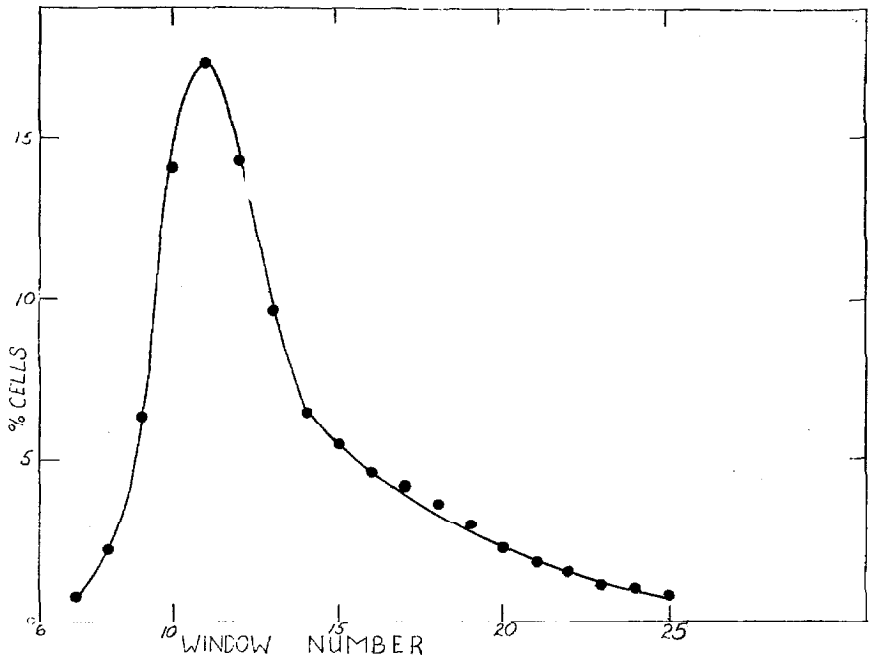

Figure 33h. -- Fraction 9.

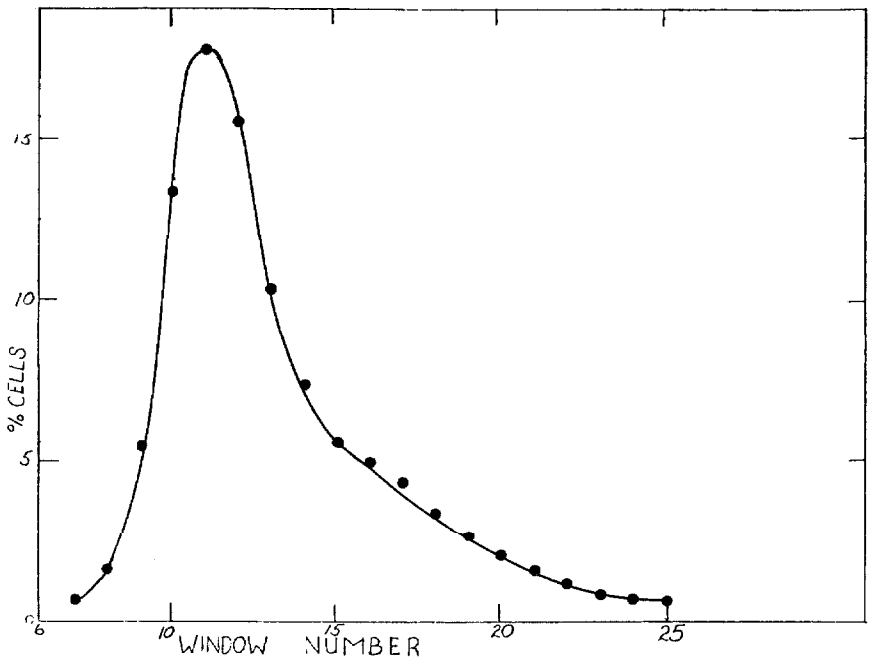

Figure 33i. -- Fraction 10.

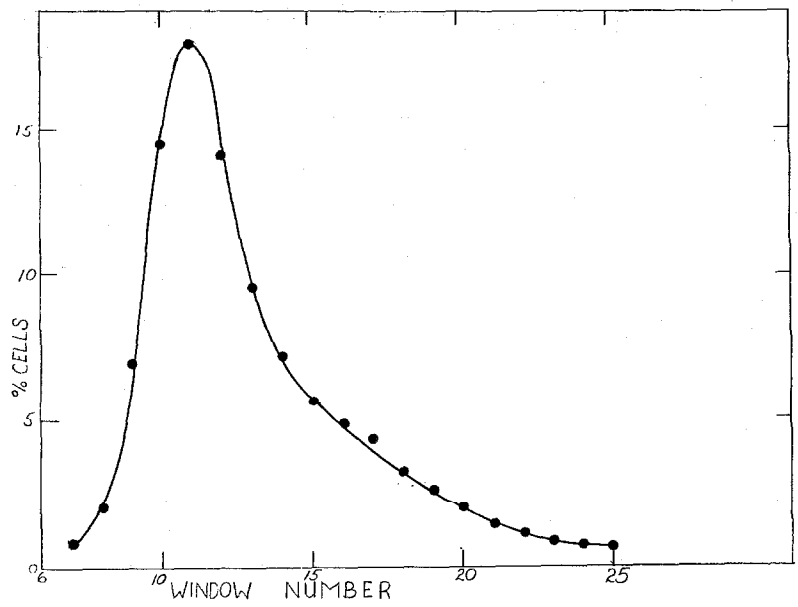

Figure 33j. -- Fraction 11.

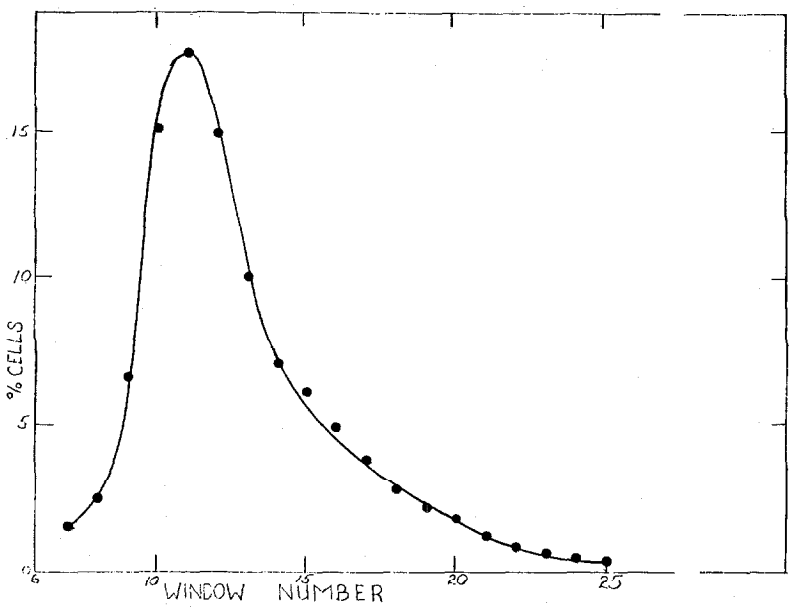

Figure 33k. -- Fraction 13.

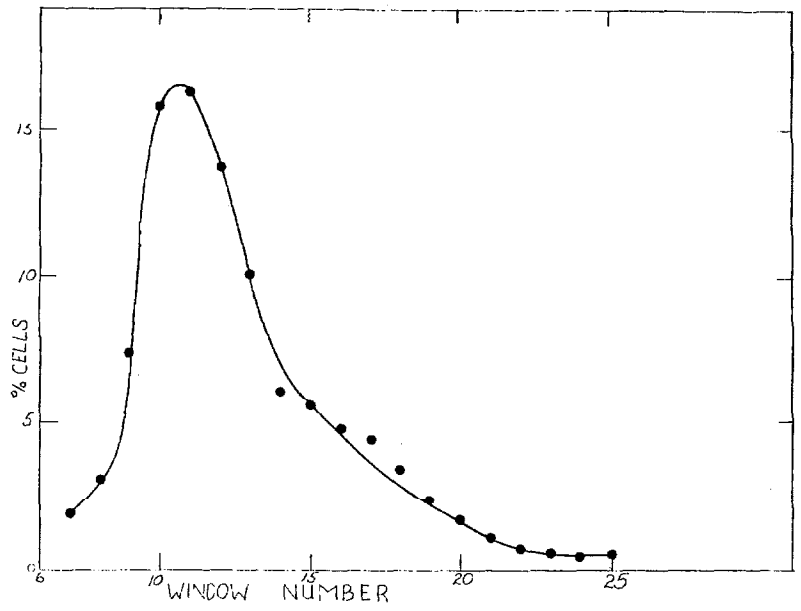

Figure 331. -- Fraction 14.

serum, and again centrifuged.

Erythrocyte morphology and white cell distributions were determined on dried cell smears stained with Wright's stain. Microphotography was performed with a Zeiss Ultraphot II microscope. This instrument is equipped with a photoelectric cell which automatically sets the length of exposure.

Reticulocyte counts were made on smears of cells which had previously been supervitally stained with Brilliant Cresyl Blue. The number of reticulocytes present in each fraction was determined from the reticulocyte counts and hemoglobin absorbances of the fractions. The reticulocyte count is the percentage of reticulocytes among the total red cells. As shown in Table VIII, only 63 per cent of the reticulocytes present in the whole blood were accounted for in the fractions. The possibility of selective loss of reticulocytes and perhaps white cells in the manipulations prior to microscopic examination cannot be totally excluded.

The loss of these cells was not due to drainage artifacts, as both methods of application of the cells gave substantially the same results. Possibilities such as the preferential sticking of these cells to the tygon or glass tubing of the apparatus exist. On the other hand, the presence of albumin is known to prevent such sticking (45).

In order to have some concrete basis for the characterizations

TABLE VIII. Distribution of Reticulocytes in Buoyant Density Fractions of Blood from R.C.L.

A	B	C	D	E	F	G
Fraction number	A. at 406 mμ	% Retics. in fractions	No. of cells counted	% of total A in fractions	C X E	% of total retics. in fractions
Bottom	0.68	0.0	whole slide	2.68	---	---
1	0.069	0.0	" "	2.72	---	---
2	0.084	0.0	" "	3.31	---	---
3	0.134	0.0	" "	5.28	---	---
4	0.196	0.0	" "	7.72	---	---
5	0.258	0.1	1,000	10.17	1.03	1.30
6	0.304	0.4	1,000	11.98	4.80	6.12
7	0.310	0.6	1,000	12.21	7.33	9.36
8	0.216	1.8	2,000	8.51	15.32	19.57
9	0.128	2.4	5,000	5.04	12.10	15.46
10	0.085	3.3	2,000	3.35	11.06	14.12
11	0.072	2.2	2,000	2.84	6.15	7.97
12	0.091	1.6	2,000	3.59	5.74	7.33
13	0.175	1.3	2,000	6.90	8.97	11.45
14	0.152	0.7	1,000	5.99	4.19	5.36
15	0.196	0.2	1,000	7.72	1.54	1.97
				Total Column F:	78.21	
Unfractionated cells		1.25	2,000	100	125	100

of these fractions which were obtained by a new method, reliable, clinically tested procedures have been used. The preparation and examination of the slides were performed in collaboration with Dr. D. Hammond and Mrs. L. Capers, Department of Hematology, Children's Hospital, Los Angeles. These clinical procedures may not be the most precise available, but they are known not to produce large random errors. The only departure in these cytological examinations from standard clinical routine was in the low concentrations of cells used; however, these were not the lowest concentrations of cells that had been examined at the Department of Hematology.

The most obvious step in the manipulations in which selective cell loss could have occurred is in the decantations of the supernatants from the washes with Alsever's solution and serum. The reticulocytes and white cells which constitute the buffy coat are normally found at the top of pelleted cells (17). Such stratification is normally ascribed to the difference in densities of the buffy coat and the rest of the cell population (17). No such density stratification would have been possible in the pellets of homogeneous density fractions. Furthermore, losses by decantation would be expected to be random and involve serious fluctuations. The curve which shows the distribution of reticulocytes (figure 35) is too smooth for such fluctuations to have occurred. Another partial fractionation by cell type

occurs when the cells are smeared on the slides. The reticulocytes and white cells have a tendency to concentrate at the edges of the slides. Counts of atypical areas of the slides would lower the relative percentage of reticulocytes. In order to prevent this, the percentage of reticulocytes was determined in populations of from one to five thousand erythrocytes. Counts across the entire smear did not increase the percentage of reticulocytes. The entire Wright's stained smear usually was checked for white cells. It is possible that some of the reticulocytes matured during the experiment into erythrocytes. This undoubtedly can occur (78). Since all manipulations except the centrifugation of the cells in Alsever's solution and the procedures in the preparation of the slides were carried out at 4°C, the extent of this maturation should have been minimal.

The above mentioned one-half ml. aliquot of cell suspension was centrifuged at 1000 rpm for 15 min. in the International centrifuge. After decantation of the supernatant solution, the cells were lysed by addition of 2.5 ml. of the 0.00005% saponin solution. To this lysate was added one ml. of a cyanide neutral pH buffer (79). After centrifugation, the hemoglobin solutions were read at the carbonmonoxy-ferricyanide isosbestic point in the Soret region, 406 mμ (80).

Results and Discussion

The human erythrocytes in fractions 3-12 were not distinguishable from the vast majority of the unfractionated cells. (figure 34). The cells in the densest fraction, 1, and in the resuspended bottom pellet, were markedly less biconcave than the lighter cells. The cells from the bottom pellet appear to be smaller than the rest of the cells.

Figure 35 shows both the normalized distributions of the hemoglobin erythrocytes and the reticulocytes. The increase in absorbance of fractions 12-15 is an example of a large drainage artifact caused by the nonsectorial shape of the centrifuge tube. The absence of a large number of reticulocytes in fractions 12-15 eliminates the possibility of this tail in absorbance being the reticulocyte peak. The reticulocytes formed a narrow distribution within the lightest quarter of the erythrocyte distribution. The maximum is displaced approximately two fractions lighter. The greatest relative concentration of reticulocytes, 3.3%, is displaced one fraction further. Clearly, the reticulocytes are not separated from the erythrocytes. This distribution of reticulocytes is very similar to that of the radioactive label two days after injection of the rabbit.

It is recognized that there is a current need to separate normal reticulocytes from erythrocytes. From the results described

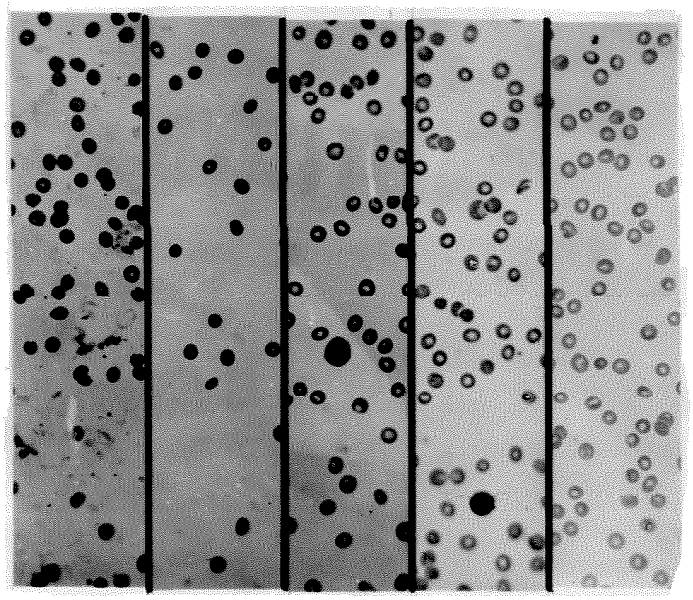

Figure 34.--Microphotographs of erythrocytes stained with Wright's stain. From left to right: cells were obtained from the bottom pellet, and fractions 1, 8, and 12 in order of decreasing density, and from an unfractionated blood sample. A white cell is present in the photographs of fractions 8 and 12.

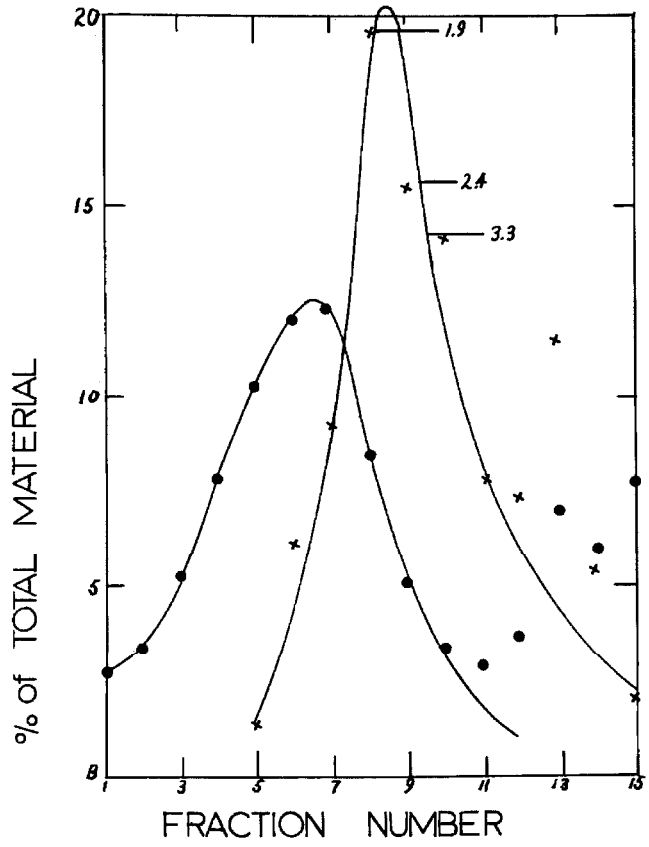

Figure 35.--Distribution of reticulocytes in the buoyant density fractions. X, percentage of the total reticulocyte population in the individual fractions (column G of table VIII). ●, percentage of the total absorbance in the individual fractions (column E of table VIII). The numbers near the crosses indicate the per cent reticulocytes referred to erythrocytes in the fraction (column C of table VIII).

above, the buoyant density method cannot be expected in its present form to provide a clean separation of these two cell populations. The use of sector-shaped tubes or sampling the column from above would eliminate the light tail drainage artifact and result in an increased reticulocyte count. The effect of tonicity or tonicity gradients could be of use in this separation.

As is shown in Table IX, the white cell distributions are quite complex. White cells are found in moderate numbers in the bottom pellet, in low numbers in the rest of the dense half of the erythrocyte distribution, and finally, in greatest numbers in the lighter half of the distribution. No density fraction which contains any significant number of white cells contains just one species of white cell, but there appears to be a definite density displacement of the various white cell distributions. No species of white cell appears to be limited to any one fraction; therefore, each species of white cell can be fractionated by buoyant density. An autoradiographic study of the time dependence of the buoyant density of cells labeled with tritium containing thymidine would show if this density fractionation is by age. For a further discussion of the complete fractionation of white cells, see Proposition 2.

TABLE IX. Distribution of White Cells in the Buoyant Density Fractions.

Fraction number	Segmented neutrophils	Lympho-cytes	Mono-cytes	Eosin-ophils	Baso-phils	Total white cells counted	Relative estimate of the number of white cells in fraction
B	8	71	5	--	--	84	4
1	3	--	--	--	--	3	1
2	1	--	--	--	--	1	1
3	7	2	--	--	--	9	1
4	10	--	--	1	--	11	1
5	44	4	--	2	--	50	2
6	37	3	--	10	--	50	2
7	96	--	--	4	--	100	3
8	92	2	--	6	--	100	4
10	33	16	1	--	--	50	4
12	51	34	9	1	5	100	4
14	52	39	4	4	1	100	4

VII. AN HYPOTHETICAL DESCRIPTION OF THE MECHANISM OF AGING OF THE ERYTHROCYTE

A. The Relationship Between Buoyant Density and Chronological Age

It has been shown in section V-C that the average buoyant density of cells of a given age is apparently directly related to age, but the density of an individual cell is not. It was noted that the linear progression of the label through the first 60 per cent of the cell distribution and the agreement of the intercept of the linear progression with the known life span of the rabbit erythrocyte are evidence that the average buoyant density of the cell of a given age and the age of the cells are directly related. The initial spread and subsequent spreading of the radioactivity disproves any direct relationship between density of an individual cell and its age.

B. The Relationship Between Physiological Age and Chronological Age

It has already been shown for both human (65, 66) and rabbit erythrocytes (68, 69, 70) that individual cells do not have absolutely fixed survival times. According to the data of Shemin and Rittenberg (65), 25 per cent of the cells have been removed from circulation at day 113, and 75 per cent of the cells have been removed at day 141. This spread for the removal of 50 per cent of the cells corresponds to 22 per cent of the average survival time, 127 days. The comparable spread for the rabbit erythrocyte is ca. 25 days and 42 per cent of the average survival time, 60 days. The foregoing result

was obtained by interpolating the data of Neuberger and Niven (69). The distribution in survival times of rabbit erythrocytes is so wide that a significant part of the cells are thought to be destroyed by a process which is not related to their age, random destruction (68, 69,70).

Because of this spread in survival times, it is convenient to define a normalized cell age, which will be called physiological age. Physiological age is the fraction of the individual cell's survival time that it has already spent in the circulation. At present, the survival time of any individual cell cannot be predicted. Whether the survival time of the cell, and consequently the rate of physiological aging, is determined before the release of the cell into the circulation or by chemical events which occur during circulation, or both, is unknown. However, both modes can be characterized by the term "biochemical environmental history." A fractionation which separates cells of different physiological ages thus constitutes a fractionation of cells with different biochemical environmental history.

Physiological age because of the spread in survival times is not directly related to age. The two quantities, buoyant density and physiological age, are both similarly, but neither directly, related to chronological age. The possibility arises that these two quantities may be directly related to each other, or at least more closely related than to the third.

In order to demonstrate that a separation is truly by physiological age, or, as stated at the beginning of this thesis, by degree of differentiation, it is necessary to know the chemical reactions responsible for these differences. But the raison d'être of this whole undertaking was to develop a method of cell separation which would provide materials for the study of these reactions. The method cannot be proven to separate cells by physiological age or degree of differentiation until the use of the method provides a chemical explanation of these processes.

C. An Hypothetical Description of the Mechanism of Aging of the Erythrocyte

The validity of the statement that buoyant density separations correspond to separations of cells of different physiological ages can be provisionally tested with the data derived from the differences observed between the cells in buoyant density fractions. The data that have been acquired are not sufficient to provide a chemical explanation of physiological aging, but are sufficient to provide a teleologically valid description of this process. This description, besides providing some conviction that cells of different physiological age have been separated, should provide a basis for future experimentation.

The red cells are formed in the red pulp of the bone marrow (81, 82). After they have become late reticulocytes, and perhaps early reticulocytes, they are carried out of the marrow by the blood stream (81, 82). The relative distribution of cell volumes is constant throughout the entire buoyant density distribution, and therefore no

fractionation by volume has taken place in the lightest, youngest, fractions of the density distribution. The newly released cells initially increase rapidly in buoyant density, but upon approaching and entering the region of mean buoyant density, increase very slowly. This buoyant density region is probably the optimum physiological state. The increase in buoyant density is not accompanied by any measurable decrease in volume.

The following discussion will present evidence that the state of the cellular hemoglobin, the integrity of the cell, and the buoyant density of the cell are all metabolically linked.

J. H. Jandl and coworkers (83-85) have shown that the state of the cellular hemoglobin and the integrity of the cell itself are coupled to the degree of oxidation of certain cellular thiol compounds. If the state of these thiol compounds were coupled to the changes in composition of the cell responsible for increasing the buoyant density, then buoyant density would be directly related to the state of the cell, the physiological age of the cell.

Jandl et al. (83, 83a) have shown that certain oxidizing agents for thiol compounds denature hemoglobin. The authors have demonstrated that these agents also cause the formation of Heinz bodies, fine grains of precipitated hemoglobin. Heinz bodies have been associated with conditions of artificially increased cell age (86). The artificially reduced rate of cell removal from spleenectomized patients who have hemoglobin H disease results in the appearance of Heinz bodies (87). Jandl and coworkers (83-85) argue that the presence of protective agents such as glutathione and catylase is

necessary to maintain the integrity of both the cellular hemoglobin and the cell itself. This coupling of the integrity of the states of both the hemoglobin and the cell has the merit of destroying cells which are no longer physiologically useful.

According to Jundl et al. (83, 83a) the cellular glutathione is responsible for protecting the easily reactable cysteines of the beta chains. The accessibility of these cysteines is decreased by oxygenation (88), and they have been linked to the Bohr effect (89). However, the latter statement is a matter of controversy (90).

Jacob and Jandl have shown that after reaction with N-ethylmaleimide and p-hydroxymercuribenzoate, erythrocytes lyse both in vitro (84) and in vivo (85). The former of these two thiol specific reagents penetrates the cell and reacts with the cellular glutathione. The latter reagent does not penetrate the cell or interfere with glycolysis, but reaction of this reagent with the cell surface thiol groups is sufficient to cause very rapid sequestration of these cells by the spleen (85).

Other evidence exists that reduced glutathione is necessary for maintaining the integrity of the cell. Triphosphopyridine nucleotide (TPNH) is 12 times as effective a cofactor for erythrocyte glutathione reductase as diphosphopyridine nucleotide (DPNH) (91). TPNH is generated by the oxidation of glucose-6-phosphate (92). The enzyme responsible for this oxidation, glucose-6-phosphate

dehydrogenase, is the shunting enzyme of the hexose monophosphate shunt (92). Otherwise, the anerobic metabolism of the cellular glucose is coupled to the formation of DPNH (92). Glucose-6-phosphate dehydrogenase is an enzyme which has been shown to have its activity greatly decreased or to disappear entirely in older erythrocytes (93). The loss of this enzymatic activity could be the catastrophic event ultimately responsible for the demise of the erythrocyte. Individuals with reduced levels of this enzyme, and presumably reduced levels of glutathione, do have shorter erythrocyte survival times (94).

The disordering of clathrate water due to the loss of lipid has been presented as a possible mechanism of buoyant density increase, section VI. If the lipid content, and thus the buoyant density, of the cell were coupled to the level of reduced glutathione or TPNH, then buoyant density would be coupled to the state of the cell, the physiological age of the cell.

This loss of lipid as the cell ages is probably the cause of the loss of biconcavity in the densest fractions. As the lipid content of the cells decreases, possible hydrophobic interactions responsible for the maintenance of the biconcavity of the cell should be weakened. Ponder and Barreto (95) have shown the existence of some structure in the center of the cell. Erythrocyte ghosts are birefringent, but this birefringence disappears if the last traces of cellular hemoglobin are

removed.

The loss of biconcavity of the cell could be a good prelude to the removal of the cell from circulation. The spleen, liver, and bone marrow are the organs cited (81) as being the organ or organs of erythrocyte removal. The mode of removal is also a matter of controversy (81, 82). The density fractionation of cells should be of use in investigating this interesting problem.

D. The Relationship of the Proposed Mechanisms of Cell Removal and the Loss of Biconcavity of the Dense Cells

Three mechanisms of cell removal suggested in the literature (81, 82) could depend upon the loss of the biconcavity of the cell. The first two of these mechanisms appear to be the most prevalently mentioned (96, 97). The third one is considered by the author of this thesis to be a good possibility.

In the first of these mechanisms, the cells as they are forced through the capillaries abrade into small fragments (96), which remain intact with their complement of cellular hemoglobin. These fragments are thought to be eventually phagocytized by the spleen or the bone marrow. The biconcavity of the cells would allow them to deform as they slip through the capillaries, and thus protect the cells from fragmentation. Biconcave cells have been shown to deform and regain shape in experiments where they were sucked into a micropipette (98).

The second mechanism of the cell destruction involves

phagocytosis of the old cells (97). The sites responsible for the initial attachment of the erythrocyte to the phagocyte could be located at the center of the biconcavity. Until the cell had lost its biconcavity it would be sterically hindered by the thick rim of the biconcave disc from approaching close enough for attachment to the phagocyte.

The third mechanism assumes the old cells to be lysed by osmotic shock (82). The spleen or some other organ could test the viability of the cells by withdrawing and later replacing some of the plasma ions. Serial osmotic shock (62, 63) has been used as a method of fractionating erythrocytes by age. This mechanism would prevent lysis in the blood stream and allow the lysis of the old cells to occur only in some specialized organ which can reutilize the cellular iron and eliminate the cellular debris. The biconcave cells could well stand these test osmotic shocks as these cells can expand in volume. The older, more spherical, cells cannot expand, and are lysed by these test osmotic shocks.

REFERENCES

1. G. Matioli, S. Brody, and B. Thorell, Acta Hemat. 28, 73 (1962).

2. G. Matioli and B. Thorell, Blood 21, 1 (1963).

3. A. H. Coons, Symp. Soc. Exp. Biol. 6, 166, published by Academic Press, New York, 1952.

4. A. H. Coons, General Cytochemical Methods, ed. J. F. Danielli, p. 399, Academic Press, New York, 1958.

5. R. G. Davidson, H. M. Nitowsky, and B. Childs, P.N.A.S. 50, 481 (1963).

6. M. F. Lyon, Nature 190, 372 (1961).

7. J. Bonner, R. C. Huang, and R. V. Gilden, P.N.A.S. 50, 893 (1963).

8. K. Hannig, Z. Anal. Chemie 181, 244 (1961).

9. H. C. Mel, personal communication, 1964.

10. H. C. Mel, Nature 200, 423 (1963).

11. P. A. Albertsson, Methods of Biochemical Analysis, Vol. 10, ed. D. Glick, Interscience, New York, 1962.

12. J. W. Ferrebee and Q. M. Geiman, J. Infect. Diseases 78, 173 (1946).

13. G. Ruhenstroth-Bauer, G. F. Fuhrmann, E. Granzer, W. Kuber, and F. Rueff, Naturwissenschaften 16, 363 (1962).

14. P. A. Albertsson, Partition of Cell Particles and Macromolecules, Wiley, New York, 1960.

15. C. G. Bass and F. M. Johns, Am. J. Trop. Dis. 3, 298 (1915-1916).

16. A. J. Key, Arch. Int. Med. 28, 511 (1921).

17. M. E. A. Powell, Nature 193, 1047 (1962).

18. D. A. Rigas and R. D. Koler, J. Lab. and Clin. Med. 58, 242 (1961).

19. L. Garby and M. Hjelm, Blut 9, 284 (1963).

20. B. W. Agranoff and B. L. Vallee, Blood 9, 804 (1954).

21. S. H. Seal, Cancer 12, 590 (1959).

22. E. Kimura, T. Suzuki, and Y. Kinoshita, Nature 188, 1201 (1960).

23. G. M. Mateyko and M. J. Kopac, Ann. N. Y. Acad. Sci. 105, 183 (1963).

24. E. L. Kuff, G. H. Hogeboom, and A. J. Dalton, J. Biophys. Biochem. Cytol. 2, 33 (1956).

25. C. de Duve, J. Berthet, and H. Beaufay, Progr. Biophys. Biophys. Chem. 9, 326 (1959).

26. G. L. Choules, Anal. Biochem. 3, 236 (1962).

27. R. M. Bock and N. S. Ling, Anal. Chem. 26, 1543 (1954).

28. T. K. Lakshmanan and S.Lieberman, Arch. Biochem. Biophys. 53, 258 (1954).

29. R. L. Millette, personal communication, 1964.

30. J. Weigle, M. Meselson, and K. Paigen, J. Mol. Biol. 1, 379 (1959).

31. R. J. Britten and R. B. Roberts, Science 131, 32 (1960).

32. J. H. Fessler, personal communication, 1963.

33. H. H. Ohlenbusch, personal communication, 1964.

34. W. R. Holmquist and J. R. Vinograd, Biochim. et Biophys. Acta 69, 337 (1963).

35. J. F. Fogh and R. O. Lund., Proc. Soc. Exper. Biol. and Med. 94, 532 (1957).

36. E. Tomkins, Jour. Lab. and Clin. Med. 44, 554 (1954).

37. D. Kabat and G. Attardi, personal communication, 1963.

38. G. Brecher, E. F. Jakobek, M. A. Schneiderman, G. Z. Williams, and P. J. Schmidt, Ann. N. Y. Acad. Sci. 99, 242 (1962).

39. E. Eagle, J. Exptl. Med. 102, 595 (1955).

40. S. C. Bukantz, C. R. Rein, and J. F. Kent, J. Lab. Clin. Med. 31, 394 (1946).

41. G. H. Hogeboom and E. L. Kuff, J. Biol. Chem. 210, 733 (1954).

42. M. R. Lipkin, J. A. Davison, W. T. Harvey, and S. S. Kurtz, Jr., Industrial and Engineering Chemistry, Analytical Edition 55, 16 (1944).

43. Hand Book of Chemistry and Physics, 42nd edition, 1960-61, Chem. Rubber Publishing , Cleveland, Ohio.

44. Coulter Counter Bulletin A-2, Coulter Electronics, Inc., Hialeah, Florida .

45. E. Ponder, Hemolysis and Related Phenomena, Grune and Stratton, New York, 1948.

46. J. E. Hearst and J. R. Vinograd, P.N.A.S. 47, 999 (1961).

47. C. Tanford, Physical Chemistry of Macromolecules (eqns. 19-13 and 21-9), John Wiley and Sons, Inc., New York, 1961.

48. S. B. Leif, personal communication, 1964.

49. P. Ohno, Rev. Sci. Instr. 32, 1253 (1961).

50. E. Ponder, J. Biol. Chem. 144, 333 (1942).

51. K. Linderstrom-Lang, Harvey Lectures, 34, 219 (1937).

52. J. W. Ferrebee, J. G. Gibson, and W. C. Peacock, J. Infect. Dis. 78, 180 (1946).

53. B. L. Vallee, W. Hughes, Jr., and J. Gibson, Blood, Special Issue No. 1, p. 82 (1947).

54. D. W. Fawcett and B. L. Vallee, Jour. Lab. and Clin. Med. 39, 354 (1952).

55. G. Scatchard, A. C. Batchelder, A. Brown, and M. Zosa, J. Am. Chem. Soc. 68, 2610 (1946).

56. J. MacLeod and E. Ponder, J. Physiol. 86, 147 (1935).

57. J. E. Hearst and J. Vinograd, P.N.A.S. 47, 1005 (1961).

58. D. B. Nevius, J. Clin. Path. 39, 38 (1963).

59. T. A. J. Prankerd, J. Physiol. 143, 325 (1958).

60. J. C. Dreyfus, G. Schapira, and J. Kruh, Compt. Rend. Soc. Biol. 144, 792 (1950).

61. E. R. Borun, W. G. Figueroa, and S. M. Perry, J. Clin. Invest. 36, 676 (1957).

62. P. A. Marks and A. B. Johnson, J. Clin. Invest. 37, 1542 (1958).

63. E. R. Simon and J. Y. Topper, Nature 180, 1211 (1957).

64. P. Clark, Australian J. Sci. 22, 216 (1959).

65. D. Shemin and D. Rittenberg, J. Biol. Chem. 166, 627 (1946).

66. W. Ashby, Blood 3, 486 (1948).

67. J. R. Bove and F. G. Ebaugh, Jr., J. Lab. and Clin. Med. 51, 916 (1958).

68. E. L. Burwell, B. A. Brickley, and C. A. Finch, Am. J. Physiol. 172, 718 (1953).

69. A. Neuberger and J. S. F. Niven, J. Physiol. 112, 292 (1951).

70. I. W. Brown, Jr. and G. S. Eadie, J. Gen. Physiol. 36, 327 (1953).

71. P. F. Hahn, W. F. Bale, J. F. Ross, R. A. Hettig, and G. H. Whipple, Science 92, 131 (1940).

72. D. L. Drabkin, Physiol. Rev. 31, 345 (1951).

73. J. G. Gibson, J. C. Aub, R. D. Evans, W. C. Peacock, J. W. Irvine, Jr., and T. Sack, J. Clin. Invest. 26, 704 (1947).

74. R. L. Evans, Nature 173, 129 (1954).

75. C. J. Price-Jones, J. Path. and Bact. 23, 371 (1919).

76. W. J. Farquhar and E. H. Ahrens, Jr., J. Clin. Invest. 42, 675 (1963).

77. L. Pauling, Science 134 15 (1961).

78. P. A. Marks, R. A. Rifkind, and D. Danon, P.N.A.S. 50, 336 (1963).

79. D. W. Allen, W. A. Schroeder, and J. Balog, J. Am. Chem. Soc. 80, 1628 (1958). Chromatographic developer #2.

80. W. D. Hutchinson and J. R. Vinograd, unpublished results.

81. M. M. Wintrobe, Clinical Hematology, 5th ed., Publishers, Lea and Feibiger, Philadelphia, Pennsylvania.

82. J. W. Harris, The Red Cell, Hardvard University Press, Cambridge, Mass., 1963.

83. J. H. Jandl, L. K. Engle, and D. W. Allen, J. Clin. Invest. 39, 1818 (1960).

83a. D. W. Allen and J. H. Jandl, J. Clin. Invest. 40, 454 (1961).

84. H. S. Jacob and J. H. Jandl, J. Clin. Invest. 41, 779 (1962).

85. H. S. Jacob and J. H. Jandl, J. Clin. Invest. 41, 1514 (1962).

86. J. G. Selwyn, Brit. J. Haemat. 1, 173 (1955).

87. D. A. Rigas and R. D. Koler, Blood 8, 1 (1961).

88. R. Benesch and R. E. Benesch, Fed. Proc. 21, 71 (1962).

89. A. Riggs and M. Wells, Fed. Proc. 19, 78 (1960).

90. R. Benesch and R. E. Benesch, Fed. Proc. 19, 78 (1960).

91. E. M. Scott, I. W. Duncan, and V. Ekstrand, J. B. C. 238, 3928 (1963).

92. J. R. Murphy, J. Lab. and Clin. Med. 55, 286 (1960).

93. P. A. Marks, A. B. Johnson, E. Hirschberg, and J. Banks, Ann. N. Y. Acad. Sci. 75, 95 (1958).

94. G. J. Brewster, A. R. Tartov, and R. W. Kellermeyer, J. Lab. and Clin. Med. 58, 217 (1961).

95. E. Ponder and D. Barreto, J. Gen. Physiol. 39, 319 (1956).

96. P. Rous, Physiol. Rev. 3, 75 (1923).

97. A. Blaustein, The Spleen, McGraw-Hill, New York, 1963.

98. R. P. Rand and A. C. Burton, Biophys. J. 4, 115 (1964).

PROPOSITION 1

The Elimination of Carboxyl Groups Present in Filter Paper by Reduction with Lithium Aluminum Hydride

The binding of carboxyl groups present in filter paper of proteins and peptides is thought (1) to be responsible for the inability to completely elute these products during electrophoreses and chromatography. It is proposed to reduce these carboxyl groups with $LiAlH_4$.

Paper chromatography and electrophoresis of peptides and amino acids are two techniques, which, though not absolutely essential to the amino acid sequence determination of proteins, are of great importance. The use of paper as a supporting medium has one great advantage when compared with other media: it can support itself even when wet. This ability of the medium to support itself greatly simplifies the techniques of both chromatography and electrophoresis. Sheets of paper can be hung by clips from solvent troughs, made into cylinders which stand up, sprayed with developers, cut into pieces, and, if need be, sewn together. Paper also has the advantage of being inexpensive.

Paper has the disadvantages that materials such as proteins, peptides, and amino acids which have positive charges tend to stick to it and cannot be eluted from it (1). This disadvantage greatly

hinders the use of paper in experiments which require elution either for the identification or isolation of materials. No matter how good a separation obtained with the use of paper techniques is, if only ten or twenty per cent of a material can be eluted from the paper, the use of other methods will be in order. One other disadvantage of the use of paper is that trailing of materials is observed (2). This trailing is probably due to the materials adsorbing on the carboxyl groups present in the paper. This chromatography retards the materials, but as these carboxyl groups are present in low concentration, they are easily saturated. Therefore, when the material is concentrated, the percentage of time that any individual product molecule interacts with the carboxyl groups is negligible. However, when the material becomes dilute, the interaction with the carboxyl groups by any individual material molecule increases. This difference in degree of interaction of the dilute and concentrated solutions of materials causes a difference in mobility and thus trailing.

In order to remove these carboxyl groups present in the filter paper, Flodin (1) has esterified them by treatment with an anhydrous ethanol HCl mixture. The author of this proposition has used this reaction to esterify the carboxyl groups present in absorbent cotton, which was to be used as a support for column electrophoresis. The cotton , initially in the form of wads, was degraded during the esterification into fine linters. Paper when so treated loses most of its

strength, which previously was mentioned as its outstanding characteristic.

$LiAlH_4$ is a widely used reductant of carboxyl, aldehyde, and ketone groups. All three are reduced to alcohols (3). It is a reagent which should not cleave hemiacetal bonds (3), and thus should not degrade the cellulose polymers. Professor Dreyer (4) of the C.I.T. Biology Department has also been interested in the problems associated with the use of filter paper as a supporting medium, and believes that aldehyde groups might form Schiff's base with the amino groups of peptides or proteins. The use of $LiAlH_4$ will not settle the question of which group is the cause of the binding of the product to the paper, but may be expected to solve the problem as it reduces both the aldehyde and carboxyl groups present in the paper.

In a preliminary experiment, filter paper was reduced for four hours with an ethyl ether solution of $LiAlH_4$. Hemoglobin had twice the electrophoretic mobility on paper so treated as it had on untreated paper. Even of greater significance, the reduction did not weaken the paper. Reduced and unreduced paper were physically indistinguishable. Ethyl ether is too dangerous a solvent to be used for routine large-scale reductions; instead, tetrahydrofuran or dioxane could be used (3). $LiAlH_4$ is more soluble in tetrahydrofuran than in dioxane (3), and therefore the former would be the solvent of choice.

Because of the flammability of the tetrahydrofuran $LiAlH_4$ solution, the amount of solution used in the reduction should be kept to a minimum. A thin stainless steel box, six inches longer and an inch wider than the paper to be reduced, would be an appropriate reaction vessel for this reduction and other chemical treatments of the paper. The top lid of the stainless steel box can be screwed on and sealed by a silicon rubber gasket. The paper can be suspended by stainless steel chromatographic clips from a rod which rests on notched supports welded to the narrow sides of the box. To one of the two large sides of the box, three thick-walled two-inch long stainless steel connecting pipes would be welded. These pipes would be grooved to take O rings and clamps. Two of the pipes would be narrow-bore and located, respectively, within an inch of the bottom and three inches from the top of the box. These pipes would each interconnect via an O ring to a glass O ring joint which was attached to a stopcock. These two stopcocks would be used in the filling and emptying of the reaction vessel. The third pipe mounted within an inch of the top would be of wider bore and would connect via an O ring to a glass reflux condenser.

After the reduction, the reducing solution can be drained into and destroyed by cold ethyl acetate. During this process, the paper could be covered with dry nitrogen or dry tetrahydrofuran. The paper could then be washed by filling and emptying the reaction vessel with

dry tetrahydrofuran. The residual $LiAlH_4$ left on the paper could then be destroyed by a wash with a dry tetrahydrofuran, ethyl acetate mixture. The paper at this point is very stiff, as the carboxyl and aldehyde groups are now in the form of an aluminum alkoxide. Washes with ethanol, water, and a dilute aqueous solution of citric acid should remove the aluminate from the paper. The paper, if still contaminated with aluminate, can then be subjected to a high-voltage electrophoresis in a volatile solvent.

The above procedure can undoubtedly be simplified, especially if it were to be undertaken as a routine step in the large-scale production of such filter paper. However, the above procedure is safe and thorough enough to establish whether $LiAlH_4$ reduction will render filter paper suitable for use as a preparative supporting medium.

The above procedure could be tested in many ways. Two of these which were the motivating factors in the development of this proposition were the elution of peptides from fingerprints and the electrophoresis of proteins on paper. Human hemoglobin is very well characterized, and is probably the best material to use for these tests.

Individual peptides obtained by column chromatography of a tryptic digest of this protein could be tested. Three equal aliquots of such a peptide would be used for the following purposes: The first aliquot would simply be hydrolyzed to amino acids and analyzed according to Spakman, Moore and Stein (5). The other two aliquots

would undergo chromatography and electrophoresis according to one of the latter versions of the "fingerprint" technique (6). One of the "fingerprints" would be stained with ninhydrin and would be used as a marker to locate the peptide on the other paper. This section of the paper would be cut out, and the peptide eluted from it. The elute would then be hydrolyzed and analyzed as before. The yield is the ratio of the absorbances from the amino acids in the fingerprinted aliquot to those of the aliquot which had not been fingerprinted. In order to verify that the piece of paper which contained the peptide was completely cut out, the remainder of the filter paper would be stained with ninhydrin.

The trailing of hemoglobin on paper after electrophoresis is readily observable because of the red color of the heme group. Electrophoresis of hemoglobin at neutral pH on paper which had been treated with $LiAlH_4$ should do away with this trailing. The paper could be scanned in the Soret region for residual hemoglobin absorbance and the hemoglobin could be eluted off the paper and the absorbance of the eluate measured. This absorbance can be compared as above with the absorbance of the hemoglobin solution that was applied to the paper.

PROPOSITION 2

A Continuous Two-Dimensional Method for Fractionating Cells

It is proposed to develop a continuous two-dimensional method for fractionating cells. The first dimension of this separation would be by buoyant density, and the second by electrophoretic mobility. Buoyant density is evidently related to degree of differentiation (1), and electrophoretic mobility to cell type (2).

Very seldom are complicated mixtures of biological materials completely separated by a single application of a single method. In the case of cells, separations based on the repeated application of a single method at different experimental conditions are not feasible, as the conditions for any experiment are essentially determined by the limitations of maintaining viability. These constraints eliminate the repeated application of any method of separation with a variation of tonicity and pH.

A two-dimensional method of separation similar to the "fingerprint" technique (3) of Ingram should greatly improve the fractionation of cells from complex tissues, and particularly bone marrow, which is presently being studied in many laboratories. As stated in the "Introduction" of the thesis, the separation by electrophoretic mobility is primarily by cell type (2). Different types of

cells such as erythrocytes and leucocytes possess different and consistent electrophoretic mobilities (2).

Cells have been separated in a Hannig curtain electrophoresis apparatus (4). This apparatus differs from previous curtain apparatuses in that the curtain contains no supporting medium. The curtain is a $\frac{1}{2}$-mm. layer of buffer which lies between two glass plates. These glass plates are air-cooled to remove the Joule heating. In the latest and best form of this apparatus (5, 6), the electrophoretic buffer is fed into six ports located at the top of the curtain. The sample to be separated is introduced into any one of several ports located near the top of the curtain. The separated products are removed through ports located at the bottom of the curtain by a 48-channel peristaltic pump. Platinum electrodes are located at the sides of the curtain in the buffer vessels. These electrodes make electrical contact with the curtain through cellophane membranes.

In the proposed method, the cells would first be distributed by centrifugation to their buoyant densities in a BSA gradient. Then, instead of fractionating the gradient, the gradient would be pumped into the sample port of the Hannig electrophoresis apparatus. In order to avoid possible electrophoretic artifacts due to the discontinuity in resistance across the curtain, which is brought about by the introduction of a concentrated BSA solution, the gradient prior to introduction may have to be continuously diluted with an appropriate amount of

electrophoretic buffer. This dilution can be accomplished with the use of another channel of the Technicon peristaltic pump and a glass helical mixer. In fact, the gradient of BSA initially present in the sample could be continuously compensated for by diluting with an inverse gradient of dilute BSA. BSA will protect the cells and minimize a possible electrophoretic anomaly due to the electrophoretic mobility of the cell being affected by binding of BSA by the cell.

Because a continuous electrophoresis apparatus is being used as the second dimension of a separation, the collection tubes of this apparatus will have to be mounted in a 48-tube wide rack which is moved forward in steps. In order to correspond to the present buoyant density fractions, the rack should be at least 15 tubes deep. The resulting distribution of cells in the tubes can be most conveniently assayed with a Coulter-Counter (7). If this Coulter-Counter is appropriately mated to a pulse height analyzer (8), the volume distributions of the fractions of the fingerprint can also be obtained.

The first test material for this two-dimensional separation will be finger punch blood from R. C. L. This material has the advantage of being practically instantaneously available to the author of this proposition, and to have been well characterized in the BSA gradient. Cells which are easily available and which are in a steady state as regards composition must be used in the development of a new method. Otherwise, if both the experimental conditions and

technique are necessarily changing while they are both being improved, and the cellular material is also changing, then it is extremely difficult to evaluate the cause of any change in the experimental results.

Once this finger punch blood has been characterized and the method is under control, then bone marrow, which is, as stated before, a tissue of great interest, can be fractionated. These purified cells could be useful in many different types of research. Some of these are the study of the differentiation and maturation of the erythroid cells, the control of hemoglobin production during this differentiation, and the isolation and characterization of the stem cell.

The stem cell is the postulated precursor of all of the cell types in the bone marrow (9). It is the undifferentiated cell which, upon mitosis, makes two different daughter cells. One of these cells is identical with the mother cell, and the other has differentiated into a precursor of one of the species in the bone marrow. Fortunately, a biological assay has been worked out for these cells (10). Stem cells in bone marrow, taken from a normal mouse, form colonies in the spleen of a mouse which has been heavily irradiated with X rays.

It should also be mentioned that, while the mating of the buoyant density procedure with electrophoresis in a Hannig apparatus

has been stressed as a solution to the fractionation of bone marrow, the techniques involved in this mating are common to a mating with the sedimentation or electrophoresis procedures (11, 12, 13) of H. Mel. The sedimentation procedure has been described in the Introduction to this thesis. The electrophoretic procedure is exactly the same except for the introduction of a field applied across the density gradient. However, the gradient formed in the Mcl apparatus would have to be made from BSA solutions with a density range of ca. 1.02-1.03 g. cm.$^{-3}$.

PROPOSITION 3

The Relationship between Human Erythrocyte Age and Buoyant Density

It is proposed to determine the buoyant density distributions of human erythrocytes which have been labeled in vivo with both radioactive iron and glycine. A study of the time dependence of the relationship between the radioactive labeled distributions and the unlabeled cell distribution will establish whether buoyant density is directly related to the average age of the cells. The double labeling of the cells will allow the study of the distribution of labeled cells during the last 40 per cent of the survival time of the cells. The distribution of radioactive glycine will not at the demise of the cells be obscured by recycling (1) of the isotope. The recycling of the radioactive iron (2) to lower densities will indicate the demise of the cells.

This proposed study with human cells would be similar to that of the buoyant density progression of the Fe^{59} pulse labeled rabbit erythrocytes reported in this thesis. The results of this study should be very similar to the previous rabbit experiment, but in order to definitively establish the relationship between chronological age and buoyant density of human cells, two or more human beings will have to be injected with ca. 100 microcuries of both $Fe^{59}Cl_3$ and

radioactive glycine. At the demise of the erythrocyte, iron is recycled (2); glycine is not (1). The ratio of the iron to glycine radioactivity should remain constant throughout the distribution of cells, except where the iron has recycled, in which case the increase in this ratio will show this recycling.

Since the buoyant density distribution of erythrocytes from normal male adults has been described in the thesis, some male adult patients with life expectancies between one and two years and normal erythrocyte buoyant density distributions might be the appropriate experimental subjects. Garby and Hjelm (3) injected Fe^{59} into schizophrenics. The use of this type of subject should also be considered.

The life span of the human erythrocyte is twice that of the rabbit erythrocyte, 120 (4) and 60 (5) days, respectively. The width of the human erythrocyte distribution also appears to be greater than that of the rabbit distribution. But accurate measurements of band width will have to wait for future improvements in the method.

In the pulse labeling experiment with rabbit erythrocytes, the linearity of the progress of the midpoints of the distribution of radioactivity through the buoyant density distribution of cells showed buoyant density to be directly related to the average chronological age of the erythrocytes. The density distribution of removal of the

erythrocytes from the circulation was obscured by the recycling of the Fe^{59} label. The use of labeled glycine, which does not recycle, will allow the observation of the distribution of radioactivity during the last 40 per cent of the life span of the cells. The glycine can be labeled with C^{14} or H^{3}, depending on the type of counter used to assay the radioactivities. The removal of the cells can be observed from the recycling of the Fe^{59}. Fe^{59} is recycled with 80 per cent efficiency (2). The probable greater range in buoyant densities of human erythrocytes and the lesser degree of apparent random destruction of these cells, as compared with rabbit erythrocytes (section V-A), should result in an improvement in the quality of the experimental results.

PROPOSITION 4

A Westphal Balance to Measure Densities of Small Volumes of Liquids

It is proposed to accurately measure the densities of small volumes of liquids, 0.1-0.3 ml., with a Westphal balance (1) based on the Cahn Electrobalance (2). The Cahn Electrobalance is a null instrument. The sensitivity of this balance should not be affected by the damping action of the viscous drag of the liquid on the Westphal bob.

The accurate measurement of densities of small volumes of liquids is necessary for many problems associated with ultracentrifugation. These measurements are essential to the determination of buoyant density distributions obtained by both density gradient equilibrium and preformed gradient techniques and the evaluation of sedimentation values and molecular weights. Accurate measurements of partial specific volumes should also be possible with this Westphal balance.

At present, the two methods of choice for density determinations of small volumes of liquids are pycnometry and Linderstrom-Lang gradient columns (3). The manipulations involved in pycnometric measurements require extreme care. The pycnometric

density determinations presented in this thesis were most time-consuming and probably were the accuracy-limiting step in the procedure.

The use of Linderstrom-Lang gradient columns allows for very precise density determinations. However, it takes time for the drops to attain their equilibrium positions, and the densities obtained are not without ambiguity. Solutes can exchange between the drop and the bromobenzene ligroin gradient columns (4). The instability in position of the drop in the gradient associated with this exchange has been observed (4). In the case of density measurements of BSA solutions which contain very complicated mixtures of solutes and erythrocytes, the possibility of the exchange of solutes between the drop and the column is so great that it rules out this very elegant technique. Ponder (5) attempted to measure red cell densities with Linderstrom-Lang gradient columns, and advised against it.

The Westphal method is presently not used because with a conventional balance the damping provided by a bob moving through a liquid is equivalent to the use of a magnetic damper. This decrease in sensitivity should not occur with the Cahn Electrobalance (6). The Cahn balance is a null instrument. The torque developed by a weight on the beam is nulled by an equal and opposite torque developed by current passing through a coil which is mounted at the center of the

beam and suspended between the poles of a fixed magnet. The current to the coil is controlled by a feedback on the position of the balance arm. The position of the beam affects the amount of light incident on a phototube. Thus, the torque generated by the weight is balanced when the arm is stationary and in a constant position.

A quartz ball suspended by a thin quartz fiber from the beam of the balance will serve as the weight or bob. For the density determinations involved in this thesis, the appropriate weight of such a bob would be 300 mg. The density of amorphous quartz is 2.2 (7). Thus, the weight loss would be ca. 150 mg. If the initial 300 mg. was tared with 140 mg. weight, then the apparent weight of the bob in the BSA solutions used in the thesis would be 10 to 15 mg. According to the Cahn Instrument Company (2), the precision of the balance when given as the fraction of the weight change is 10^{-4}. Thus, the balance would have a precision of ca. 1 microgram. The precision of the density differences would then be $\pm 8 \times 10^{-6}$ g. cm.$^{-3}$. At 4°C, the density change of water is 1.4×10^{-5} g. cm.$^{-3}$/°C. Even if this theoretical discussion of the precision of the proposed Westphal balance had underestimated the errors by a factor of ten, the proposed instrument would still be five times as precise as the pycnometric measurements given in this thesis.

It might be added that for partial specific volume measurements, the mounting of two bobs of equal weight at opposite ends of the balance arm would allow the measurement of small density differences between solutions with very small increments of solute.

An ambiguity in these Westphal measurements is the surface tension on the thin quartz fiber at the interface of the BSA solution and the atmosphere. Firstly, Cahn balances are presently used to measure surface tension (8). The surface tension of the BSA solutions used in this thesis is presently not known. However, the most direct way to correct for this surface tension effect is to measure it with the Cahn balance. This measurement could be made with the use of a second quartz fiber and bob, with the bob now located at the center rather than at the end of the fiber. This bob and fiber can be weighed in air, and with the tip of the fiber just submerged under the surface of the BSA solution. The difference in the weights is the surface tension blank.

PROPOSITION 5

A New Peptide Mapping Technique

It is proposed to modify the peptide mapping technique of Ingram (1) to render it more suitable for the comparison of proteins that differ by 3 or more amino acids or for the identification of neutral amino acid substitutions. The tryptic digestion and subsequent electrophoresis would be unchanged, but digestion with papain or pepsin and electrophoresis at acid pH would replace the chromatographic separation.

The peptide mapping technique has been used to study small differences in amino acid composition of proteins which were closely related in primary structure. This was the technique which Ingram (1) invented and first used to detect the differences between hemoglobins A and S (2, 3). It has been extended to many other proteins. Zuckerkandl et al. (4) have traced the phylogenetic pathways of hemoglobin by the peptide mapping technique. From the results of Zuckerkandl et al. it is apparent that relationships between orders or, more distantly, classes, exhibit the proper trend, but that a semiquantitative evaluation of the degree of congruence of the peptide sequences is extremely difficult. What is much more discouraging is that the peptide maps of all the hemoglobins taken together exhibited no other common spot except lysine.

The strength , and for these cases the weakness, of the peptide mapping technique lies in its extreme sensitivity, especially for charged amino acids; it is most effective when the proteins differ by one or perhaps two charged amino acids. If a tryptic peptide contains one or more substitutions, the resulting spot on the fingerprint will be displaced and only identifiable by difference. That is, all the other spots have remained in their positions and only one spot has moved. Chemical analysis of many displaced spots would be possible but not feasible if the peptide mapping technique were to be of use as a survey method. The great difficulty in evaluation of peptide maps of widely separated species is that, if ten spots have been displaced, the question of how many amino acids have been changed in the spots cannot be answered. One amino acid substitution can, in these long tryptic peptides, hide common di-, tri-, tetra-, and penta-peptides. The tryptic peptides of adult human hemoglobin, according to the data of Guidotti et al. (5), average 12 amino acids in length and range between 2 and 40 amino acids. The large size of the tryptic peptides could mask changes in neutral amino acids. Ingram (6) has postulated such change to be the cause of thalassemia.

The following modification of the peptide mapping technique should render it suitable for use as a survey method, allow the discovery of small common peptides, and enhance the possibility of the

identification of neutral amino acid substitutions. The normal tryptic digestion and subsequent electrophresis in Michl's buffer on Whatman 3 MM would be unchanged. The chromatographic separation would be eliminated. Instead, the stripe of tryptic peptides would be digested by spraying a solution of a second less specific preolytic enzyme on the paper. Pepsin in a formate buffer of pH ca. 2 would probably be a reasonable starting condition for the development of the technique. Papain might also be a good possibility. The action of pepsin or of papain on proteins is not specific to the extent that one can a priori predict which peptides will be cleaved, but these cleavages are reproducible (7). The digest would then be separated in the second dimension by electrophoresis. The diffusion of the peptides during this procedure should be approximately that of the chromatographic separation of the conventional finger print technique. The time involved is about the same.

The digestion of the tryptic peptides would be according to the procedure of Naughton and Hagopian (8). These authors have reported the removal by carboxypeptidase B of the C terminal arginines and lysines from the peptides of a tryptic digest of the γ chain of human fetal hemoglobin. The enzyme in ammonium carbonate buffer of pH 8.8 was applied as a fine spray until the paper was moist. The moist paper was then hung for 18 hrs. at room temperature in a jar

which had been lined with paper wet with ammonium carbonate buffer.

The tryptic peptides would now be identified by examination of their products. The tryptic peptides would be displaced according to their electrophoretic mobility in the first dimension. The products of the subsequent digestion would all be displaced according to their individual electrophoretic mobilities in the second dimension. Hence, the digest products of identical tryptic peptides would appear as stripes of spots with the entire stripe displaced the same distance in the first dimension and the individual spots displaced the same distances in the second dimension.

The case of interest is, however, when the two tryptic peptides differ by one and perhaps two amino acids. During the first electrophoresis, the tryptic peptides would be displaced according to their individual electrophoretic mobilities. The identical products of the subsequent digest would appear as spots on stripes which usually were displaced in the first dimension, but which were identical in the second dimension. The relationship between two tryptic peptides would be demonstrated by the identical distribution in the second dimension of all except one or possibly two of the products of the digestion. The digest peptide which contains the substitution will be displaced in the second dimension; however, it will be identifiable

as it lies on the same stripe as the other digest peptides.

In the case of a substitution in a tryptic peptide which does not result in a change of electrophoretic mobility, the position in the first dimension of the stripe of spots will be the same, but the position of the digest peptide which contains the substitution will be more sensitive to the substitution. The contribution of a single amino acid to the electrophoretic mobility of a small peptide is going to be greater than that to a large peptide.

References

PROPOSITION 1:

1. P. Flodin and D. W. Kupke, Biochim. et Biophys. Acta 21, 368 (1956).

2. H. G. Kunkel and A. Tisselius, J. Gen. Physiol. 35, 89 (1951).

3. W. C. Brown, in Organic Reactions, Vol. 6, 469; R. Adams, Editor in Chief, New York, J. Wiley and Sons Inc., 1951.

4. W. J. Dreyer, personal communication, 1963.

5. D. H. Spakman, W. H. Stein, and S. Moore, Anal. Chem. 30, 1190 (1958).

6. A. M. Katz, W. J. Dreyer, and C. B. Anfinsen, J. Biol. Chem. 234, 2897 (1959).

PROPOSITION 2:

1. H. Borsook, J. B. Lingrel, J. L. Scaro, and R. L. Millette, Nature 196, 346 (1962). These authors fractionated rabbit reticulocytes in BSA density gradients with methods developed in the early stages of this research.

2. G. Ruhenstroth-Bauer, G. F. Fuhrmann, E. Granzer, W. Kuber, and F. Rueff, Naturwissenschaften 16, 363 (1962).

3. V. M. Ingram, Nature 178, 792 (1956).

4. K. Hannig, Z. Anal. Chemie 181, 244 (1961).

5. E. F. Haag, Sales Engineer, Brinkmann Instruments, Inc., Long Island, N. Y., personal communication, 1964.

6. Presently such an apparatus is in use in the laboratory of Prof. A. Hodge, California Institute of Technology.

7. G. Brecher, E. F. Jakobek, M. A. Schneiderman, G. Z. Williams, and P. J. Schmidt, Ann. N. Y. Acad. Sci. 99, 242 (1962).

8. B. Cassen, personal communication, 1964.

9. E. P. Cronkite, T. M. Fliedner, V. P. Bond, and J. S. Robertson in The Kinetics of Cellular Proliferation, editor, F. Stohlman, Jr., Grune and Stratton, N. Y., 1959.

10. J. E. Till and E. A. McCulloch, Radiation Res. 14, 213 (1961).

11. J. W. Ferrebee and Q. M. Geiman, J. Infect. Diseases 78, 173 (1946).

12. H. Mel, J. Theoretical Biol. 6, 159 (1964).

13. Ibid., 181.

PROPOSITION 3:

1. N. I. Berlin, T. A. Waldmann, and S. M. Weissman, Physiol. Rev. 39, 577 (1959).

2. J. G. Gibson, J. C. Aub, R. D. Evans, W. C. Peacock, J. W. Irvine, Jr., and T. Sack, J. Clin. Invest. 26, 704 (1947).

3. L. Garby and M. Hjelm, Blut 9, 284 (1963).

4. D. Shemin and D. Rittenberg, J. Biol. Chem. 166, 627 (1946).

5. A. Neuberger and J. S. F. Niven, J. Physiol. 112, 292 (1951).

PROPOSITION 4:

1. N. Bauer, Determination of Density, Physical Methods of Organic Chemistry, Vol. 1, editor, A. Weissberger, Interscience, N. Y., 1945.

2. Cahn Instrument Co., Bulletin 109B, Paramount, California.

3. K. Linderstrom-Lang, Harvey Lectures 34, 219 (1937).

4. G. L. Millere and J. M. Gasek, Anal. Biochem. 1, 78 (1960).

5. E. Ponder, J. Biol. Chem. 144, 333 (1942).

6. L. Cahn, President, Cahn Instrument Co., Paramount, California, personal communication, 1964.

7. The Merck Index, 7th edition, P. G. Stecher, editor, chemical monographs, published Merck and Co., Inc., Rahway, N. J., 1960.

8. Cahn Instrument Co., Bulletin 111, Paramount, California.

PROPOSITION 5:

1. V. M. Ingram, Nature 178, 792 (1956).

2. J. A. Hunt and V. M. Ingram, Biochim. et Biophys. Acta 28, 546 (1958).

3. V. M. Ingram, Biochim. et Biophys. Acta 28, 539 (1958).

4. E. Zuckerkandl, R. T. Jones, and L. Pauling, P.N.A.S. 46, 1349 (1960).

5. G. Guidotti, R. J. Hill, and W. Konigsberger, J. Biol. Chem. 237, 2184 (1962). The average number of amino acids in the tryptic peptides of adult human hemoglobin were calculated from the data.

6. V. M. Ingram and A. O. W. Stretton, Nature 184, 1903 (1959).

7. F. Sanger and H. Tuppy, Biochemical J. 49, 481 (1951).

8. M. A. Naughton and H. Hagopian, Anal. Biochem. 3, 276 (1962).